AN ABSTRACT OF THE THESIS OF

Kamal Fouad Bichara for the degree of Doctor of Philosophy

in Electrical and Computer Engineering presented on August 16, 1975

Title: LIQUID CRYSTAL THERMOGRAPHY: A NEW SYSTEM FOR BREAST CANCER DETECTION

Redacted for privacy

Abstract approved: _____
Dr. C. C. Chang

A liquid crystal thermographic technique was developed for application to several problems in clinical medicine and physiology. The procedure was inexpensive, rapid, simple, versatile and acceptable to patients. Investigators in the past have used cholesteric liquid crystals for thermography but their use was limited to research in the medical field because the methods involved called for the direct spraying of the skin surface with the liquid crystals over a black paint.

The present research has been involved in the development and fabrication of a liquid crystal dispersion thin film with very high elastomeric properties which provides perfect contact with the skin surface of a body of

any configuration. Different films were prepared using plasticized vinyl resins in which the liquid crystals are dispersed. The final film yields optimum optical, thermal and mechanical characteristics and a long shelf life. Liquid crystal dispersions in plasticized polyvinyl chloride or copolymers of vinyl chloride and vinyl acetate were fabricated. However, polyvinyl butyral was selected since it forms strong, highly resilient films and yields optimum optical characteristics.

After the film was perfected, a clinical comparative study was conducted to evaluate the new system. In this study, seventy-five volunteer women were given a breast examination using three modalities:

(1) Liquid crystal thermography using the thin film.

(2) Liquid crystal thermography using the direct spraying of the liquid crystals over a pre-blackened coat (Trade name--Lix Kit).

(3) Infrared thermography using AGA Thermovision model 680 infrared thermography system.

All positively read thermograms were followed up by a xeroradiography examination, the most recent and widely spread method for breast cancer detection.

Positive thermographic signs were defined and a new interpretation scheme was introduced intended to reduce the

false positive rate and to free the thermographic interpretation from the dependency on the experience of the reader.

The new interpretation method was applied to one thousand random cases of patients who had breast examinations using infrared thermography, xeroradiography and pathological tests. This interpretation scheme is based on a trinary point system which penalizes each positive symptom by 1 or 2 points according to its severity. The total number of points which are assigned to the thermogram would make it negative, positive or equivocal. As a result of this method, the false positive rate which constitutes a major disadvantage of infrared thermographic techniques was reduced from 57.4% to 20.37%.

Liquid Crystal Thermography: A New System for Breast Cancer Detection

by

Kamal Fouad Bichara

A THESIS

submitted to

Oregon State University

in partial fulfillment of
the requirements for the
degree of

Doctor of Philosophy

Completed August 16, 1975

Commencement June 1976

APPROVED:

Redacted for privacy

Assistant Professor of Electrical and Computer Engineering
in charge of major

Redacted for privacy

Head of Department of Electrical and Computer Engineering

Redacted for privacy

Dean of Graduate School

Date thesis is presented August 16, 1975

ACKNOWLEDGMENTS

Because of the interdisciplinary nature of this dissertation, a large number of people have aided in its evolution and success.

Many individuals and institutions were directly and indirectly associated with the success of this project. I would like to thank my advisor, Dr. C. C. Chang, for initiating my interest in biomedical research and for his confidence and interest in my work. Particular thanks go to the members of my committee whose special efforts through my Ph.D. program helped make this work successful. I would like to express my sincere thanks to Dr. Thomas W. Davison at Kent State University and Liquid Crystal Biosystems for inviting me to complete my research work at Kent State University and for his enthusiasm and support through the completion of the research. I would also like to express my sincere gratitude to Dr. Keith L. Ewing at Kent State University for making my visit a most productive learning experience.

I am grateful to Dr. Austin Kuster at Akron City Hospital for his confidence and encouragement through the completion of the research. I would also like to thank

Miss Joanne Bonish, R.N., for her assistance and the long hours she put in the clinical study that made the completion of this work possible.

TABLE OF CONTENTS

LIST OF ILLUSTRATIONS

LIST OF TABLES

LIQUID CRYSTAL THERMOGRAPHY: A NEW SYSTEM FOR BREAST CANCER DETECTION

I. INTRODUCTION

Definition

Thermography is the technique of photographically portraying the surface temperature of a body. The optimum thermographic technique provides a quantitative, instantaneous thermogram equivalent to the maximum possible number of individual temperature measurements per unit area. Therefore, the criteria of an optimum thermogram is both a high temperature sensitivity and spatial resolution in real time.

In the clinical comparative study, Xeroradiography is used as a follow-up method on all volunteers with positively read thermograms. Xeroradiography is the use of a modified X-ray irradiation technique for the distinction between normal and abnormal tissues.

Liquid Crystal Thermography Characteristics

Liquid crystal (L.C.) thermography is a relatively new technique that provides many of the optimal characteristics desired in thermography. L.C. thermography was

developed by utilizing the color temperature properties of cholesteric liquid crystals. When applied over a blackened surface, cholesteric liquid crystals give rise to iridescent colors, the dominant wavelength being influenced by a very small temperature change. L.C. thermography is capable of producing a color thermogram with a temperature sensitivity of 0.1°C and a spatial resolution of 1000 lines per inch.

A major advantage of L.C. thermography over other techniques is that it may be viewed in real time since no scan is required. The time constant observed in L.C. thermograms is 0.1 second (Fergason, 1968); a significant factor for dynamic thermographic applications.

The L.C. thermographic technique utilizes mixtures of cholesteric liquid crystal materials that display color-temperature properties when applied in a thin layer over a blackened skin surface. A typical material used for medical and physiological applications responds with a 4°C color-temperature range; however, the range can be varied depending on the cholesteric esters used and their relative proportions. All colors of the visible spectrum are seen on the L.C. thermogram with shades of blue, green and red being most dominant on simple observation. The highest temperatures on the thermogram are shades of blue, the lowest temperatures are shades of red and the intermediate are

shades of green and yellow. Through a well designed photographic set up, a perfect reproduction of the thermogram can be obtained.

How the study was done

The study was done in three phases:

(1) Development of the thin liquid crystal dispersion film.

(2) Comparative clinical study using thermography in three modalities.

(3) The development of an interpretation scheme for thermographic diagnosis and its application on 1000 randomly selected cases which were previously read.

Each phase of the study was important and necessary because:

(1) Casting films from solutions of volatile solvents was the first method of applying cholesteric liquid crystals, although alternatives have been developed such as a rigid encapsulation of liquid crystals by the National Cash Register Company. The majority of cholesteric liquid crystal formulations are at present used as solutions. Despite the very promising potential of cholesteric liquid crystals (Davison, 1972), their use in the medical field was limited because:

(a) The cholesteric liquid crystal formulation

is protected against degradation right up to the moment of application. The solution, once cast, is very vulnerable to degradation from oxygen and UV light as it is totally exposed. Fergason (1968) quotes a lifetime of 3-4 hours before the performance is impaired.

(b) Re-use of cholesteric liquid crystal formulation is only possible by scraping off the solution and reconstitution in a solvent.

(c) The surface to which the cholesteric liquid crystal solution is applied must be free from grease, oil and fat traces which can depress the color-temperature play for a temperature sensitive system.

(d) Unless formulation containing built-in blackening material is used, the surface must first be coated with a water-soluble black paint, a process which is not well accepted in medical practice. In addition, time has to be allowed for evaporation of solvents.

(e) In order to maximize the intensity of the colors observed, the cholesteric liquid crystal solution should be orientated in the plane texture by mechanical disturbance to convert the focal-conic texture to the plane texture as reported by Gray (1962) and Adams (1969).

(f) It is not possible to obtain a perfectly uniform film.

(2) Importance of early breast cancer detection

It has been reported that successful treatment of breast cancer by mastectomy and radiotherapy depends significantly upon its stage of development at detection. If metastasis has not occurred beyond the axillary lymph nodes, the cancer may be completely ablated (Aartz, 1967).

Self-examination has been recommended. However, Gershon-Cohen, et al. (1970) stated that self-examination should not be decried, but that in advocating this approach, we are, in effect, making the woman responsible for discovering her own cancer. Women do discover their own cancer in 95% of the cases. Cancers are then found large and late. They average 3.5 cm in diameter and have metastasized in about 65% of the cases by the time surgery is performed. The five-year survival rate in these circumstances is about 45-50%. In contrast, when the physicians assume responsibility for finding evidence of breast cancer by periodic examination aided by such procedures as thermography, mammography or xeroradiography, lesions are found to average 1.0 cm in diameter and to be associated with metastases in only 30% of the cases. About 80% of women with the early, Stage 1 lesions will attain a survival rate of five years or longer. It was shown that breast cancer grows on a linear scale from the time of clinical recognition until terminal acceleration in the phases of

systematic dissemination (Delarue, 1969). Projection of the linear scale into the preclinical or occult stage suggests that carcinoma has been present for many years (see Figure 1). Thus, there must be some signs present when the carcinoma is in the preclinical stage such that recognition might be feasible by combined clinical and screening techniques. Delarue (1969) showed that cases recognized in mass screening programs have been identified 20 months earlier than would be possible by clinical palpation.

(3) The most widely accepted technique for early diagnosis of breast cancer is xeroradiography, a modified technique of X-ray mammography. The lesion is seen as an area of increased tissue density with spotty calcifications. Even though the method is very reliable in localizing cancerous lesions, it has little value in women of younger age due to high tissue density of younger breast. The major practical limitations of xeroradiography are its expense and the time required by radiologists and technicians. Some researchers are very cautious about the use of xeroradiography since it calls for the exposure of the breast tissues to X-ray irradiation, a factor which is believed to increase the frequence of occurrence of cancer if successive exposure is used (Evers, 1974).

(4) Thermography is a recent method aiding in the diagnosis and screening of breast cancer. Many researchers

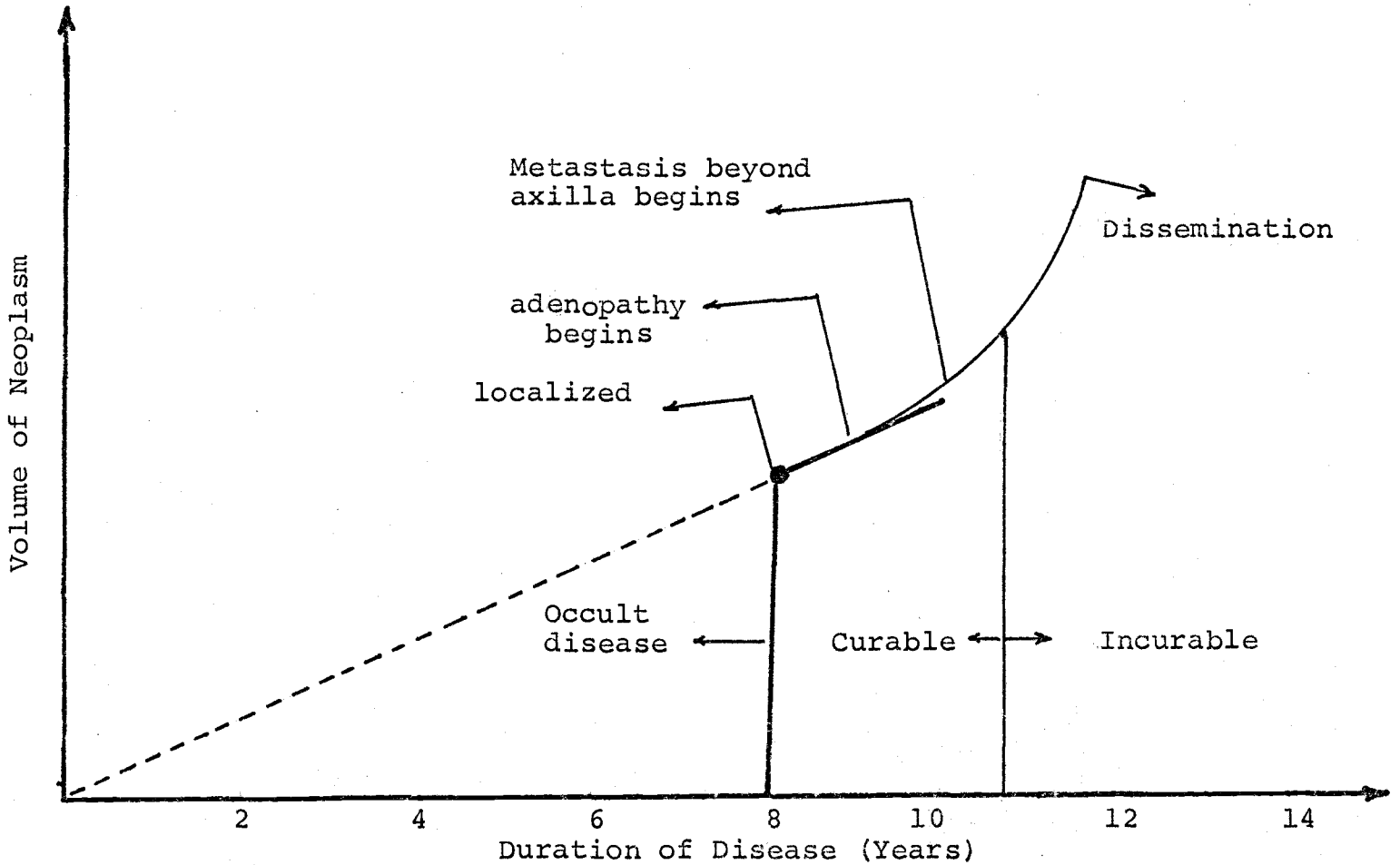

Figure 1. Natural history of untreated mammary carcinoma (After Delarue 1969)

have screened large numbers of women with and without suspicious breast characteristics using infrared (IR) thermography. The IR scanner picks up the emission of infrared radiation from the skin. The infrared emission is proportional to the fourth exponent of the absolute temperature. A thermal pattern is recorded as a permanent black and white or color scan. Thermography is given priority when other techniques show no evidence for carcinoma (Gershon-Cohen et al., 1970; 1971). Though IR thermography proved its effectiveness in breast cancer screening, its application for diagnosis and screening is limited due to unavailability as a result of high instrumentation costs.

(5) Some investigators in the field using IR thermography Isard (1974) showed their concern about the inconstancy of the IR thermographic diagnosis when read by different radiologists, a major factor in the accuracy of interpretation. This necessitated the development of a systematic interpretation scheme which applies for L.C. and IR thermography.

The inexpensive, simple and rapid liquid crystal thermographic technique developed in this study offers an answer to the unavailability of thermography in most hospitals and clinics. The development of the thin elastic film technology was undertaken to correct the lack of a reliable and easily available method for early detection of

breast cancer at the mass screening level. The development of the point interpretation scheme is designed to make L.C. and IR thermographic interpretation a science rather than an art, and by doing so freeing thermographic interpretation from its dependency on the experience of the reader.

The liquid crystal phenomenon

Commonly all matter is classified in three states; solid, liquid or gas with increasing molecular disorder occurring as one passes from the solid to the gaseous state. The liquid crystalline state is in many respects a fourth state of matter intermediate in molecular ordering between a crystalline solid and an ordinary liquid (Carroll, 1973). Hence, its more accurate name is the "mesomorphic" or intermediate state. However, the term "liquid crystals," first used by Lehmann (1889), has remained in use because it describes so directly the properties of this intermediate state: the mechanical properties of liquids combined with the optical properties of crystals.

Anisotropism of crystalline solids

Between all molecules attractive and repulsive forces exist. In a crystalline solid the attractive forces between the molecules are strong enough to hold them packed into a regular three dimensional geometrical array over

large volumes. Hence, crystals are said to show long range ordering of the molecules. One result of this ordering is that for certain crystals the physical properties, for example, the speed at which light travels through the crystal, will vary with the angle between the direction in which they are measured and the axes of the crystal.

Isotropism of liquids

In an ordinary liquid the cohesion between the molecules has been reduced to a point where they are free to move and so adopt a random arrangement. There is still some degree of ordering since each molecule can be considered to be surrounded by a spherical shell of its neighbors. However, this spherical arrangement only holds for the short distances between neighboring molecules. Over the longer distances the short range ordering breaks down to form a random arrangement. Therefore, the physical properties of a liquid are the same in whichever direction they are measured; that is, the liquid behaves isotropically.

Molecular arrangement in a liquid crystal

For most organic compounds the transition from the crystalline state to the isotropic liquid occurs rapidly once the cohesive forces holding the molecules in a fixed

arrangement in the crystal have been overcome. There is no stable intermediate level of molecular cohesion between the high level present in the crystal and the lower level present in the isotropic liquid as Carroll (1973) showed (Figure 2a).

But some organic compounds, because of their rod-like structure and the particular attractive forces between the molecules, can have a stable intermediate level of molecular cohesion (Figure 2b). It is this category which forms "liquid crystals." In the figures the horizontal axis can represent any factor (such as increasing temperature), which reduces molecular cohesion. Thus, in the liquid crystalline state, the cohesion between the molecules has been reduced enough, compared to the crystalline solid, to allow a rearrangement of the molecules. Some freedom of movement is possible (thus the liquid properties), but not enough to allow the complete random alignment of the rod-like molecules (thus the anisotropic crystalline behavior). Eventually, with a further increase of temperature, the cohesive forces in the liquid crystalline state (mesophase) are overcome and an ordinary isotropic liquid forms (Carroll, 1973).

Normally there are said to be three main subdivisions or mesophases of the liquid crystalline state: smectic, nematic and cholesteric.

In the smectic mesophase, the molecules are arranged in "raft-like" layers, with their axes parallel, either normal to the plane of the layer or tilted. The molecular packing within the layer can be either regular or random (Carroll, 1973).

In the nematic mesophase, the long axes of the molecules retain a parallel alignment, but, in contrast to the smectic, there is no separation into layers so that otherwise their positional arrangement is random. Thus, this type of liquid crystal is that much closer to an ordinary isotropic liquid than the smectic phase.

The cholesteric phase is a "twisted" form of the nematic phase. There is no layering and the positional arrangement of the molecules is random. But as shown in Figure 3, the direction in which the parallel molecules are aligned twists around as one passes through the cholesteric phase. This twisting forms a screw-like, helical arrangement of the molecules in the cholesteric phase, like the steps of a spiral staircase (Carroll, 1973). Because of this helical structure, a property very important to the optical behavior of the cholesteric phase is produced. That is, a periodicity corresponding to the pitch of the helix (the distance between areas where the molecules are pointing in the same direction) which is roughly equal to the wavelength of visible light.

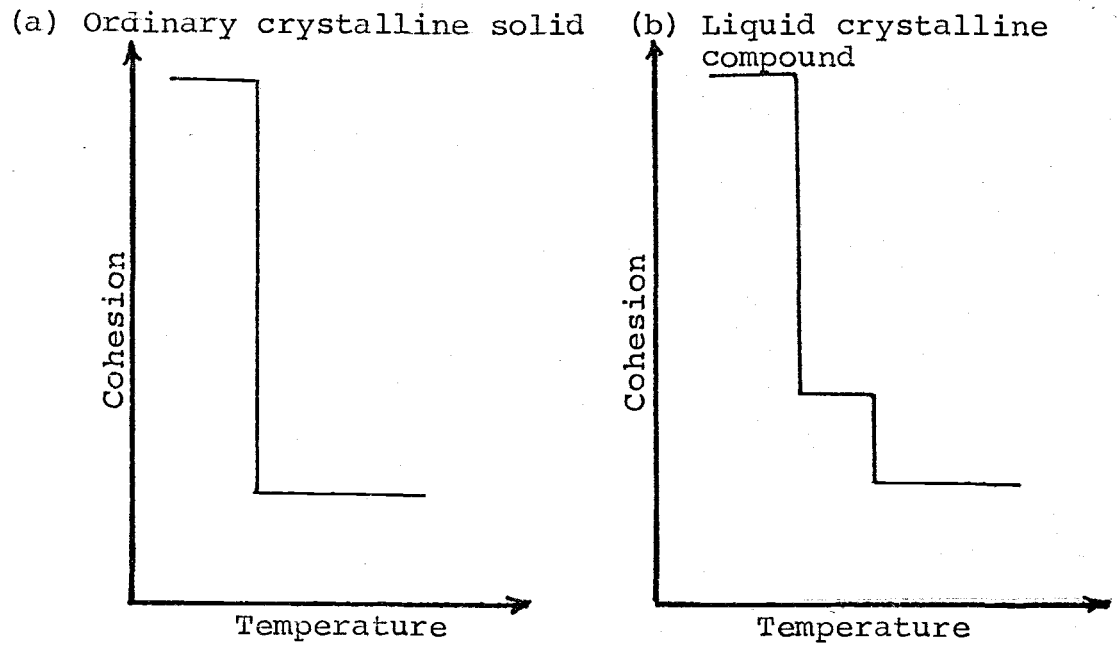

Figure 2. Levels of molecular cohesion

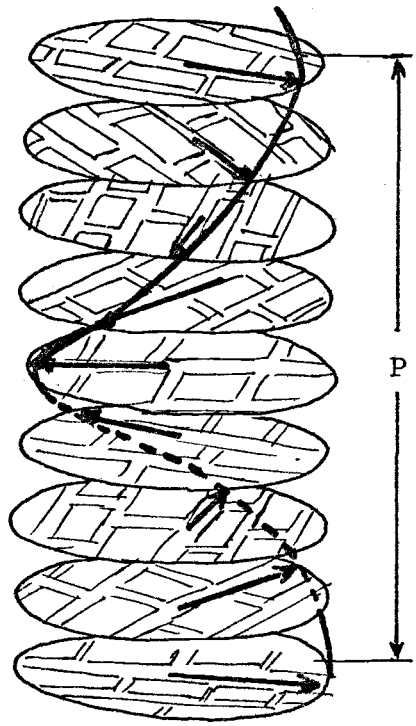

Figure 3. DeVries model of helical C.L.C. structure (after Fergason 1966a)

The most striking optical property of the cholesteric phase is that under the right conditions it displays a vivid color when illuminated with white light. The color depends on the pitch distance of the helix in the cholesteric liquid crystal (CLC) and this pitch can be easily altered. The distance between the molecular layers in the CLC which determines the final pitch distance depends on a balance of weak intermolecular attractions and repulsions. Once this balance is changed by a stimulus such as a temperature change, shear force, presence of other chemicals or an applied electrical or magnetic field, a color change will be seen. It is this direct, visible response to stimuli which gives CLC's their important versatility as detector systems. Accordingly the CLC can be regarded as a modulation system altering either the amplitude or the frequency of the light falling on it.

Optical properties of cholesteric liquid crystals

The combination of anisotropic melting coupled with the helical arrangement of the molecules in the cholesteric phase has a very pronounced effect on light passing into CLC. As De Vries (1951) and later workers have shown, all the optical properties of CLC: its characteristic appearances, ability to selectively reflect a narrow band of wavelengths, and polarization properties can be related

to the birefringence properties of the cholesteric phase (Carroll, 1973).

Birefringence of cholesteric phase and related properties

For an anisotropic material there are only certain directions at right angles to each other in which the vibrations of a light wave can be transmitted through the material. These "privileged" directions or planes have different orientations with respect to the molecular alignment of the anisotropic material and so light will be transmitted along them with different velocities. Because the index of refraction for a material is a function of the velocity at which light is transmitted through it, the result is that the material has different indices of refraction for light waves propagated along the different privileged directions. Thus, when a beam of unpolarized light encounters a birefringent substance, it is split into two polarized components whose transverse vibrations are at right angles to each other. The two components are refracted at different angles through the substance and emerge as parallel beams of polarized light (Fergason, 1964), see Figure 4. If the angle of incidence of the unpolarized beam is changed, one of the birefringent beams will change its angle in accord with the laws of normal refraction, and, therefore, is called the ordinary ray.

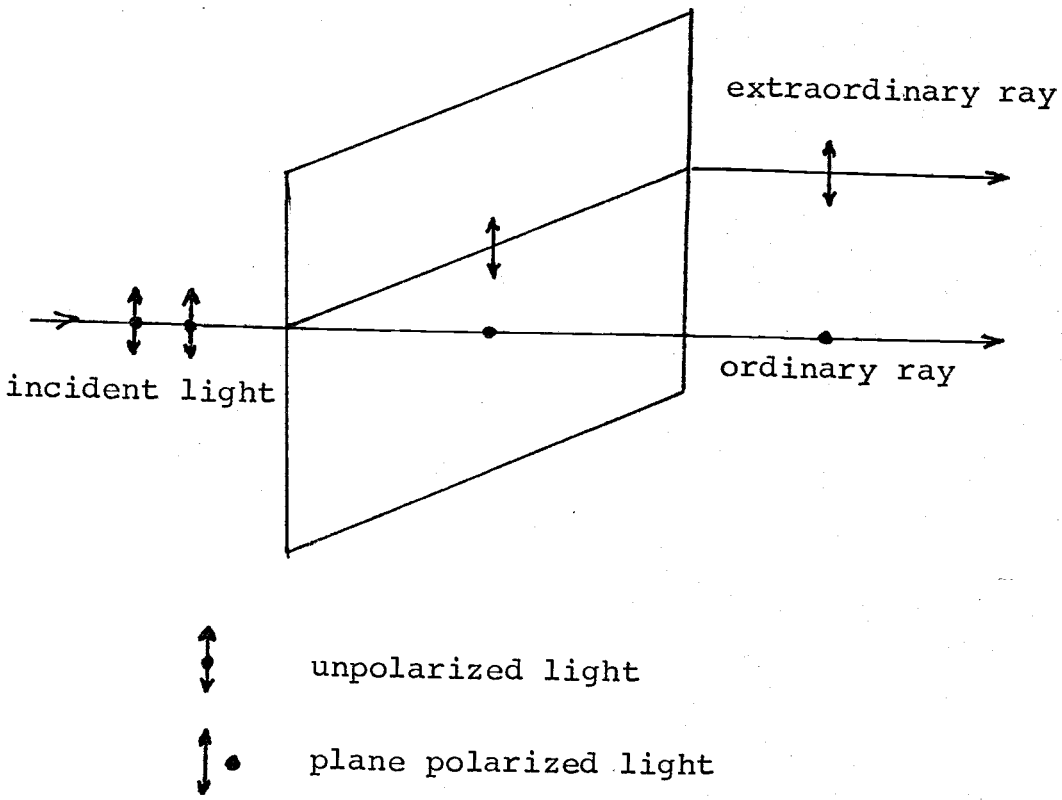

Figure 4. Birefringence (double refraction)

The other will not and this beam is called the extraordinary ray. If the velocity of the ordinary ray is less than the velocity of the extraordinary ray, i.e., if the refractive index n_o for the ordinary ray is greater than the refractive index n_e for the extraordinary wave, then the material is said to be optically negative. This is the case for the cholesteric mesophase.

Fergason (1966) derived a formula for the bandwidth of a CLC formulation which related it to the relative birefringence of the material:

$$2(n_o - n_e) / (n_o + n_e) = \text{(Bandwidth)} / \text{(wavelength of maximum reflectance)}$$

where n_o is the refractive index for the ordinary ray and n_e is the refractive index for the extraordinary ray.

Reflection of light in the CLC phase

Because the reflection of incident light occurs from many different molecular layers with the CLC, the colors seen are analogous to the colors observed when light is scattered back from a multi-layer interference filter. The helix structure present in the cholesteric mesophase causes the areas in which the parallel aligned molecules point in the same direction to be separated by a regular, periodic distance equal to the pitch of the helix (Carroll, 1973). This periodicity means that a CLC can act as a

three dimensional diffraction grating for light of visible wavelength and, therefore, shows similar behavior to the Bragg scattering effects observed in crystalline solids with their greatly smaller periodicities when short wavelength X-rays are passed through them as Carroll (1973) showed.

For a CLC the distance between reflecting planes is taken as half the pitch distance since molecules aligned in one direction and molecules aligned in the opposite direction have the same reflecting properties. Carroll (1973) has shown, by considering the path length for light reflected from the different Bragg reflecting planes of the helix, that maximum reflection will occur when

$$m\lambda = 2 d \sin(B) \qquad (1)$$

where m = 1,2,3,4, etc.

and λ = wavelength of incident light

d = separation between reflecting planes

B = Bragg angle of incident light

For a CLC, only first order scattering is observed under normal conditions (m = 1). Equation 1 says that the light reflected by the CLC at an angle equal to the Bragg angle of incidence B will be of wavelength

$$\lambda = N.P.\sin(B)$$

Where N = average value of index of refraction for the CLC

P = pitch of helix (equal to 2X distance between reflecting planes).

Fergason (1966) developed the relationship between the wavelength (color) seen and the angle of illumination and viewing of the CLC material:

$\lambda = \lambda_{max}$ (cos ($\sin^{-1}$ ((n_1/n_2) sin I) + $\sin^{-1}$ ((n_1/n_2) sin R)))

Where λ_{max} = wavelength of reflected light for illumination and viewing normal to the surface

λ = wavelength of reflected light

I = angle of incidence

R = angle of reflection

n_1= refractive index of viewing medium

n_2= refractive index of CLC

For viewing in air n_1 is taken as 1.0, n_2 as 1.5 (Figures 5 and 6).

Polarization effects on CLC phase

The cholesteric mesophase affects both linearly and circularly polarized light:

(a) Linearly polarized light

The cholesteric phase is strongly optically active and will rotate the plane of linearly polarized light by several thousands of degrees per mm.

(b) Circularly polarized light

The cholesteric phase is circularly dichroic for certain wavelengths of light. This means that the CLC will

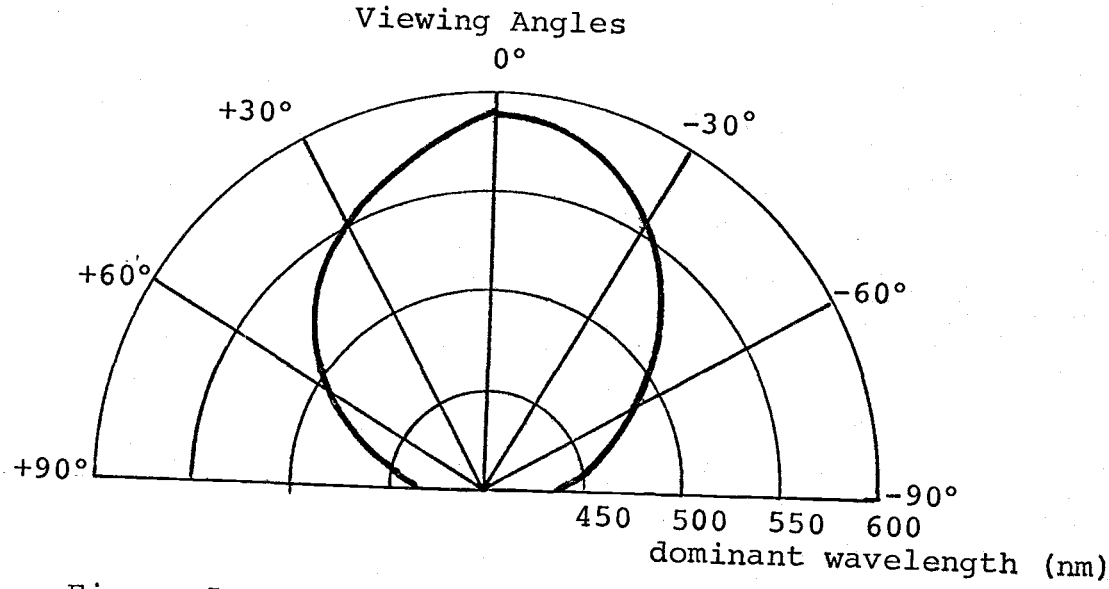

Figure 5. Wavelength of maximum scattering with normal illumination and varying viewing angles.

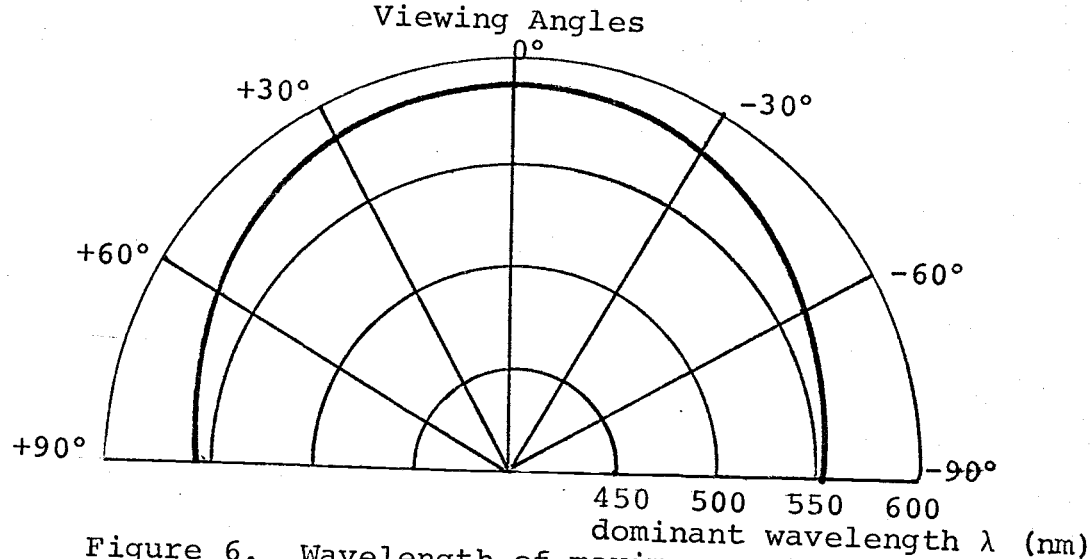

Figure 6. Wavelength of maximum scattering with light source and viewing angle moved together (after Fergason 1966).

totally reflect, for example, right hand circularly polarized light, but transmit left hand circularly polarized light.

It is those properties that gives the cholesteric phase its characteristic iridescent color in response to temperature stimuli when illuminated by white light.

II. LITERATURE REVIEW

History of thermography

Less than 200 years ago the existence of the infrared portion of the electromagnetic spectrum was not suspected. It was not until the discovery by Sir William Herschel in 1800 that the first thermogram was developed. He observed the heat producing capability of invisible infrared radiation and postulated that these waves had the peculiar power of heating objects in their path (Gershon-Cohen, 1964).

It is known now that these waves are emitted from any surface above absolute zero as a spectrum of waves whose distribution and amount varies with absolute temperatures and the nature of the surface (Lloyd-Williams, 1964).

It can be shown that every object in nature emits radiant energy as a function of its absolute temperature. The basic relationship derived by Max Planck in 1901 shows that the energy radiated by a black body can be expressed as

$$W_\lambda = C_1\lambda^{-5} \left(e^{\frac{C_2}{\lambda T - 1}}\right)^{-1} \qquad (1)$$

W_λ is the spectral radiant emittance, C_1 and C_2 are constants and T is absolute temperature (degrees Kelvin).

The wavelength of peak energy emission is obtained by differentiating equation 1.

$$\lambda_{max.} = \frac{2897}{T} \quad \text{(Wien's displacement law)} \qquad (2)$$

By integrating Planck's equation, we get the total power radiated over all wavelengths at a temperature T

$$W = \sigma T^4 \quad \text{(Stefan-Boltzman law)} \qquad (3)$$

where σ is the Stefan-Boltzman constant.

For a non-perfect radiator such as human skin, an efficiency factor ε is introduced in equation (3) giving $W = \varepsilon\sigma T^4$. It is this relationship which permits the translation of infrared radiation sensed by infrared detectors to the corresponding temperature of the radiating body (Figure 7).

In the past 40 years, many infrared sensitive devices have been developed for military, industrial and scientific needs. Infrared thermography has been applied to clinical medicine in the last 18 years. Now it is the most widely accepted thermographic technique.

The basis for liquid crystal thermography were introduced by Fergason (1964, 1965a, 1965b, 1968), who was the first to recognize the unusual color-temperature sensitivity of cholesteric liquid crystals. Crissey et al. (1964, 1965) and Selawry et al. (1966) further explored the

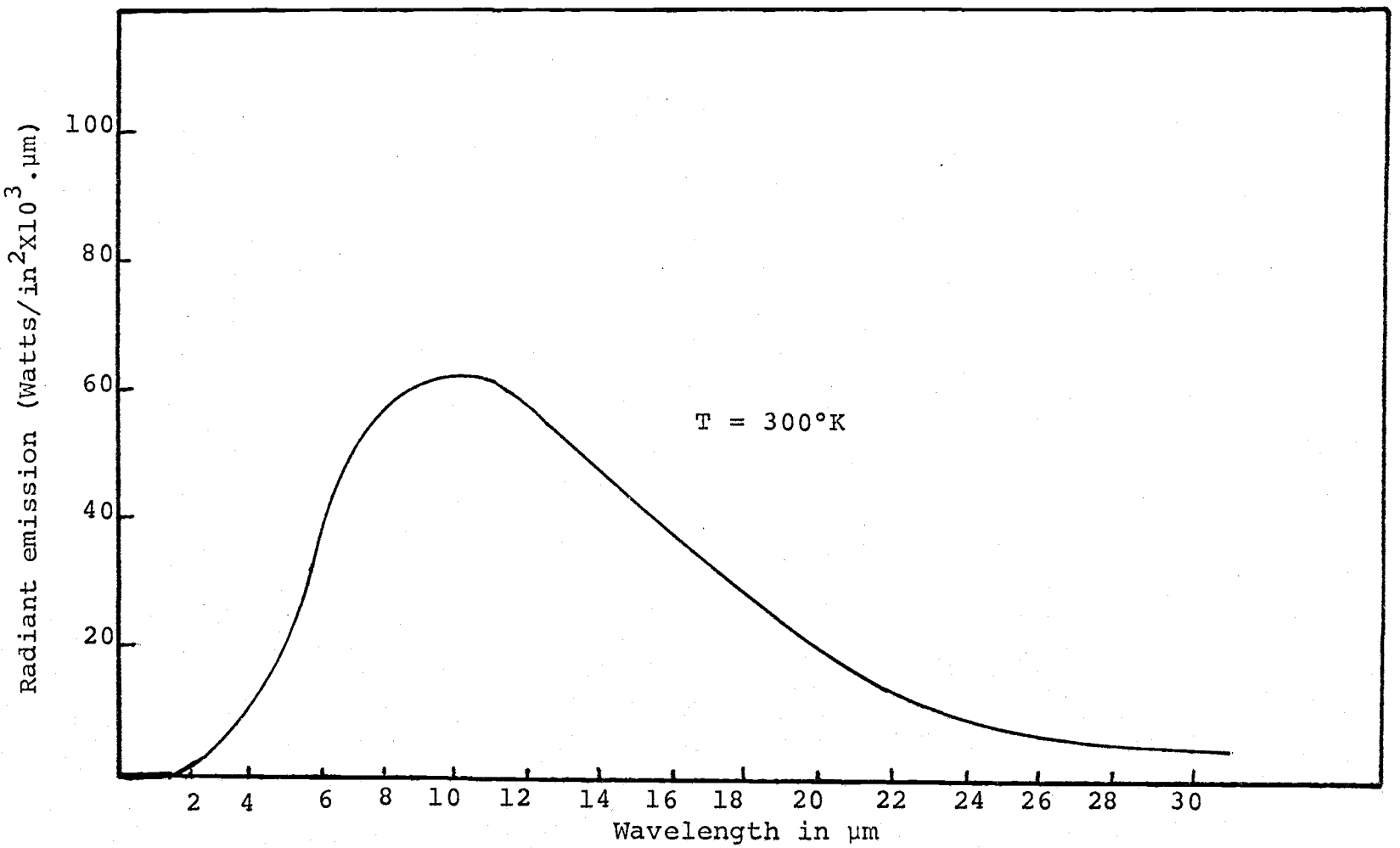

Figure 7. Infrared emission from a black body at 300 degrees Kelvin

potential of liquid crystal thermography.

Thermography in breast cancer detection

(a) Infrared Thermography

Many researchers have examined a large number of women for breast cancer over the past 10 years using infrared thermography. Lloyd-Williams (1964) and Lloyd-Williams et al. (1960, 1961) showed, using an infrared thermopile which measures the skin temperature of a small area as a function of the infrared emission without contacting the skin, that skin temperature over 95% of the histologically proven breast cancers were at least 1°C greater than the temperature of the contralateral area of the unaffected breast. He also found that more advance carcinomas were warmer.

Brasfield et al. (1964) used an improved infrared scanning thermograph to examine patients with one breast removed by radical mastectomy. They found that the area of increased skin temperature over the malignant tumor was larger in diameter than the tumor and that the areolar temperature of the affected side was usually warm.

Gershon-Cohen et al. (1964, 1965) examined 750 women with a scanning infrared thermograph. One hundred fifty biopsies of the breast were done after the thermographic examination. The skin temperature over 40

histologically proven carcinomas was elevated by 1 to 7°C while the temperature over benign lesions was never greater than 1°C over the contralateral area of the unaffected breast. This observation set the criteria for thermographic interpretation of malignant lesions. According to this study, all thermograms demonstrating a unilateral area more than 1°C warmer than the opposite side were considered suspicious. This criteria is found to be insufficient since too many normal patients had suspicious thermograms resulting in a high false positive rate.

Swearingen (1965) examined 100 patients with suspicious breast characteristics using both thermography and mammography. He reported that the use of both methods eliminated many false negatives (false interpretation of malignant lesions) and also false positives (false alarm on benign lesions).

Harris et al. (1966) examined 150 women by IR thermography and IR photography, a technique which gives a picture of the superficial veins. The comparison of the IR thermogram to the IR photograph showed that spots, patches, and lines of elevated temperatures followed the venous drainage pattern. These observations support the findings of Massapust and Gardner (1953), who used IR photography and mammography to study the venous patterns of cancerous breasts. They reported that the venous pattern was

disrupted and often associated with venous engorgement when associated with carcinoma.

The improved spatial resolution of the latest available IR scanners has shown clearly the importance of the superficial venous drainage pattern in the thermographic interpretation (Dodd et al., 1969b). Investigators have been considering the overall thermal and associated vascular pattern when looking for areas of increased local metabolism or inflammation (Isard et al., 1968; Dodd et al., 1969a; Draper and Jones, 1969; Forrest et al., 1969; Jones, 1969).

Isard et al. (1969) reported that malignancies are often difficult to interpret by IR thermography as cancerous breasts do not always display hyper-vascularity and increased temperature while some benign lesions show the same thermal signs as malignancies. Dodd et al. (1969a) reported that the most difficult malignant lesions to detect by thermography have been large, slow growing tumors and small intraductal tumors. The latter do not pose a problem as they are evident clinically. However, the former cannot be detected unless a thermograph with better optical resolution is used. Dodd et al. (1969a); Shaw (1969) reported that the strongest thermographic evidence is demonstrated by small duct infiltrating carcinoma.

Draper and Jones (1969) and Lapayowker et al. (1971) examined subjects with no clinical abnormalities by IR thermography to classify the normal breast thermal patterns. They distinguished four distinct thermal patterns. They noticed that false negative and false positive interpretations occur predominantly in the normally asymetric pattern.

Several investigators (Gershon-Cohen, 1964; Isard et al., 1968; Isard et al., 1969; Draper and Jones, 1969) studied the effects of pregnancy, the menstrual cycle and contraceptives on thermographic patterns. They all concluded that the slight changes from day to day during the menstrual cycle should be of no significance in the detection of breast cancer. They noted that oral contraceptives and pregnancy caused an increased overall vascularity and, therefore, could make thermographic interpretation more difficult.

In an attempt to determine the sensitivity of infrared thermography in detecting breast cancer before and after it is clinically evident, Aartz (1967, 1969); Freudlich (1968); Dodd et al. (1969a); Isard et al. (1969); Shaw (1969); Wallace et al. (1965) showed that thermographic interpretation gives too many false positives and that combined thermography and mammography decreased the percentage of the false positives and false negatives.

However, most investigators mentioned that the high percentage of false positive was necessary to detect malignancies in the occult stage. Hoffman (1967) recorded a large percentage of false positives; yet he detected four carcinomas which otherwise would not have been detected for another eight years.

Many researchers are not satisfied with the past performance of infrared thermography in breast cancer screening (Hitchcock et al., 1968; Lilienfield et al., 1969; Farrow, 1969). They feel that the rate of false positives is too high because the infrared thermographs available to clinicians lack the optical resolution required to differentiate between benign and malignant lesions. In order to improve the results of thermographic breast examinations, a new thermograph for clinical use is being developed. The new thermograph gives high spatial resolution and an excellent morphological view of the subject. These qualities make easier recognition and classification of breast thermal patterns and are expected to decrease the number of false positives (Wallace, 1965; Dodd et al., 1969b). Information concerning the heat transfer process has been obtained and the new IR scanner has demonstrated more accurately that the normal breast thermal patterns are related to varying process of superficial vein distribution and the heat transfer process drainage heat convection (Dodd et al., 1969b).

The most recent improvements of IR thermography have made it the most desirable technique for mass-screening of breast cancer. Thermography is given priority as it often gives evidence of carcinoma when other techniques show no evidence of cancer (Gershon-Cohen et al., 1970; Gershon-Cohen, 1971).

Davey et al. (1970) screened 1768 women by physical examination, mammography and IR thermography. They reported 15 patients with carcinoma of the breast, a rate of 8.5 cancers per 1000 women.

Isard et al. (1972) examined 10,000 women; 56% of these women were symptomatic and 44% were asymptomatic cases. They reported 36% positive thermograms in the symptomatic group and 23% in the asymptomatic group. According to biopsy reports, they found the ratio of malignant to benign to be 1:2.3 in the symptomatic group and 1:5.3 in the asymptomatic group. They recommended the use of IR thermography as a preliminary screening of asymptomatic women to focus attention upon those who should be examined more intensively because of greater risk of breast cancer.

Isard et al. (1974) examined 5662 women using IR thermography, mammography and physical examination. He reported that accuracy was improved to 92% using all three modalities for breast cancer detection.

The full potential of breast thermography is yet to be realized. While thermography does not diagnose cancer, it can serve as a signal for abnormality. Moreover, its total safety, lack of irradiation, and minimal expense make it a very attractive modality (Isard et al., 1974).

Though IR thermography has been successful in breast cancer detection, its application is limited due to high instrument costs.

(b) Liquid crystal thermography using spray on techniques

Davison et al. (1972) examined 105 women with abnormal breast characteristics using liquid crystal thermography. The breast surface was painted black and the liquid crystal material was sprayed over the black surface. They reported that palpable malignancies with L.C. thermography had a true positive rate of 82.3%. The false positive rate was 13.6%, and one of 17 histologically proven malignancies gave no thermographic signs of malignancy.

Liquid crystal thermograms of 197 apparently healthy women with no breast abnormalities were classified according to pattern type. Six distinct thermal patterns were characterized with three subgroups distinguishable in each of 3 vascular pattern groups. The L.C. pattern type was studied as a function of age, past pregnancies, previous

lactation, use or non-use of oral contraceptives, and breast size (Davison et al., 1972).

The method proved to be reliable, accurate, and inexpensive. However, the thermogram application procedure was cumbersome and somewhat messy.

(c) Plate thermography using encapsulated liquid crystal sheets

The National Cash Register Company (NCR) introduced a process to form encapsulated liquid crystal (ELC) sheets. The principle of micro-encapsulating cholesteric liquid crystals is to first emulsify the CLC to micro droplets in an aqueous solution of polymeric material. Then, by addition of another agent, the water soluble polymer is converted to a water insoluble form which, as it comes out of solution, wraps itself around the CLC droplets to encapsulate them.

The ELC sheet has proven to be of little use in medical application due to the rigidity of the sheet and its thickness. Also, the color intensity of the scattered light is low. Because the cholesteric liquid crystal material is in the form of discrete capsules, the resolution (fineness of detail observable) of the ELC's is low when used to map thermal patterns (Carroll, 1973).

Some investigators overseas have used the ELC sheets in a method called plate thermography. Introduced by Tricoire (1970), the method consists of mounting the ELC sheets on a plate which is compressed on the breast surface. Tricoire et al. (1970) examined 300 patients with plate thermography. They reported the diagnosis was true 291 times.

Bothmann et al. (1974) examined 1919 patients using plate thermography. They reported that the chance of missing a carcinoma with L.C. plate thermography is between 0.3 and 3%.

Fochem et al. (1974) and Gautherie et al. (1974) reported on the use of plate thermography and its limitations as a mass screening technique. A major disadvantage that limits the use of plate thermography is its inadequacy to conform to surfaces which require the compression of the breast surface in order to accomplish a 2-dimensional contact between the breast surface and the sheet, a factor that affects thermographic findings. Another disadvantage of plate L.C. thermography is that the examination of each breast is done separately, which results in more difficulty in interpretation (Fochem et al., 1974).

Xeroradiography

Xeroradiography is the science of recording radiographic images electronically on a selenium plate. The principal element in xeroradiobraphy is a re-usable photoreceptor plate measuring approximately 24 x 36 cm. It consists of a thin photoconductive layer of selenium adhering to an aluminum backing. The selenium semi-conductor is given a uniform positive charge by an ionizing device consisting of a number of electrodes and a grid called a scorotron.

When the selenium plate is exposed to light or to radiation (X-rays), the electrical conductivity of the semi-conductor layer increases and allows the positive charge on the plate to discharge. Since the discharge of the plate varies according to the number of photons reaching it, an electric charge pattern which corresponds to the density of the object being X-rayed is left on the plate. This resultant charge pattern is the latent image (Brebner, 1974).

A developer consisting of a blue powder called the toner is then aspirated on to the plate to which it is attracted by the charge pattern in the form of a diffuse powder cloud. The image thus formed is made permanent by transferring and fixing it by heat on a special paper. This is the xerogram (XR). An image of various shades of

blue is produced. The dense regions of the breast being examined will strongly absorb the X-rays. This will allow less discharge from the plate and will lead to a stronger residual charge on the plate. More toner will be attracted to it and the area on the XR will be dark blue in color. Thin regions of the subject will allow the X-rays to pass through almost unaffected. These cause considerable discharge of the plate and little residual charge. Only a few toner particles will be attracted, and the area will be light blue in color (Wolfe, 1974).

Recently, Malone et al. (1975) reported 185 breast cancers demonstrated by xeroradiography in a study on 6238 patients. They reported that 62 of those cancers were occult.

Principle of surface temperature mapping in tumor detection

Surface skin temperature measurements over malignant tumors were first made by Lawson (1956, 1957) who believed that a malignant lesion should exhibit a higher temperature than surrounding tissues because it is characterized by an increased local metabolism and supported by greater lymphatic and blood vascularity. Lawson demonstrated with a Baird evapograph and other temperature measuring devices that the skin over a malignant breast lesion and areola of the affected breast averaged a 1.2°C

(2.3°F) temperature increase over the contralateral area of the unaffected breast. Later (Lawson, 1957) tested several IR scanning thermographs and found that they lacked the sensitivity and optical resolution required for thermographic breast examination.

Since then several investigators studied the effect of transmission on temperature measurements of human skin in an attempt to develop a relationship between the actual temperature of a tumor and the surface temperature (Watmough, 1969).

The basic principles of the theory of transmission by partially transparent bodies were developed by McMahon (1950). Steketee (1973) showed that the same theory can be applied to a slab of partially transparent skin (Figure 8). When the spectral emissive power density is $j(\lambda,T)$ radiation generated in a unit area layer with thickness x is $j(\lambda,T)dx$. For unit solid angle the emitted radiation is

$$\frac{j(\lambda,T)dx}{4\pi} \tag{1}$$

For a very small solid angle dw, containing radiation traveling essentially by normal to the surface of the slab, the spectral radiant emittance is:

$$1/4\pi j(\lambda,T)\ dx\ dw$$

When $a(x)$ is the spectral absorption coefficient, then the radiation arriving at the surface from the layer lying on a

depth x below the surface of the slab is given by

$$\frac{dw}{4\pi} j(\lambda,T)\exp(-a(\lambda)x)dx \tag{2}$$

Suppose that T is uniform within the slab, equation (2) can be integrated between x = 0 and x = ∞ giving

$$\frac{j(\lambda,T)dw}{4\pi a(\lambda)}$$

If the spectral reflectivity of the surface is $\rho(\lambda)$, the radiation which penetrates the surface and escape is

$$(1-\rho(\lambda))\ \frac{j(\lambda,T)dw}{4\pi a(\lambda)} \tag{3}$$

Equation (3) must be equal to

$$(1-\rho(\lambda))N(\lambda,T)dw \tag{4}$$

in which $N(\lambda,T)$ is the spectral radiance of a black body and $1 - \rho(\lambda)$ is the spectral emissivity of a non-transparent body.

Combining equations (3) and (4) yields

$$j(\lambda,T) = 4\pi a(\lambda)N(\lambda,T). \tag{5}$$

Substitution of equation (5) in equation (2) leads to

$$a(\lambda)dwN(\lambda,T)\exp(-a(\lambda)x)dx \tag{6}$$

Steketee (1973) modified the theory of McMahon, assuming a thermal gradient across the epidermis, in which case $T = T(x)$ and $N(\lambda,T)$ also depends on x. The total radiation penetrating the surface is given by

$$a(\lambda)(1 - \rho(\lambda))dw \int_0^\infty N(\lambda,T)\exp(-a(\lambda)x)dx \tag{7}$$

Watmough (1969) has shown that over narrow temperature ranges for $N(\lambda,T)$ the Dreyfus rule may be used

$$N(\lambda,T) = K(\lambda)T^n \tag{8}$$

where $K(\lambda)$ is a constant for a particular wavelength and where $n = hc/\lambda KT$.

According to Hensel (1952) it is justifiable to assume that the temperature across the epidermis and underlying tissue varies as shown in Figure 9. Thus we can write

$$T = T_s(1 + \beta x)$$

or

$$T^n \simeq T_s{}^n(1 + n\beta x) \text{ where } x \leq d \tag{9}$$

and

$$T = T_c \text{ when } x>d \tag{10}$$

Using equations (8), (9) and (10), equation (7) can be integrated by parts leading to

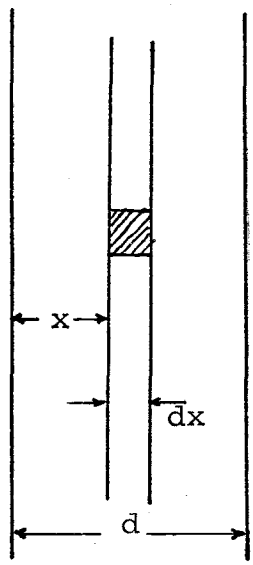

Figure 8. A slab of partially transparent skin

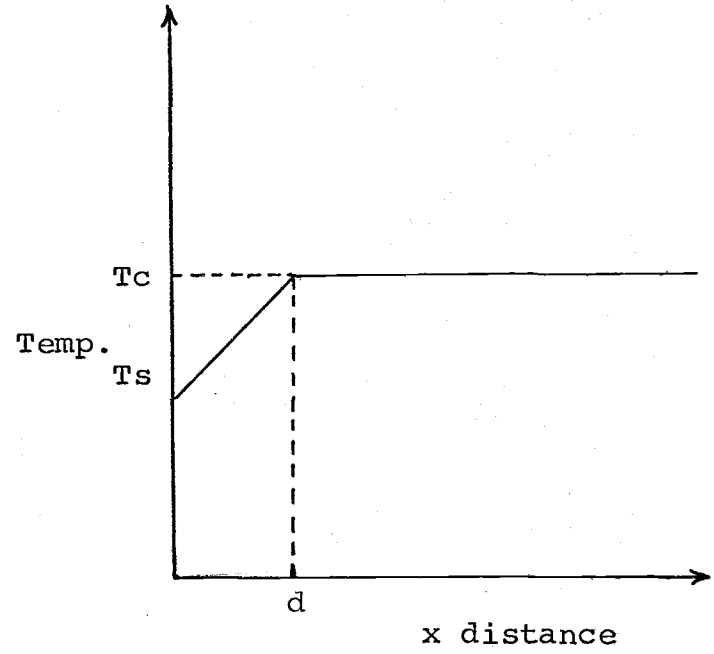

Figure 9. The thermal gradient across the epidermis

$$(1 - \rho(\lambda))K(\lambda)T_s^{n}(1 + \frac{n\beta}{a(\lambda)}\ [1 - \exp(-a(\lambda)d)])dw \qquad (11)$$

When T_{eff} is the effective temperature as measured by the radiometer equation (11) is also equal to:

$$(1 - \rho(\lambda))K(\lambda)T_{eff}^{n}dw$$

Thus we get:

$$T_{eff}^{n} = T_s^{n}(1 + \frac{n\beta}{a(\lambda)}[1 - \exp(-a(\lambda)d)] \qquad (12)$$

Equation (12) shows that if the skin temperature is determined by measurement of the infrared radiation, this effective temperature may be somewhat higher than the true surface temperature (Steketee, 1973).

The thermal gradient according to Hensel (1952) is $0.2\text{-}0.5 Kmm^{-1}$. Hence, the value of β in equation (9) is given by

$$\frac{dT}{dx} = \beta T_s = 0.5\ Kmm^{-1}$$

Putting $T_s = 300°K$ and $T_c = 310°K$, we have

$$\beta = 1.7 \times 10^{-3} mm^{-1} \quad \text{and} \quad d = 20\ mm$$

Hardy (1956) showed that for the most penetrating radiation with a wavelength $\lambda = 1.2$ micrometer (μm) the absorption coefficient is about $1.0\ mm^{-1}$. This means $\exp(-a(x)d)$ is very small, so that equation (12) can be written as

$$T_{eff}^{n} \simeq T_s^{n}\left(\frac{a(\lambda) + n\beta}{a(\lambda)}\right) \qquad (13)$$

Taking the nth root of equation (13), we find

$$T_{eff} \simeq T_s\left(1 + \frac{\beta}{a(\lambda)}\right) \qquad (14)$$

Substituting

$$a = 1.0\ mm^{-1}\ ,\quad \beta = 1.7 \times 10^{-3}\ ,\quad T_s = 300°K$$

equation (14) leads to

$$T_{eff} = 300.5°K \text{ when } \lambda = 1.2\ \mu m$$

Steketee (1973) showed that for other wavelengths a (λ) has a higher values, so that we may conclude

$$300.0°K < T_{eff} \leq 300.5°K$$

Comparing equations (14) and (9) we can conclude that T has the same value as the temperature of a point lying at a depth x = 1/a. When $a = 1.0mm^{-1}$ this means x = 1mm, and the temperature at this depth is 0.5 K higher than T_s.

Under clinical conditions the values of β and $a(\lambda)$ will differ from those determined by Hensel (1952) and Hardy et al. (1956). Further investigations have to be done to account for the variation in thermal properties of the different components of the breast structure and for their irregular configuration.

III. EXPERIMENTAL PROCEDURE

The elastic film is composed of five layers:

(a) The substrate

(b) Release agent layer

(c) Opaque polyvinyl butyral layer

(d) Liquid crystal dispersion layer

(e) Polyvinyl alcohol protective layer

Fabrication criteria and properties of film layers

Each layer plays an important role in the final film properties and therefore, each will be described in detail. In the following analysis, all compositions are given as percentage by weight of dry components.

(a) The substrate is used for film deposition. It is to be disposed at the time of use. The main criteria in the choice of the substrate is that it should not be affected by isopropyl alcohol and hydrocarbon solvents used in casting the film.

(b) The release agent layer serves two purposes:

(1) It allows the pulling of the final film easily from the substrate at the time of use.

(2) It serves as an adherent agent to insure perfect contact when applied on the skin and therefore, should be water soluble.

(c) The opaque polyvinyl butyral layer serves two purposes:

(1) It makes the visual observation of the colors possible when the L.C. film is subject to thermal energy.

(2) It serves as a U.V. absorber to protect the next L.C. layer.

The mechanical properties of this layer affect significantly the final properties of the film.

(d) The liquid crystal dispersion layer is responsible for the color-temperature play of the film and, it therefore, will be studied in detail.

The cholesterol esters, carbonates and halides are not usually used by themselves in cholesteric liquid crystal applications because the temperature range for the cholesteric mesophase or other properties of the pure compound often does not fit the requirements of the application. However, by mixing cholesterol derivatives, the properties of the eventual cholesteric liquid crystal system can be tailored to meet a wide range of requirements.
Narrow low temperature range:

The following are agents which lower the color-play temperatures without broadening the range:

(1) Low temperature mesomorphic compounds such as cholesteryl oleyl carbonate, cholesteryl oleate.

(2) Lipid soluble compounds. Fergason (1966) found that addition of fatty acids, esters (such as methyl oleate) and alcohols to a cholesteric liquid crystal formulation depressed the temperature for color play without appreciably broadening the range of play.

Broader low temperature color range:

Table 1 shows that the addition of cholesteryl lower alkyl esters both broadens and depresses the color play temperature. The broadening effect would appear to be inversely proportional to alkyl chain length because cholesteryl acetate has a greater effect than cholesteryl butyrate.

TABLE 1.--Effect of adding cholesteryl alkyl esters to cholesteryl nonanoate

Formulation (wt. %)	Red (625 nm) scattering temp. °C	Blue scattering temp. °C (475 nm)
100 CN	74.6	75.9
80 CN:20 cholesteryl butyrate	53	57
80 CN:20 cholesteryl proponate	45	54
80 CN:20 cholesteryl acetate	20 (590 nm)	45

Source: Fergason 1966. CN: cholesteryl nonanoate.

Cholesteryl benzoate (CBz) was used in this study as a broadening agent.

Narrow high temperature color range:

Cholesteryl nonanoate (CN) is commonly used to narrow and raise the temperature range for color play in a cholesteric liquid crystal formulation. Other long chain alkyl esters such as cholesteryl myristate are usable. Woodmansee (Boeing U.S. patent 3,441,513) disclosed the use of cholesteryl paranitrobenzoate in concentrations of 1-4 wt % in cholesteric liquid crystal formulations to narrow the temperature range for red-blue color play to about .4°C.

Cholesteryl halydes as temperature desensitizing agents:

The effect of adding cholesteryl chloride (CC) in increasing concentrations to CN can be seen from Figure 10. For a mixture of 75 wt % CN: 25 wt % CC the color shown is nearly constant for a temperature range of approximately 50°C. Fergason (1966) mentioned that other compounds which have a similar effect are cholesterol, cholesteryl bromide and, to a lesser degree, cholesteryl chloroformate.

Formulations showing thermal hysterisis:

In most temperature indicating cholesteric liquid crystals formulations, heating cooling hysterisis can occur (Dixon and Scala 1970). Table 2.

In the final analysis, the three component system formulation of cholesteryl oleyl carbonate (OCC),

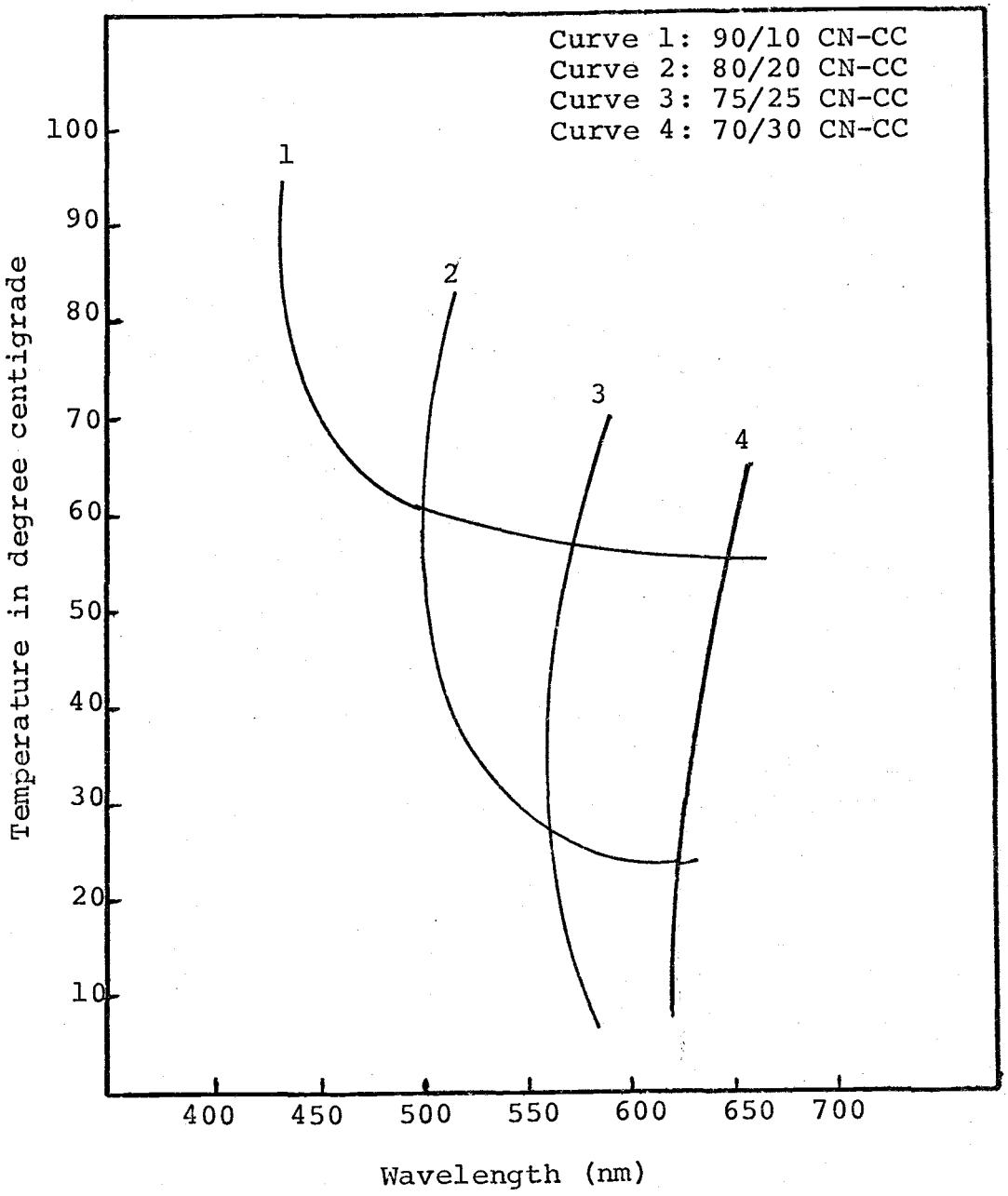

Figure 10. Effect of adding cholesteryl chloride on scattering wavelengths

After Ex DT 2227720
Hoffman-La-Roche Inc.

TABLE 2.--Temperature against scattered wavelength for materials exhibiting thermal hysteresis

Wavelength (nm)	Temp. (Heating) °C	Temp. (Cooling) °C
420	152	152
500	115	110
600	110	88
700	105	75
780	60	60

Source: Dixon & Scala 1970.

cholesteryl nonanoate (CN) and cholesteryl benzoate (CBz) proved to be the most useful for biomedical applications called for in this study. Therefore a thorough investigation was made on the properties of different formulations of this system and calibration curves were obtained in order to fabricate L.C. dispersion films that cover the total temperature range of interest (Figure 12).

The color-temperature response of each liquid crystal compound was obtained using the following photometric method: A sample material was applied to a black film which was placed on an aluminum temperature block. The block temperature is increased slowly by a thermal electric unit and measured by a thermistor which drives the X-axis of an X-Y recorder. The cholesteric phase is illuminated by monochromatic light and its temperature increases so that, as the wavelength of maximal scattering passes through the wavelength of the light source, the

intensity of the light increases to a maximum and then decreases. The intensity of scattered light is measured by a photoelectric detector which drives the y-axis of an X-Y recorder (Figure 11). The wavelength of the light source is altered to give a series of scattering peaks at corresponding temperatures. The calibration curves for a 29-32°C liquid crystal material are shown in Figure 12. In this study, the liquid crystal range is defined as the range between the temperature of scattering peak at 625 nm and the temperature of scattering peak at 475 nm.

The color-temperature characteristics of different compositions of the OCC-CN-CBz system were obtained (Figures 13, 14, 15, 16, 17). In the practical application, once a color-temperature range was specified, it was desired to choose the composition which would give the color response in this temperature range. Figures 13-17 would predict (given any color-temperature range in the medical temperature ranges) the corresponding exact percentages of OCC-CN-CBz.

(e) The polyvinyl alcohol protective layer serves as an added protection to the L.C. dispersion layer against the major degradation factors of liquid crystal materials such as oxygen, U.V. radiation, dust and fibre particles.

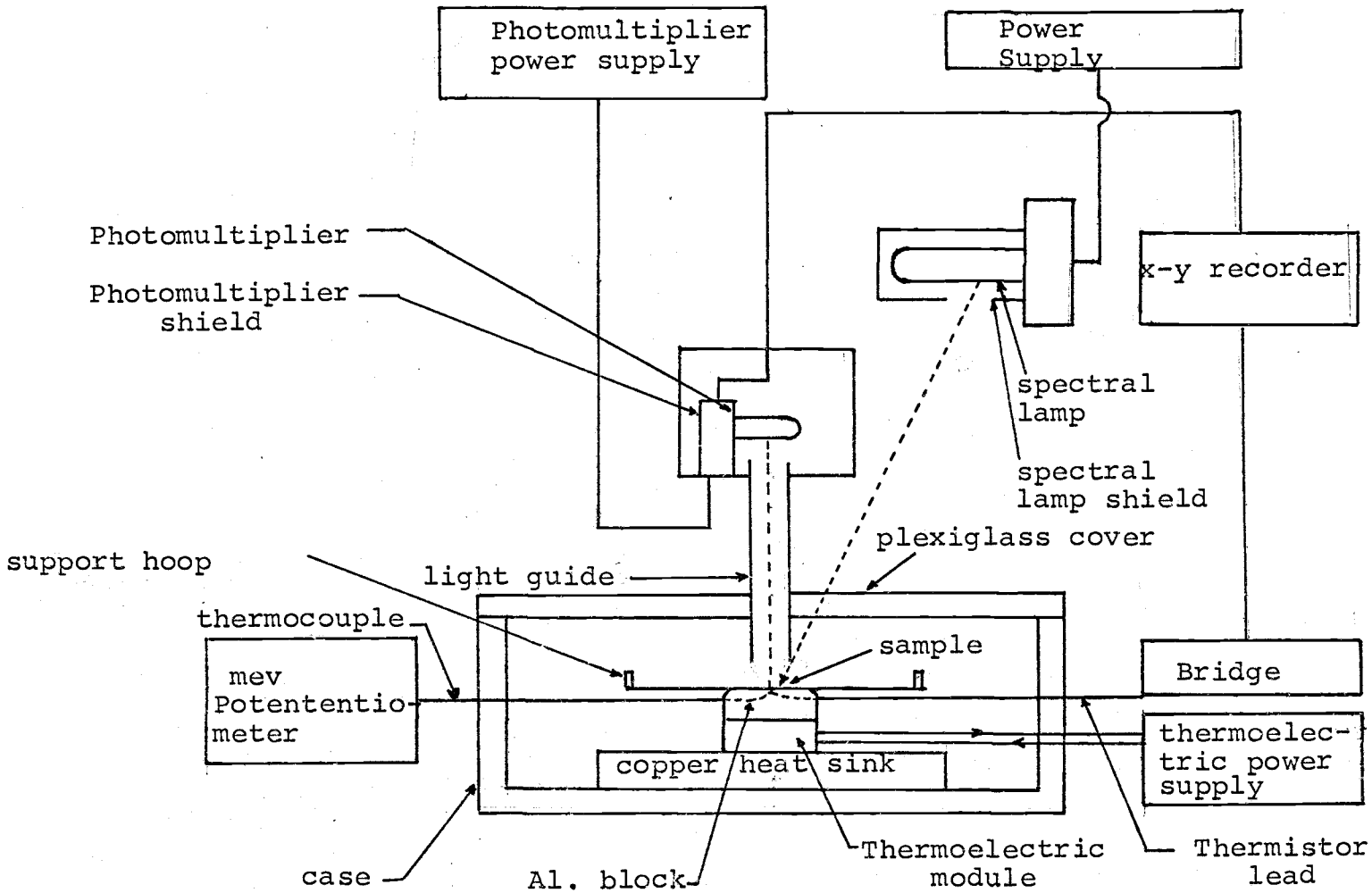

Figure 11. A block diagram of the apparatus used to calibrate L.C. films

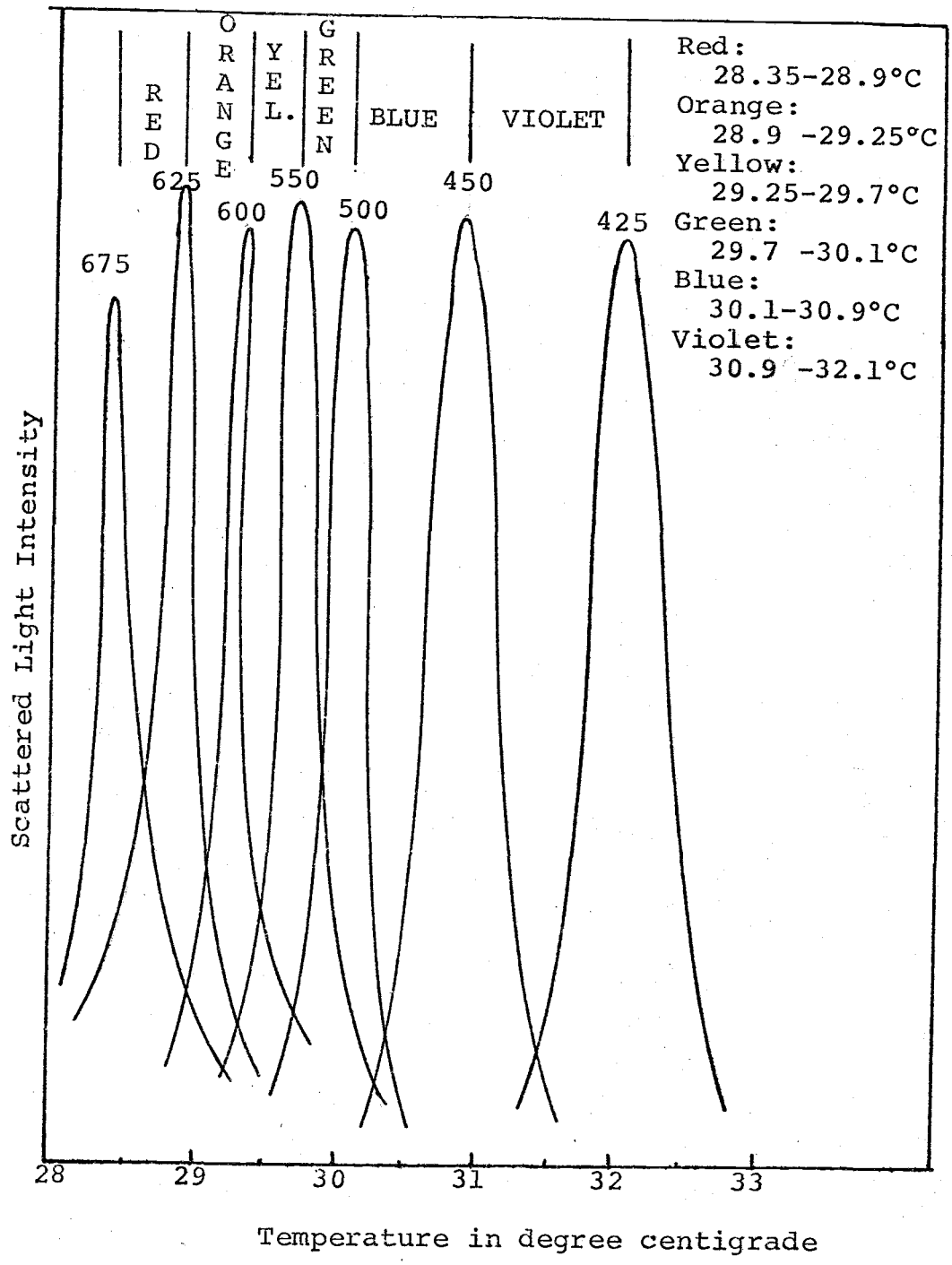

Figure 12. Calibration curves for a liquid crystal film with a color temperature range of 29-32°C

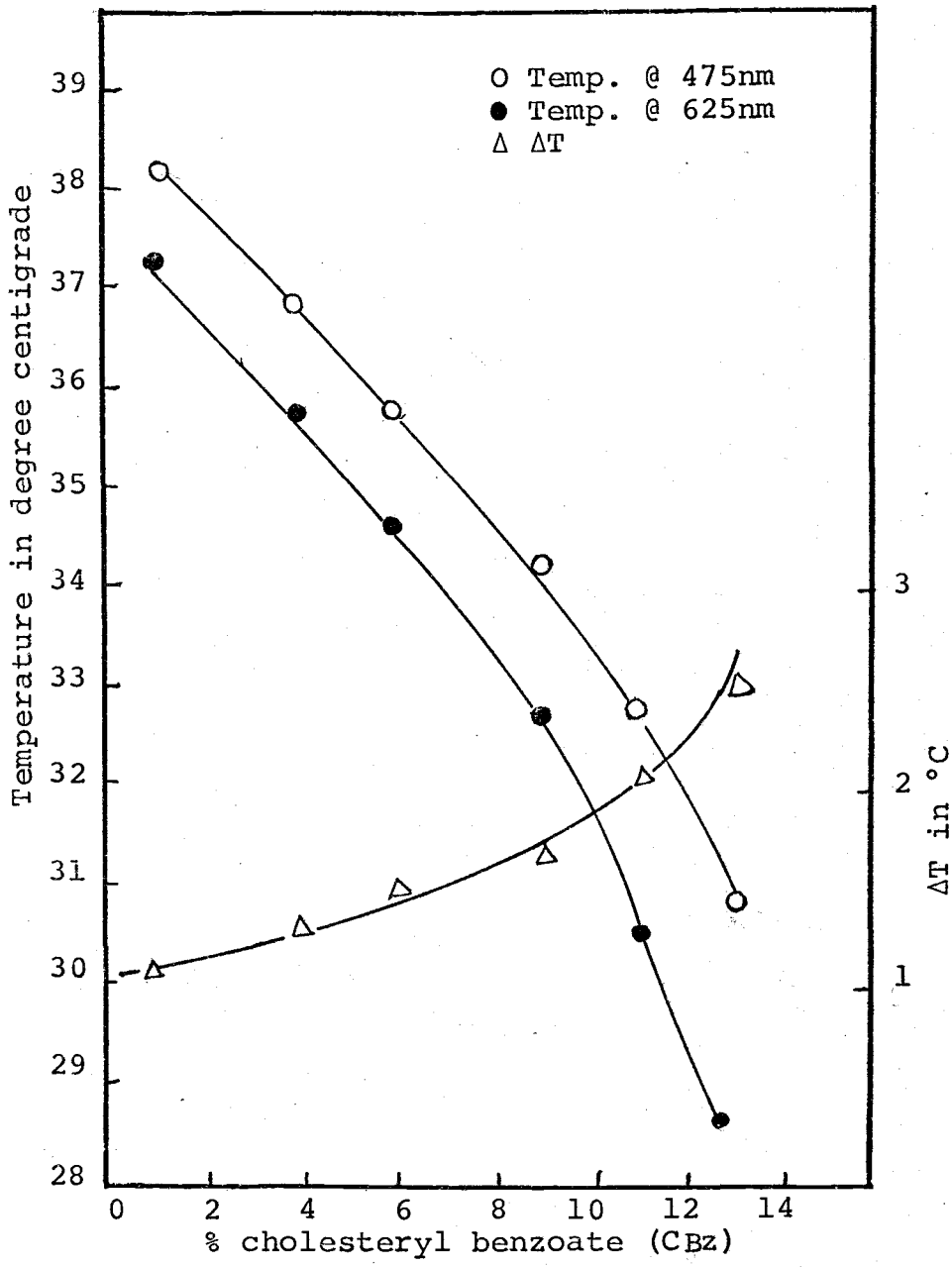

Figure 13. Effect of adding cholesteryl benzoate on color-temperature play for a 40/60 OCC-CN mixture

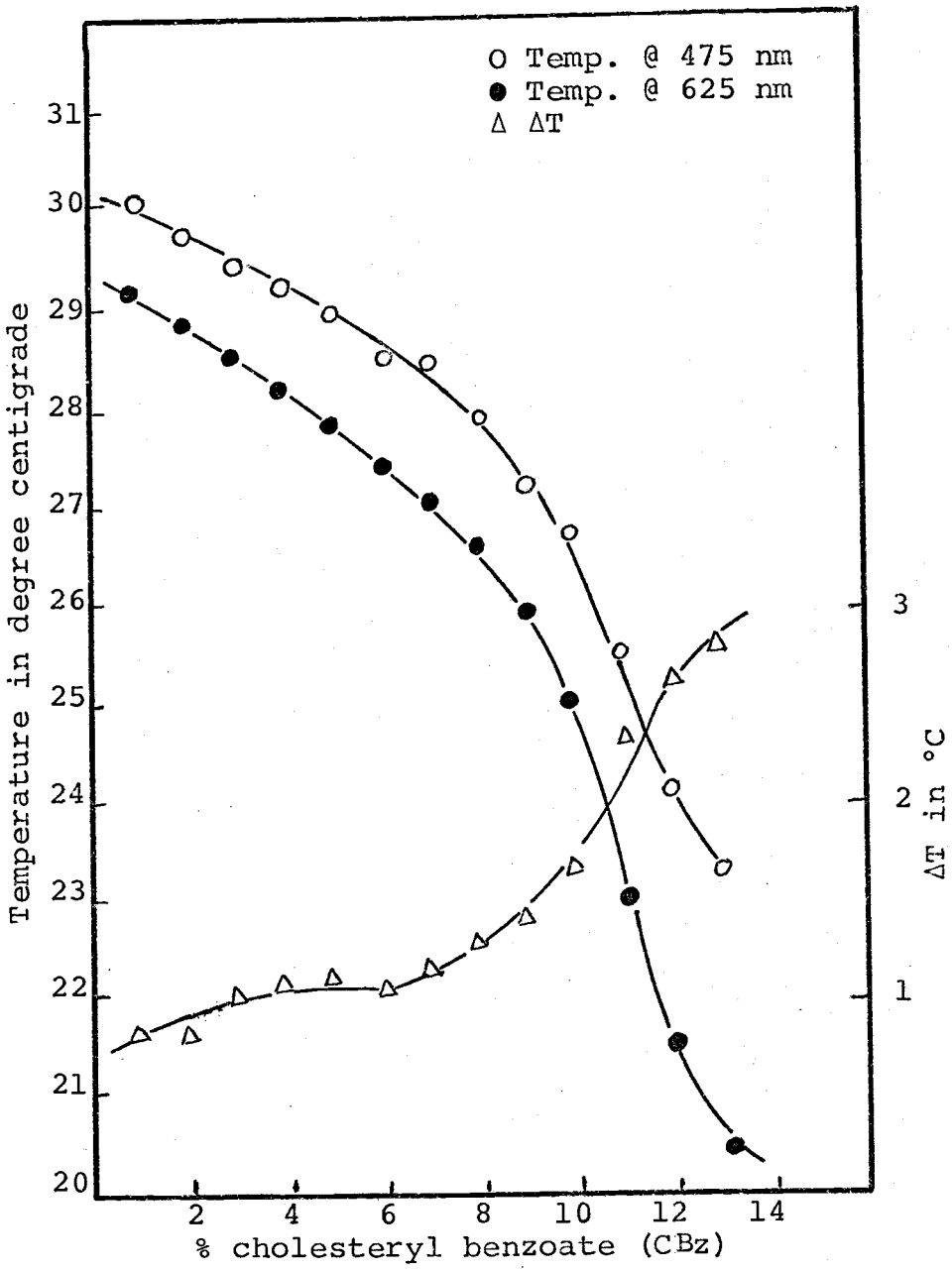

Figure 14. Effect of adding cholesteryl benzoate on color-temperature play for a 60/40 OCC-CN mixture

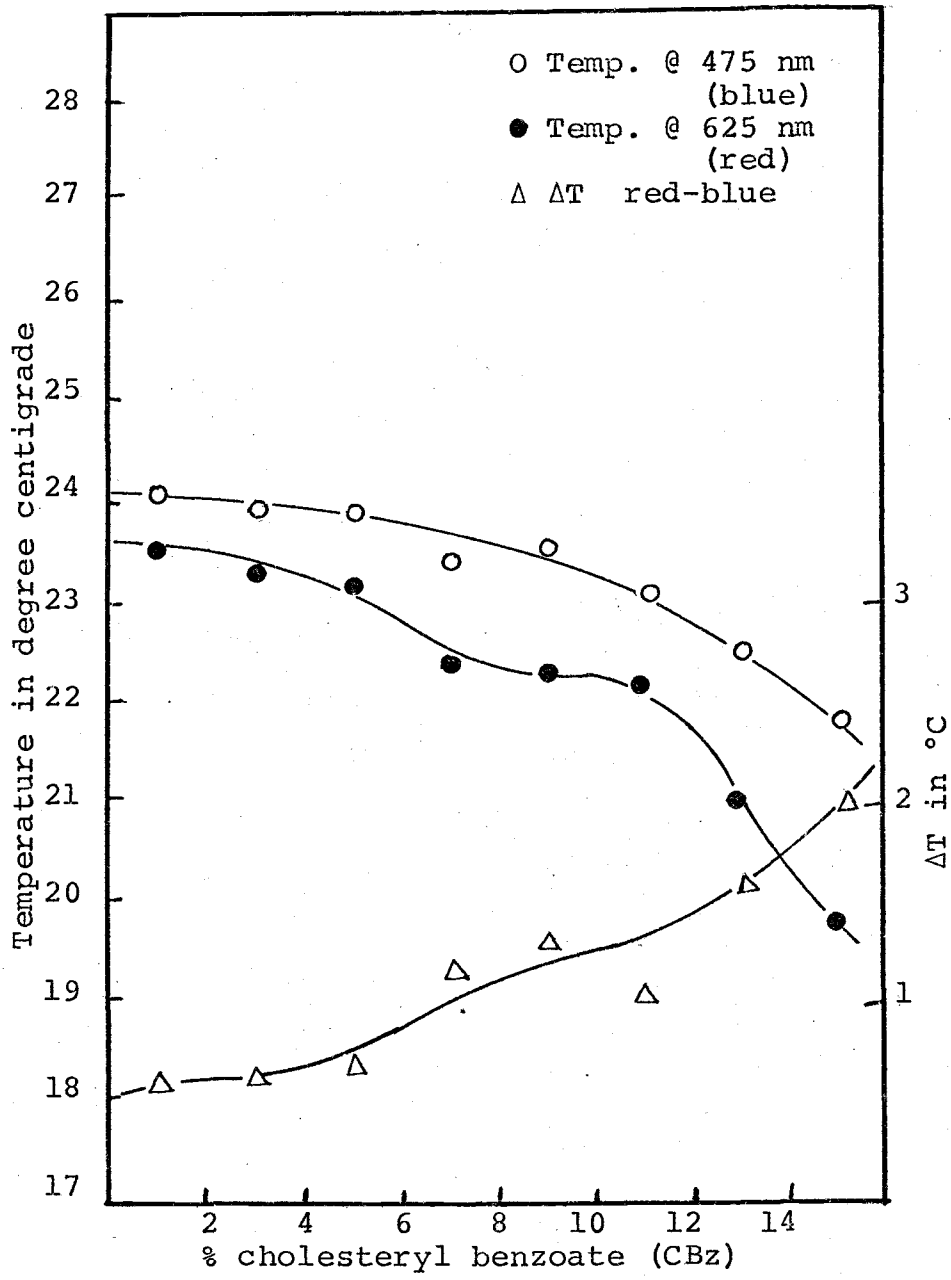

Figure 15. Effect of adding cholesteryl benzoate on color-temperature play for a 80/20 OCC-CN mixture

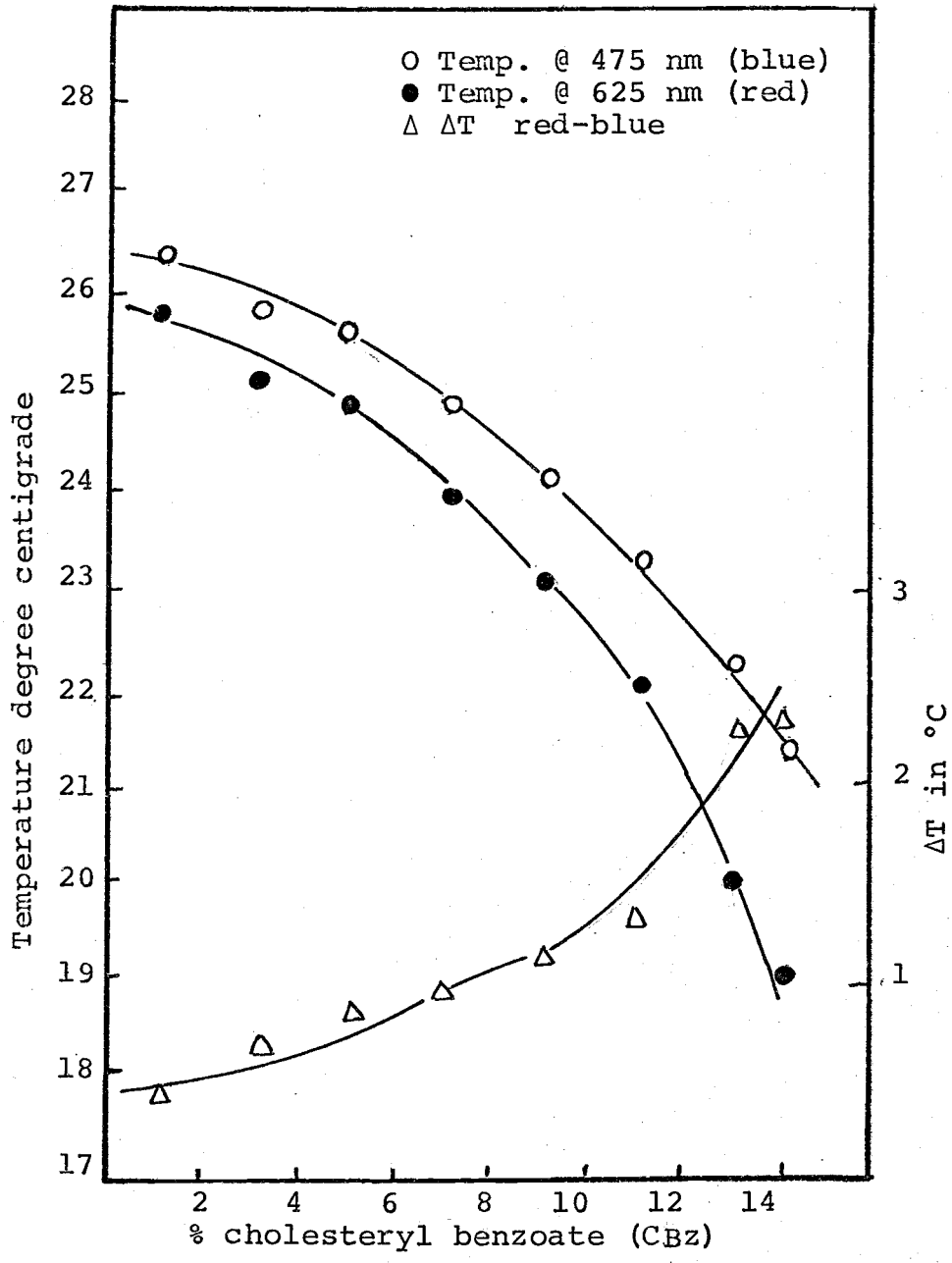

Figure 16. Effect of adding cholesteryl benzoate on color-temperature play for a 70/30 OCC-CN mixture

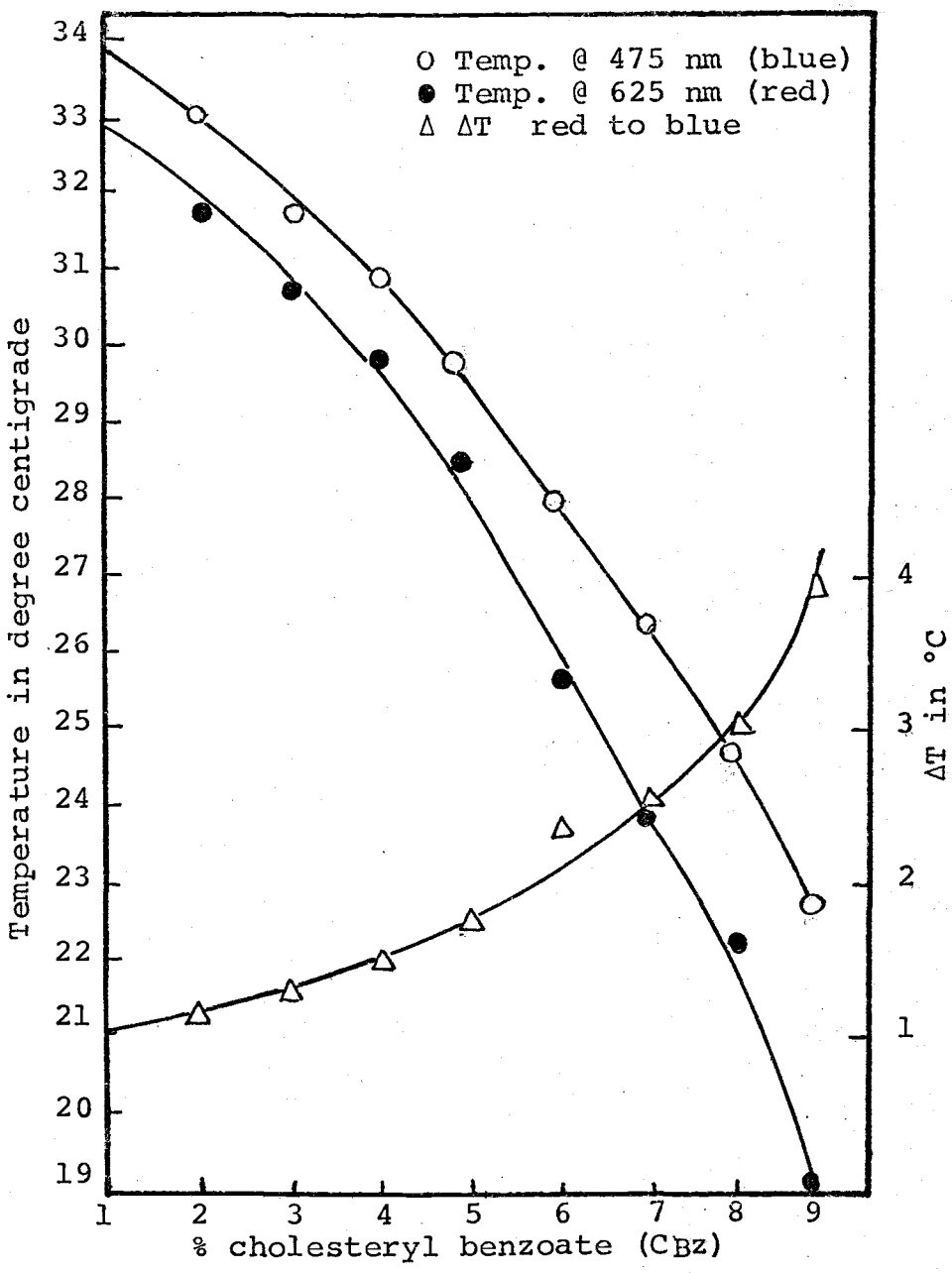

Figure 17. Effect of adding cholesteryl benzoate on color-temperature play for a 50/50 OCC-CN mixture

Fabrication procedure

(a) The substrate

Polyethylene terephthalate film of .05 mm (2 mil) thickness such as is sold under the trade name Mylar was used. The width of the substrate was chosen to be 10 inches.

(b) Release agent layer

To form this layer, Polyvinyl acetate 80% hydrolyzed to alcohol, in 10 parts to 90 parts isopropyl alcohol is cast on the substrate to a wet thickness t = .04mm (1.5 mil) and is allowed to dry 8-10 minutes leaving a coat of approximately .004 mm (.15 mil) on the substrate. The viscosity is 5500 centipoise at a room temperature = 27°C to insure proper flow (Figure 18).

In casting this layer and the succeeding three layers, a roller casting unit is used which consists of two very well machined stainless steel cylinders with a 1 inch diameter and an adjustable gap between the rollers where the film is pulled. The substrate is placed in the gap and is pulled at a constant rate to allow the flow of the fluid on the substrate.

Figure 18. Effect of concentration on viscosity of different grades of P.V.A.
a) at T = 20°C
b) at T = 50°C

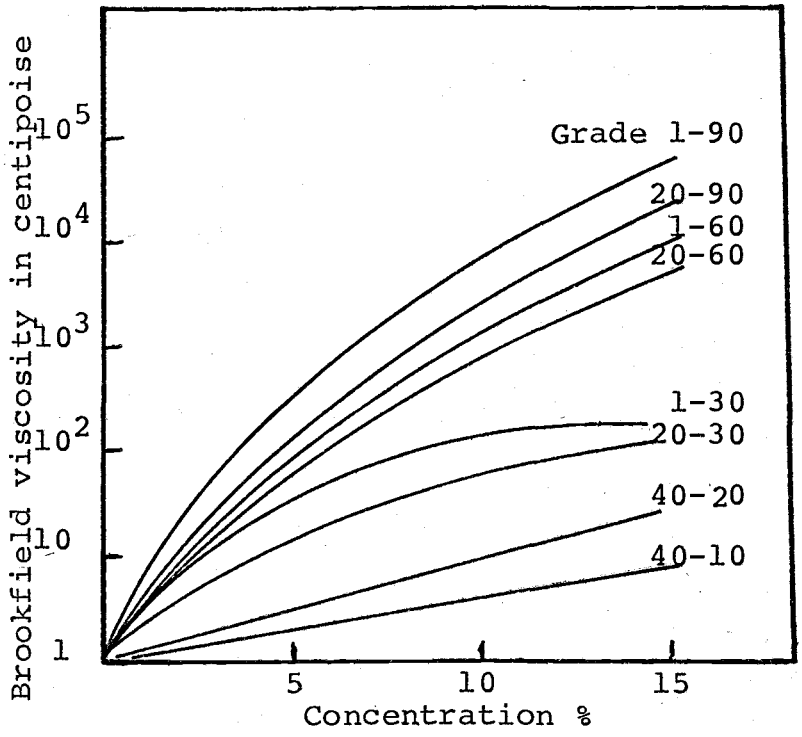

(a) Temperature = 20°C

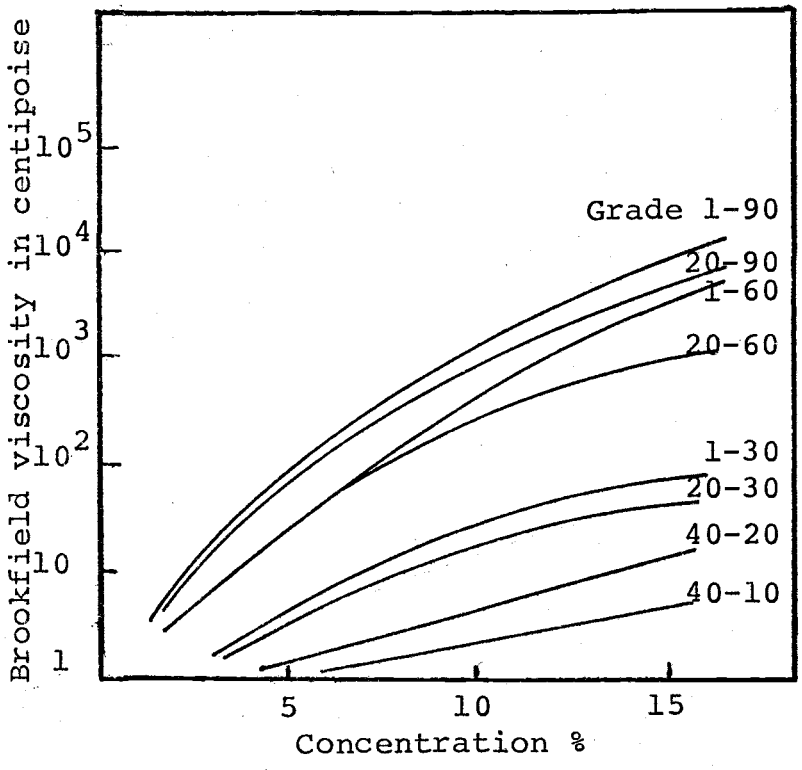

(b) Temperature = 50°C

(c) Opaque polyvinyl butyral layer

Polyvinyl butyral (P.V.B.) with 19% residual vinyl alcohol content in the polymer and not over 2.5% vinyl acetate content is very well dispersed in isopropyl alcohol using dispersator at 3000-4000 RPM to form a homogenous solution of 15% concentration. The Brookfield viscosity is a direct function of the solvent concentration (Figure 19). The final solution should have a viscosity of 20,000-30,000 centipoises at R.T. to insure a good flow rate for casting.

The addition of elasticizers and plasticizers to this solution gives the film the very low elastic modulus that allows it to conform perfectly to irregular surfaces. Several plasticizers and elasticizers were used in different proportions to get the optimal properties desired. Elasticizers such as polyether plasticizer which is a diaryl ether of polyoxyethylene twenty-seven (27) parts for each 100 parts of polyvinyl butyral resins in the solution yield optimum characteristics. Plasticizers such as castor oil 30w was used (27 parts for each 100 parts of polyvinyl butyral resins). Both the elasticizer and plasticizer were very well dispersed in the P.V.B. solution.

The solution obtained was divided into two parts. One part was used to obtain the opaque layer and the other was used to obtain the next layer (L.C. dispersion layer).

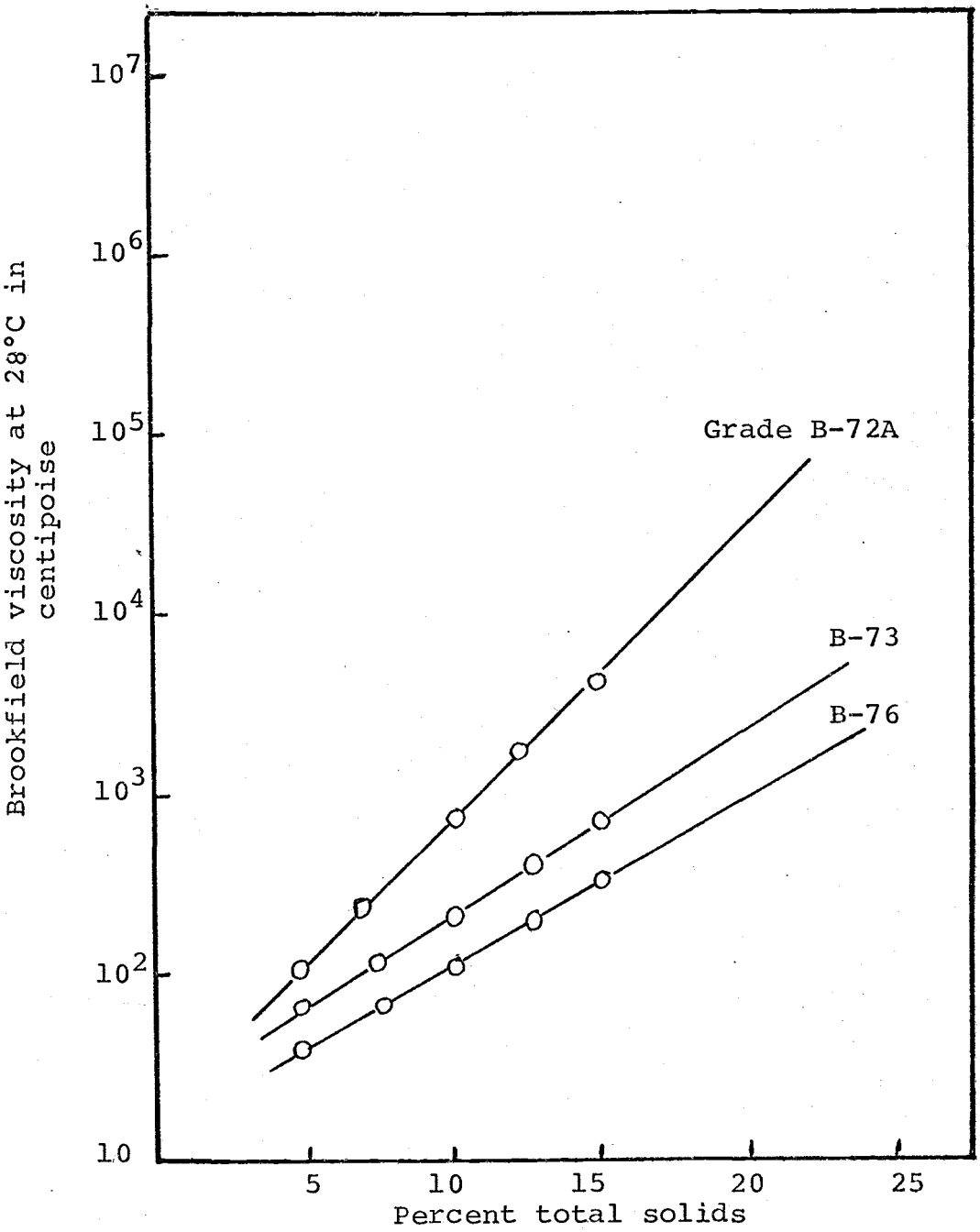

Figure 19. Polyvinyl butyral viscosities in isopropyl alcohol % by weight

To obtain the opaque layer, the solution previously described was further dispersed with 8 parts of a 40% carbon black suspension in alcohol for each 100 parts of P.V.B. to form a light absorbing and opacifying layer. This layer is cast with a wet thickness of .09 mm (3.5 mil). The film is allowed to dry 40-50 minutes producing a dry lamina of about .02 mm (.8 mil).

(d) Liquid crystal dispersion layer

The cholesterol esters are melted together in a melting pot until the mixture becomes a homogenous yellow solution. Melting time and temperature depends on the composition of the mixture.

The addition of 4% by weight of 4-(4'-ethoxyphenyl-azo) phenyl hexanoate to the liquid crystal mixture serves a U.V. inhibitor.

The liquid crystal mixture is well dispersed in the portion of the clear elasticized P.V.B. solution prepared in layer (c). The result is 80 parts of L.C. to 100 parts of P.V.B. resins. The final solution should be free of air bubbles.

The final solution was homogenous and bubble free and had a brookfield viscosity of 22,000-30,000 centipoises at a room temperature of 81°F (27.22°C). The solution was cast over the black lamina to a wet thickness of .1 mm

(4 mil) producing a dry lamina of .015 mm (.5 mil). The solvent evaporation time is 4-5 hours. The evaporation time can be reduced significantly if a proper ventilation system is available.

(e) Polyvinyl alcohol protective layer

This protective surface lamina is applied by casting a 17% water solution of polyvinyl alcohol in a wet thickness of .05 mm (2 mil) which results in a dry thickness of .007 mm (.3 mil). This layer is to be washed off with water at the time of use in medical applications and can be left as an added protection for other applications.

The five layer film has a total thickness of .095 mm (3.75 mil). This thickness represents the packaged thickness. However, at use the substrate, release agent and protective layers are removed leaving a film with .033 mm (1.3 mil) thickness.

Analysis of film properties

Mechanical properties

Ten samples of films with different color-temperature ranges and optimum compositions were tested to determine the final elasticity and strength of the film.

The tests were performed using an Instron Stress Analysis machine and plotter at Cleveland State University,

Cleveland, Ohio. Specimens were: 1" X 1" X .0013".

The results gave an average modulus of elasticity of μ = 894.6 PSI with a standard deviation σ_μ = 26.26 PSI. Tensile strength $\overline{T}$ = 2.0395 X 10^3 PSI, σ_T = 151.39 PSI. The stress-strain curve was linear from no load to rupture. It was noted that the samples were strained to maximum elongation (just before rupture) with no signs of creep in the specimen.

Five samples were subjected to maximum allowable stress without rupture and were allowed to recover. The results were that they all recovered to original length within a period of 8-20 seconds. The 5 recovered samples were further tested for optical properties. The results showed perfect correlation between the original films and the recovered specimens in terms of intensity of scattered light and color-temperature range.

Ten samples were tested for the change in the intensity of light scattered with stress. The samples were driven gradually from no load to maximum elongation and the relative intensity of color was noted for the same input monochromatic light with λ = 625 nm. The results showed that the change in light intensity from no load to maximum elongation is between -11 to -18%.

Stability considerations

A cholesteric liquid crystal material is only useful as long as it continues to behave predictably. Most applications of CLC materials utilize thin films of 10-100 micron thickness. This means a large surface area to volume ratio resulting in susceptibility to degradation whether from oxygen in the atmosphere, which can diffuse in the shallow film easily or ultraviolet (UV) radiation or dust and film particles.

CLC films are very sensitive to certain chemicals especially fats, greases and many of the organic solvents commonly used. The presence of small concentrations (sometimes as low as a few parts per million) of these chemicals changes the color-temperature range of the CLC material.

The inherent high viscosity of the cholesteric mesophase means that unless it is protected it will trap dust and fibre particles.

A study was conducted to optimize the stability of the L.C. dispersion film.

A UV inhibitor was incorporated in the L.C. layer as described in the previous section. In addition, several factors were taken into consideration to immunize the film against the two major degradation factors: UV radiation and oxygen.

A closer look at the film composition shows that the L.C. layer is sandwiched between an opaque layer on a mylar substrate and a protective clear PVA layer. Therefore, in order for any U.V. light to reach the L.C. layer, it has to come through one of those two paths. A test was made to determine the filtering characteristics of the opaque-mylar path (Figure 20). The figure shows that in the ultraviolet part of the spectrum, the transmittance is less than 1% of the incident flux. In addition, the mylar substrate has low permeability to oxygen.

A packaging material was chosen with high UV absorption properties to protect the other side of the L.C. layer. This package consists of 2 sheets, one of 5 mils manila paper and the other of 5 mils black paper. The transmittance properties of this package are shown in Figure 20. This package transmits less than 2% of the incident radiation in the UV region. As to the oxygen permeability, the PVA layer offers total protection against oxygen exposure.

A stability test was performed to evaluate the L.C. dispersion film. Twenty samples of different color-temperature ranges were monitored for stability evaluation over a period of 12 weeks. Ten samples of the film were placed in a control chamber under vacuum with a total UV elimination. Ten identical samples were packaged as

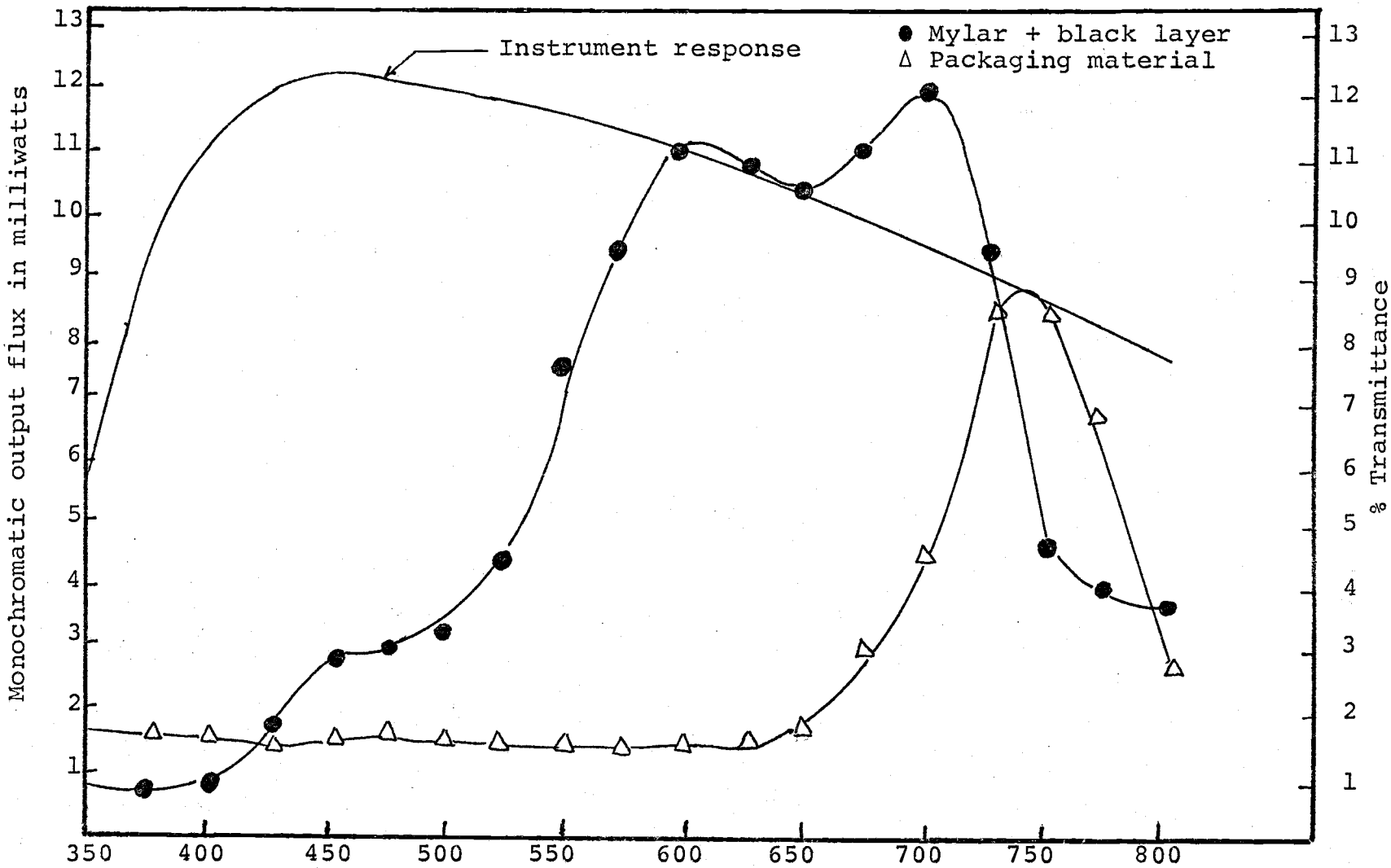

Figure 20. Wavelength in (nm)

described above, and left on exposed shelves under normal room condition illumination and temperature in the laboratory room. The samples were initially calibrated, and were recalibrated every week for 12 weeks. The temperatures of maximum reflection at wavelengths λ = 625nm (red), λ = 525 nm (green) and λ = 475 nm (blue) were noted.

The results are shown in Figure 21. The figure shows the average temperature variation of the samples under total UV and oxygen protection and the samples under normal shelf exposure for the maximum reflection at a wavelength λ = 625 nm over the 12 week period (variations of other wavelengths gave similar results). It was noticed that there is an initial temperature drop varying between 1.6-2.1°C from the L.C. solution to the L.C. dispersion film due to solvent evaporation.

Optical properties

A test was conducted to determine the relative intensity of reflection of the L.C. dispersion film. Five samples of varying liquid crystal layer thickness were tested and the percentage light reflected at a wavelength λ_{max} = 625 nm was noted as shown in Figure 22.

Fergason (1968) derived a formula relating the amplitude of the reflected circularly polarized light wave

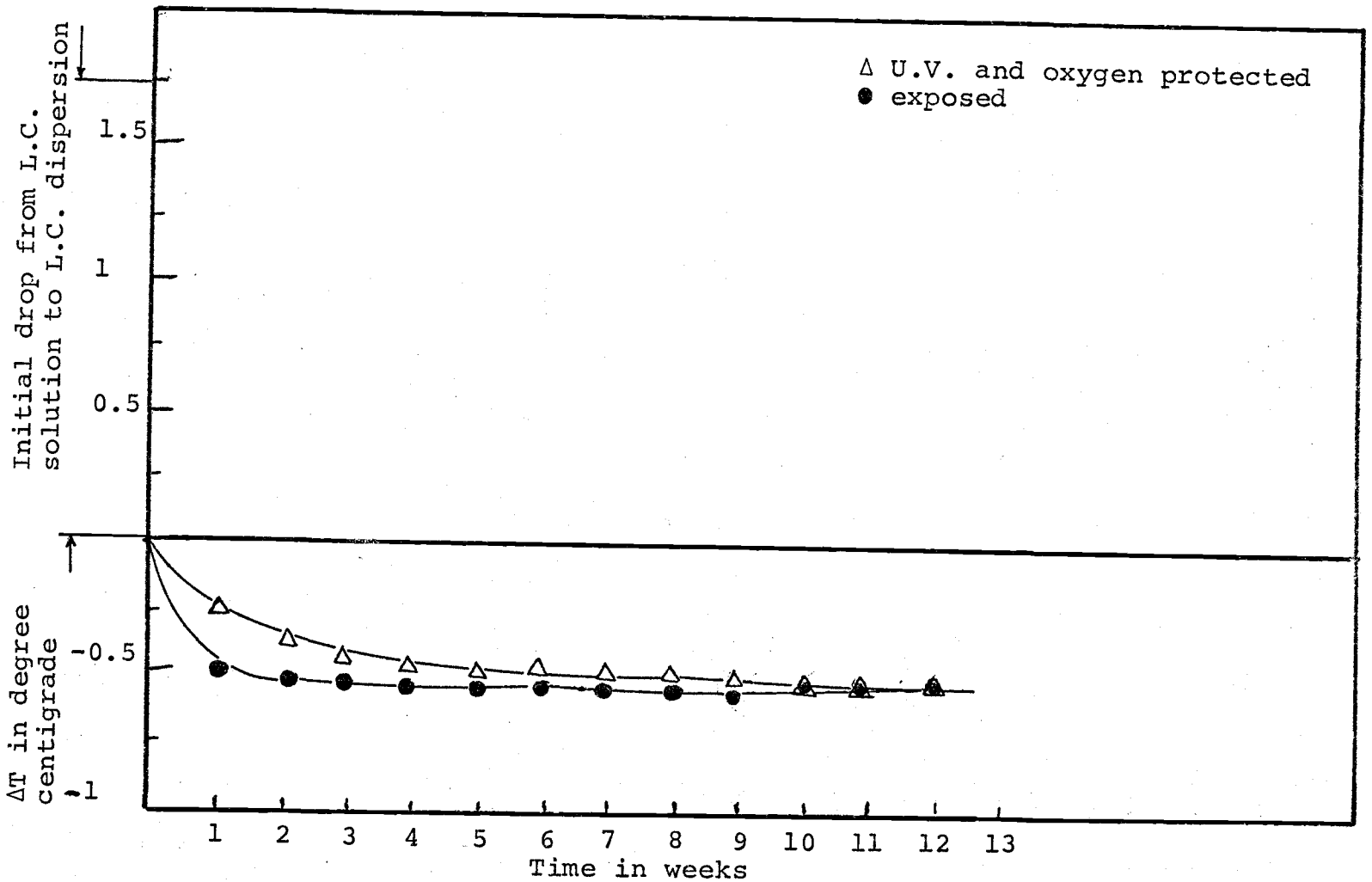

Figure 21. Stability results for control and normally exposed sample

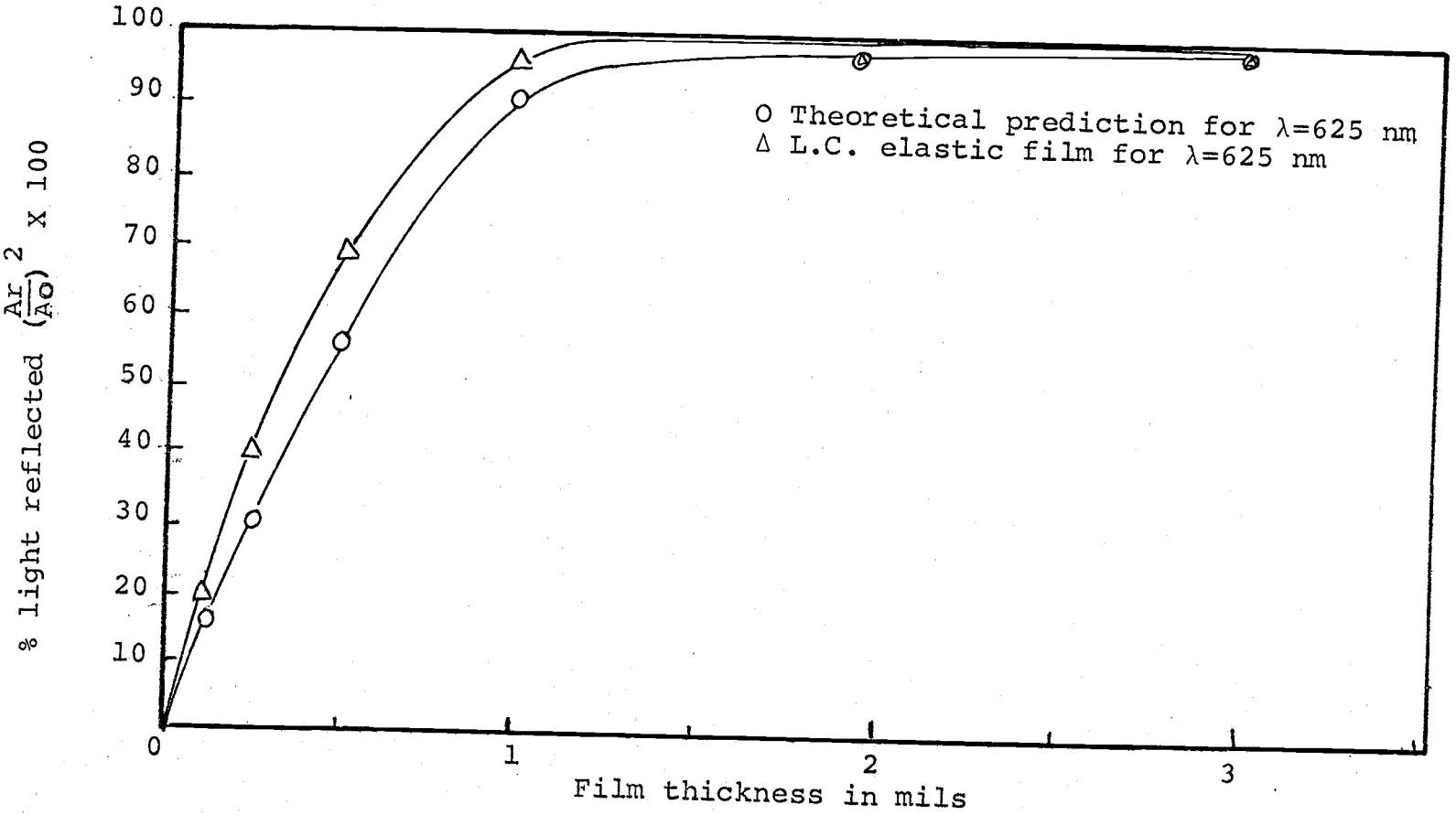

Figure 22. Effect of film thickness on reflected light

to the film thickness in the form:

$$A_r = A_0 \left(1 - (n_0/n_e)^{8t/\lambda max}\right)\left(1 + (n_0/n_e)^{8t/\lambda max}\right)$$

where A_r = amplitude of reflected circularly polarized light of reflection sense.

A_0 = amplitude of incident circularly polarized light of reflection sense.

n_0 = refractive index for ordinary ray

n_e = refractive index for extraordinary ray

t = thickness of CLC film

$\lambda_{max.}$ = wavelength of reflected light in vacuo.

In Figure 22 Fergason's formula is plotted for the same thickness and wavelength. The relative intensity of reflection is given by $(A_r/A_0)^2$.

Methods, materials, and protocol for breast cancer screening using thermography in three modalities

Permanent equipment

1. IR thermography system AGA Thermovision 680
2. Temperature controlled examining room
3. Air blower drier
4. Photographic equipment
   --Single lens reflex 35mm film loading 55mm lens camera
   --2 Strobonar 202 electronic flash units

--2 light stands for flash units

--Rotating polarizing lenses for camera

--2 rotating polarizing lenses for flash units

--Photographic black drape

Expendable materials

1. Elastic L.C. films each with a different range covering 28.2-31.2°C, 29.1-32.1°C, 30.1-33.1°C

2. Lixkit, liquid crystal thermography kit contains 2 aerosol cans of black base, four cans of liquid crystal; each with a different temperature range including 28-31°C, 29-32°C, 30-33°C, and aluminum temperature test probes with an alligator clip handle.

3. 70% isopropyl or ethyl rubbing alcohol.

4. Cotton pads 2 to 4 inches square, disposable paper drapes or towels 18 to 24 inches square, disposable paper wash cloth or towels 6 to 12 inches square.

5. Lixkit release for thermographic clean-up.

6. Infrared film, 35mm color film; Ektachrome X for slides or Kodacolor II for negative prints.

Breast examination procedure

1. The patient fills out examination forms before entering the examination room.

2. During this period, the investigator sets up the IR equipment and the photographic liquid crystal set up. Each volunteer is assigned a number that serves as identification; this number is taped on IR display scope.

3. The temperature of examining room is kept at 68°F at all times.

4. Upon completion of test information forms, the volunteer is directed to the dressing room where she disrobes from above the waist. The cooling room fan is turned on and the volunteer is directed to the cooling area where the breast area is cooled. The volunteer is advised to keep her arms away from the sides in order to insure uniform cooling of breast area.

5. Cooling time is 10 minutes.

6. After cooling, the volunteer is guided to sit facing the IR camera and is reminded to keep her arms away from the rest of body while walking to the IR camera section.

7. The volunteer is seated and is asked to hold on to an overhead bar to insure thermal isolation of the arms from the breast area. Through rotation of chair and/or camera, the subject is put in focus as seen in the viewfinder.

8. A picture is taken of the volunteer identification with camera setting in normal mode. Then the film is

advanced and the mode switched to "inverted." Both remain so through the rest of the test.

9. Contrast is adjusted to get the best picture and middle temperature level (MTL) is noted. A series of pictures is taken in the following order:

(a) Anteroposterior (A.P.) picture

(b) Left oblique

(c) Right oblique

(d) Isotherm set at delta T = 0°C

(e) Isotherm set at delta T = 1.0°C

(f) Isotherm set at delta T = -1.0°C

(g) Isotherm set at delta T = -0.5°C

(h) Isotherm set at delta T = +0.5°C

10. The time for the IR pictures is estimated to be 10 minutes.

11. The volunteer is redirected to the cooling area with the fan on for a cooling period of 7 minutes.

12. The volunteer is assisted to the supine position on the examining table with her hands behind the neck.

13. During this time, the investigator prepares the elastic L.C. film to be tested. The MTL obtained in step (9) serves as a good indicator for the choice of a film that shows a green color (λ = 525nm) at this temperature.

14. The investigator pulls the L.C. film off the substrate, holds one end of the film and lays it down on breast area with slight stretch to cover the whole anterior and lateral breast.

15. Upon film application, the ends are taped laterally, superiorly and inferiorly to provide intimate contact. A black photographic drape is used as a background for subject. The black background optimized photographic reproduction.

16. A series of 5 pictures is taken to reproduce the whole breast surface. The patient number is put on embossing tape both on front, left and right sides. The pictures are taken as shown below:

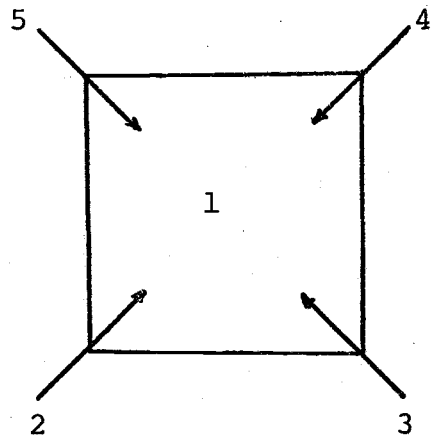

17. The estimated time for steps 12-16 is 10 minutes. Film is then removed.

18. The volunteer is redirected to the cooling area for five minutes with the fan on.

19. The volunteer is assisted to the supine position on the examining table.

20. The black photographic drape with a window opening of 24" x 12" is placed on the volunteer with the breast area exposed. The window is draped on the four sides.

21. The breast area is wiped copiously with an alcohol (isopropyl alcohol) moistened cotton swab. Residual alcohol is wiped with a dry towel.

22. The exposed breast area is draped to limit overspray.

23. The proper liquid crystal aerosol temperature range is selected.

24. The black coating is sprayed evenly to cover the entire breast area using Lixkit black base aerosol. A dryer is used to speed up drying of black base.

25. Liquid crystals are sprayed evenly over the blackened breast surface. Solvents evaporate from the liquid crystal layer. The dryer can be used to speed up the evaporation.

26. Pictures are taken similarly to step (16). A total of 5 pictures is taken to reproduce the whole breast area.

27. After pictures are taken, alcohol is used to remove the liquid crystals.

28. The volunteer returns to the dressing room and is advised to use soap and warm water to remove completely the black base coat.

29. Time for steps 19-27 is estimated to be about 20 minutes.

30. Total time is estimated to be about one hour.

IV. RESULTS AND DISCUSSION: PART I

COMPARATIVE STUDY

This study was conducted to evaluate the liquid crystal dispersion film developed and to compare it to existing thermographic methods. A random sample consisting of seventy-five (75) women was examined using thermography in three modalities: elastic L.C. dispersion film, direct spraying of the liquid crystals and infrared thermography. All cases with a positive thermogram in any one of the three modalities were given a xeroradiography examination.

Through the course of this study, major considerations were: to establish a protocol for liquid crystal thermography that would make it a practical and reliable tool in clinical mass-screening, to define clearly the factors that affect the breast thermographic findings, to spell out the advantages and limitations of breast thermography. In this comparative study the results of the correlation between the three thermographic modalities served in defining the features and characteristics of the normal thermogram.

Very little attention has been paid to the thermal patterns existing in the breasts of a normal healthy female, and it is impossible to draw conclusions of

abnormality without first having a background knowledge of normality (Harris et al., 1966). Later Draper and Jones (1969), Davison et al. (1972) studied the normal thermal pattern, but, to date, thermography lacks a simple, quantitative interpretation scheme.

A. Sample description

The sample was selected on a purely random basis from volunteers at Akron City Hospital, Akron, Ohio.

The sample had an age distribution with a mean $\bar{X}$ = 39 years old and a standard deviation σ = 11.79 years. Seventeen women (22.6%) had present complaints in one or two breasts, six of whom (8%) had complaints in both breasts. Twenty-two women (29.3%) had fibrocystic disease or mastitis in one or both breasts, eight of whom (10.6%) had it in both breasts. Thirty-four women (45.3%) had one or more family histories of cancer. Forty-two women (56%) had one or more pregnancies. Fourteen women (18.7%) were on current oral contraceptives.

B. Factors affecting thermograms

Medical thermography requires that the area under investigation be completely uncovered so that the unobstructed natural heat emission of the skin may be sensed by the liquid crystals in L.C. thermography or by

the infrared detector in IR thermography. The translated image is observed as different colors of the visible spectrum on the L.C. surface or is displayed on the face of a cathode ray tube in IR thermography and is then photographically recorded. The quality of the processed thermogram is, therefore, dependent upon both of these processes.

Factors that influence the thermogram are: ambient temperature, positioning of the patient and photographic techniques.

(1) Ambient temperature and pre-conditioning for thermographic examination

The examining room should be free of drafts and be maintained at an ambient temperature 20°C (68°F) at all times to promote infrared radiation.

Davison (1971) reported on the breast L.C. thermographic examination of women under uncontrolled room temperature. The resulting temperature distribution under those circumstances is shown in Figure 23. This distribution shows that the MTL (λ = 525 nm) of the coldest breast was 31°C and the MTL (λ = 515 nm) of the warmest breast was 35°C. These findings show a range of 4°C for the MTL between the coldest and warmest sample in the study.

In this study, with a room temperature controlled at 20°C (68°F), and a standard cooling procedure for each case it was found that the temperature distribution was shifted to the cooler side as shown in Figure 24. This distribution shows that the MTL (λ = 525 nm) of the coldest breast was 29.2°C and that the MTL (λ = 525 nm) of the warmest breast was 31.1°C. These findings show a range of 1.9°C for the MTL between the coldest and warmest sample in the study. The distribution under controlled ambient temperature is more selective and is positively skewed.

The examination of the two distributions demonstrates the effect of ambient condition on breast temperature. The difference in the two distributions can be explained considering an uncontrolled ambient room condition to be a random variable which would follow approximately a Gaussian normal distribution over a period of time (the period of the study). If the breast surface temperatures have the distribution shown in Figure 24 under controlled ambient temperature, and considering that the random variation of ambient temperature is a variable added to the system; by the central limit theorem and applying the convolution principle, the resulting distribution would approach the one reported by Davison (1971).

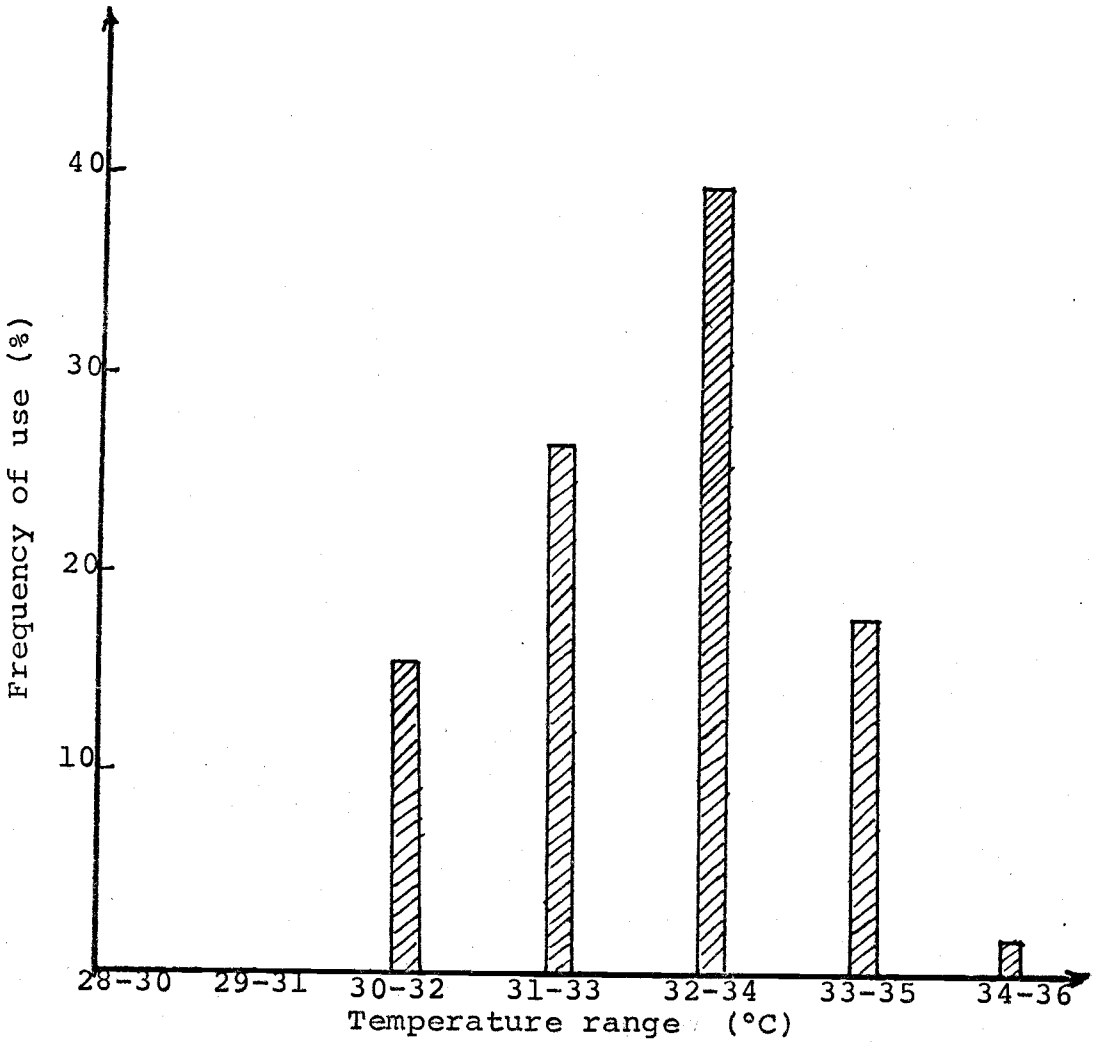

Figure 23. Breast temperature range histogram

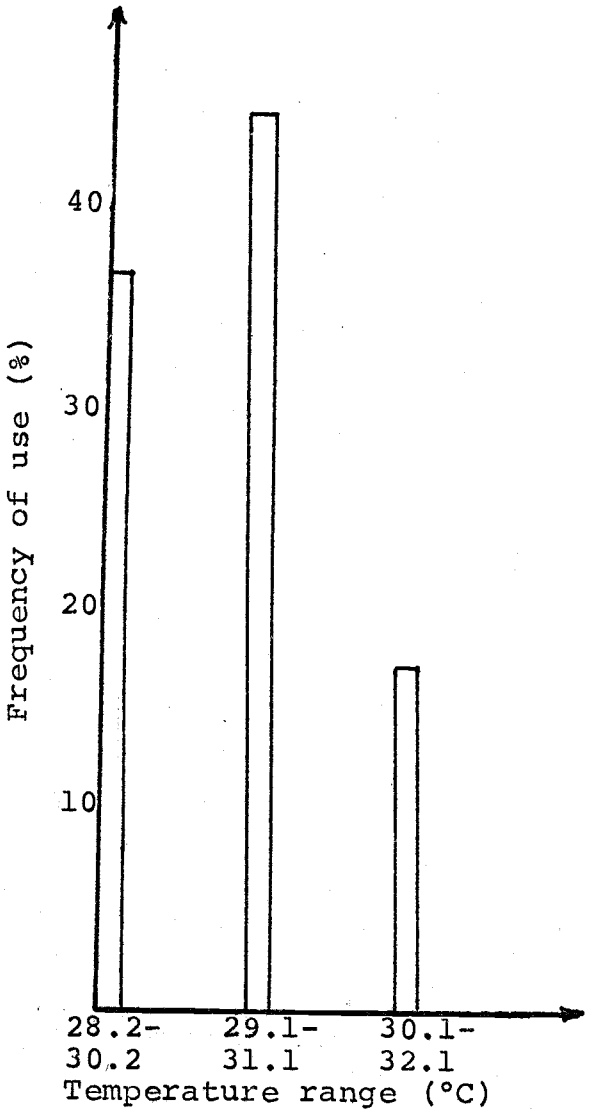

Figure 24. Distribution under control ambient temperature

Illumination should be by sources with a minimum heat emission and window shades or drapes should be used as shields in the examining room against sunlight.

Previous reporters mentioned the need for prolonged waiting periods prior to examination. Adjustment of surface temperatures of the human body is a highly complex physiologic process and external environment is only one of many factors which include the emotional state of the person (Isard, 1974).

In this study 10 cases were examined under different waiting times varying between 0-15 minutes. The results showed no significant differences in thermograms with waiting times between 7-15 minutes. Therefore, 7 minutes was chosen as optimum cooling and preconditioning time.

(2) Positioning

Examination of the breast is best conducted with the patient disrobed to the waist and in the erect position.

In this study the L.C. thermograms were obtained in both the supine and sitting position in 40 cases using the L.C. dispersion film and the L.C. spray in an effort to determine whether there are any significant thermographic differences between the two positions. The results showed

a perfect correlation between the thermographic patterns in both positions with minor differences which do not effect the thermographic interpretation. Thus, the supine position was used and recommended for L.C. thermography.

In the IR thermographic examination, the sitting position is used with the patient facing the IR camera and inclined slightly forward so that the breasts assume a natural dependency. By holding onto a bar suspended from the ceiling, cross radiation from the arms and body is avoided.

In this study the temperature recordings in each case showed perfect correlation using the three modalities under the same controlled ambient condition as shown in Figure 27.

In the following L.C. thermograms the color-temperature conversion will follow the code below:

Temperature	Wavelength (nm)	Color
T_1	625	red
T_2	600	orange
T_3	575	yellow
T_4	525	green
T_5	475	blue
T_6	425	violet

with: $T_1 < T_2 < T_3 < T_4 < T_5 < T_6$.

Thermographic evaluation

The 75 women involved in the comparative study were all examined using thermography in three modalities. The resulting thermograms were read independently and all positive thermograms were followed up by a xerogram. The results showed that 10 (13.33%) had a positive L.C. thermogram, 12 (16%) had a positive IR thermogram.

The xerograms of the 12 women with positive thermograms were obtained and the results showed that 8 (10.66%) had benign lesions (fibrocystic disease with sclerosing adenosis, papillomatosis or epithelial hyperplasis). There was no case of malignancy.

Since only malignant tumors are considered true positive, the results of the L.C. thermographic study of the 75 cases are: 13.33% false positive, 86.67% true negative, 0% false negative, 100% true positive (no malignant cases).

Despite the false positive occurrence in thermography, a more objective study shows that if a breast cancer detection method is to detect early stages, those women with benign lesions such as fibrocystic disease (which are considered as false positive) are very likely to develop carcinoma of the breast in the future.

Farrell et al. (1971) reported that of 72 cases (10%) that were false positive in a study of 682 women

using IR thermography of the breast, 7 cases which were originally considered as false positive turned to malignant cases of carcinoma in a period of three to six months after the first examination, therefore, becoming true positive.

An analysis of the figures given by Delarue (1969), which were discussed in an earlier section of this study, and the results of Farrell et al. (1971) means that one has to be very careful in the interpretation of false positive cases in thermography of the breast. The classical statistical meaning of a false positive being a false alarm may have to be modified. In this case it may mean an alarm for a future occurrence in some of the cases may mean more routine follow up would be necessary in this case.

In this study both the normal and abnormal thermograms were carefully studied and analyzed. This allows one to isolate the positive signs and classify them according to their relative importance in relation to carcinoma of the breast.

Researchers in the past have classified the normal thermal patterns of women's breasts into several groups and subgroups which were considered normal. If a given thermogram did not fit into one of the normal patterns it was considered abnormal. As a result, thermography suffered from a high incidence of a false positive rate.

In this study three patterns were recognized: vascular, avascular and mottled. Cases with these three basic patterns can be either normal or abnormal depending on the abnormal signs in the thermogram.

Figures 25 A, B, C show sample L.C. thermograms of vascular, avascular and mottled patterns.

Figure 26 shows an illustration of the consistency of the thermographic pattern in the supine and sitting positions using L.C. and IR thermography.

Figure 27 shows the thermographic findings in the three modalities. It is clear that there is a correlation between the three thermograms and the optimum optical characteristics of the film in terms of the iridescent colors and the high resolution.

Figure 28 shows another illustration of the one-to-one correspondence between the liquid crystal and infrared thermograms. One major advantage of L.C. thermography is that the temperature isotherms are readily identified because each isotherm would represent the contour of the corresponding color.

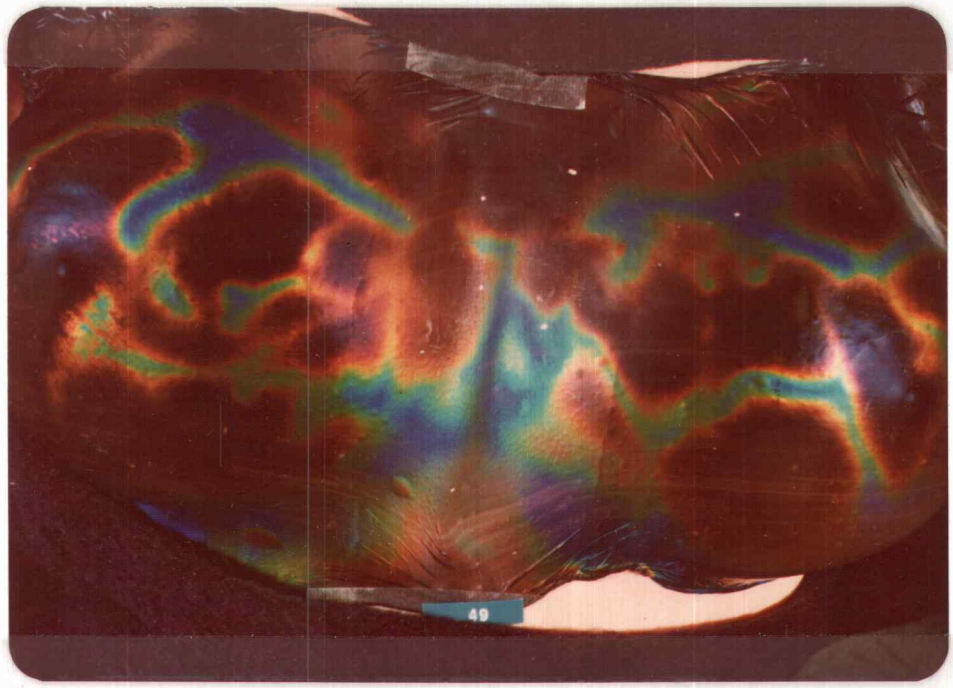

Figure 25A. Vascular thermogram

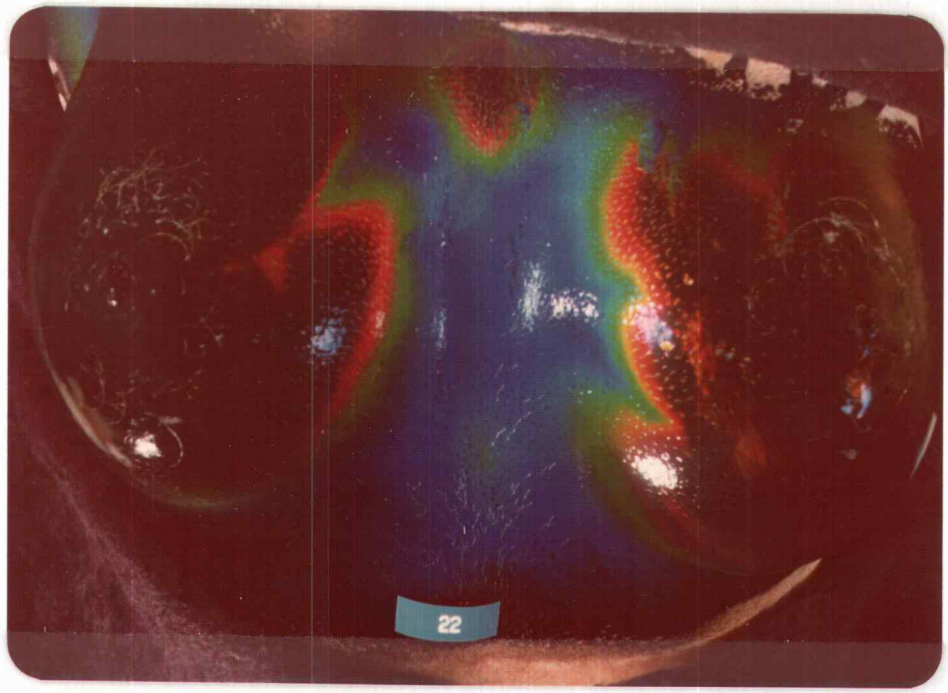

Figure 25B. Avascular thermogram

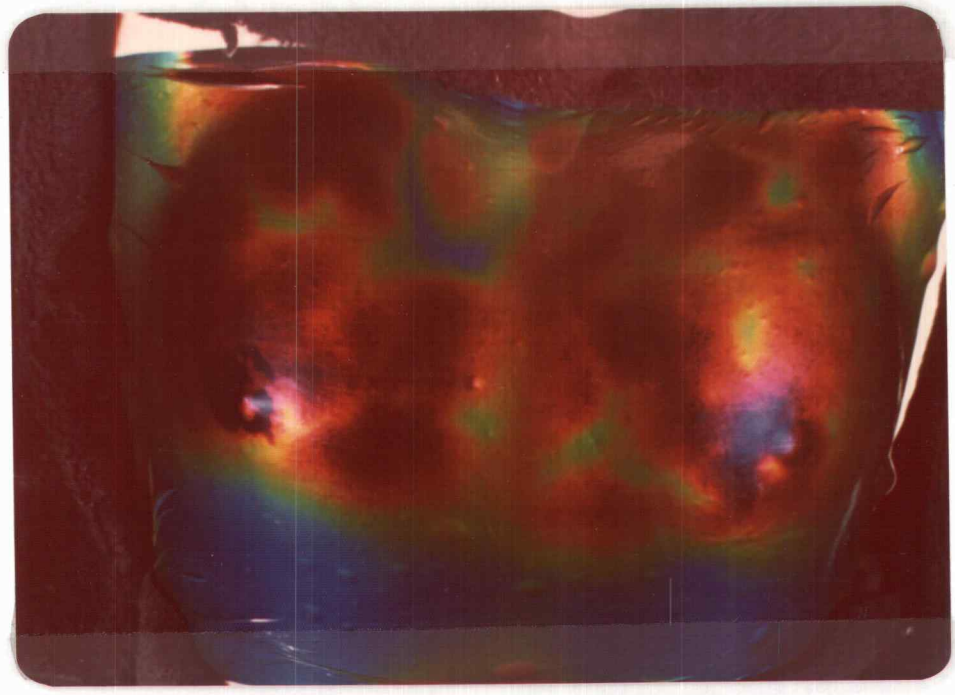

Figure 25C. Mottled thermogram

A

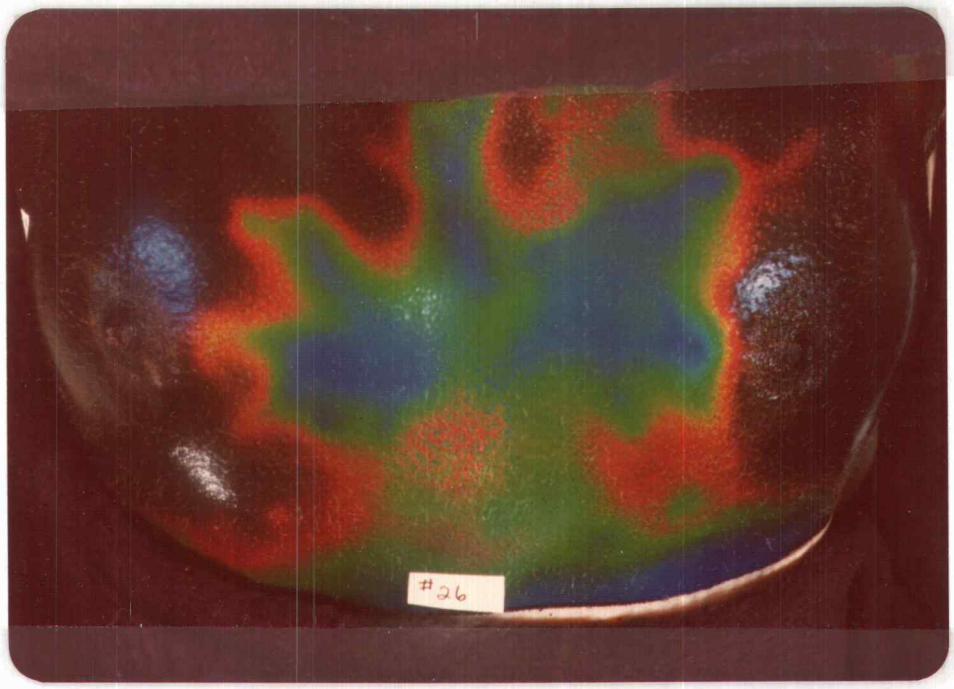

B

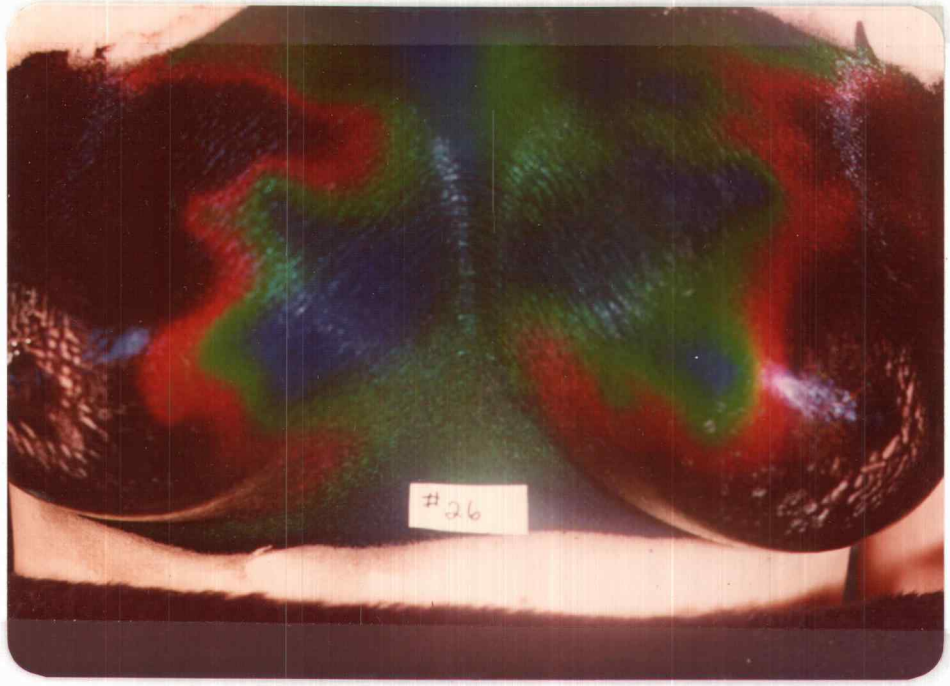

Figure 26. A--Liquid crystal thermogram in supine position
B--Liquid crystal thermogram in sitting position

Figure 27 shows (A) L.C. thermogram with thin elastic film showing T_1(red) = 28.2°C, T_4(green) = 29.2°C, T_5(blue) = 30.2°C; (B) L.C. thermogram with direct application of liquid crystals showing T_1(red) = 28°C, T_4(green) = 29°C, T_5(blue) = 30°C; (C) Infrared thermogram with isotherms taken at MTL (Δ=0), (Δ=-1), (Δ=+1°C).

A

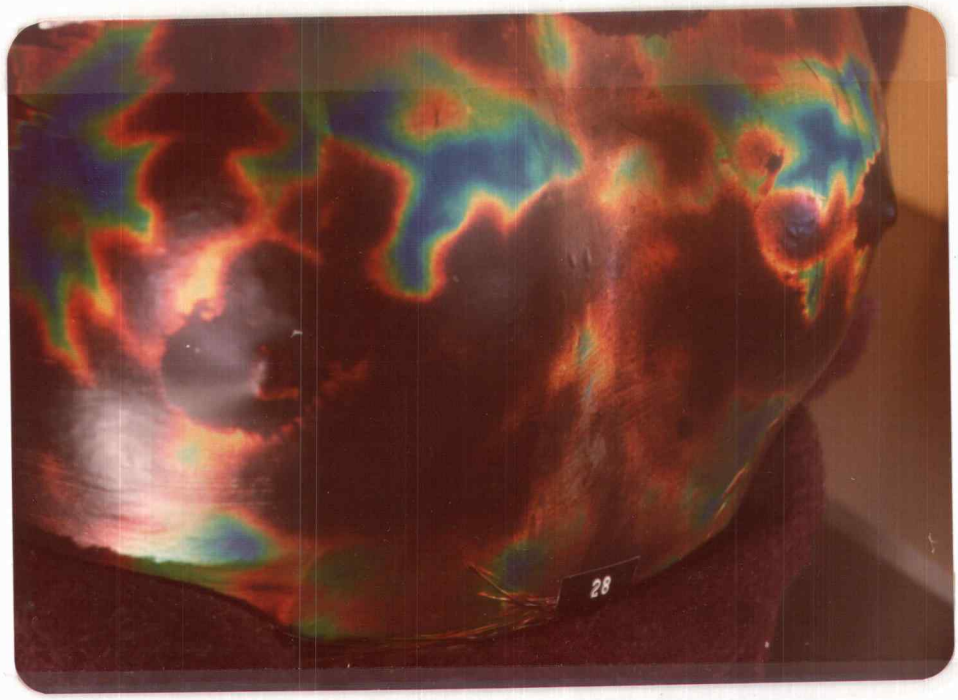

B

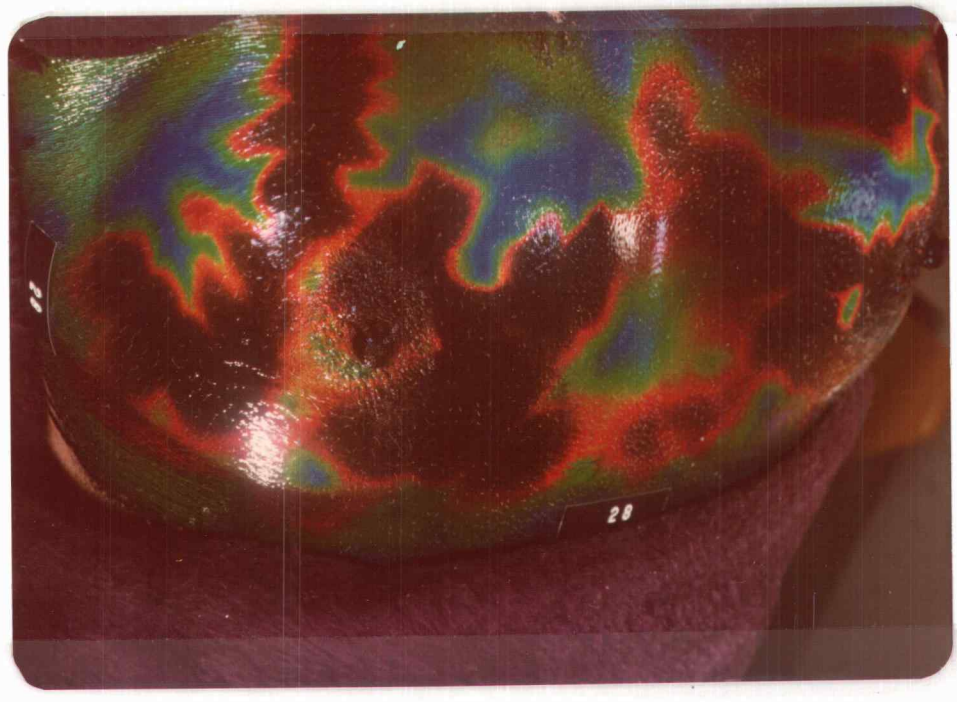

C

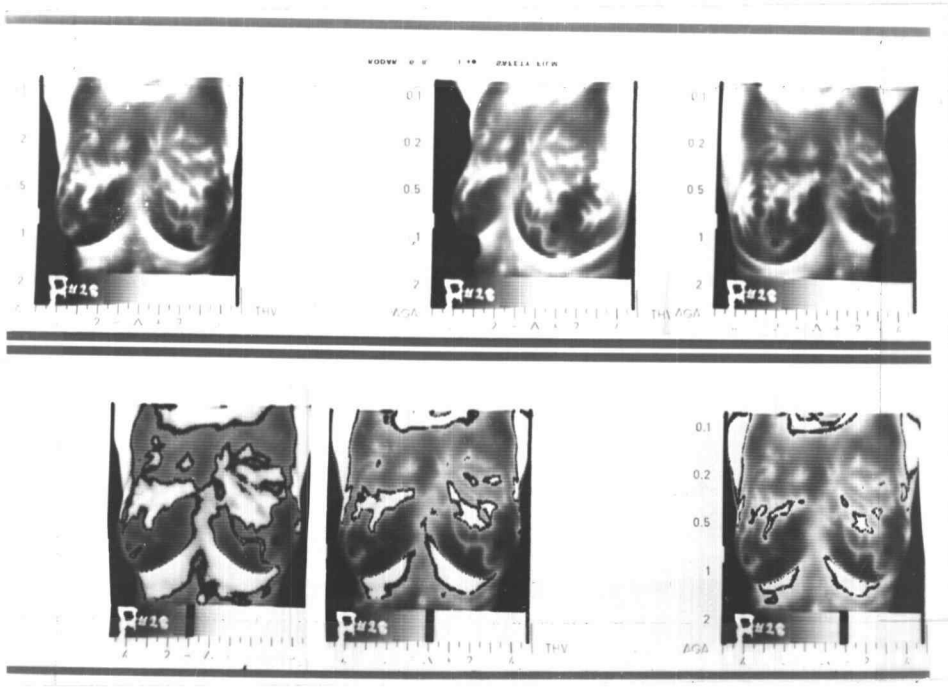

Figure 28. Breast thermograms of a normal subject (A) shows the L.C. film thermogram with range 28.2-30.2°C for (λ= 625-475 nm); (B) shows the L.C. thermogram with direct application of the L.C. (spray on) with range 28-30°C for (λ = 625-475 nm); (C) shows the corresponding IR thermogram.

A

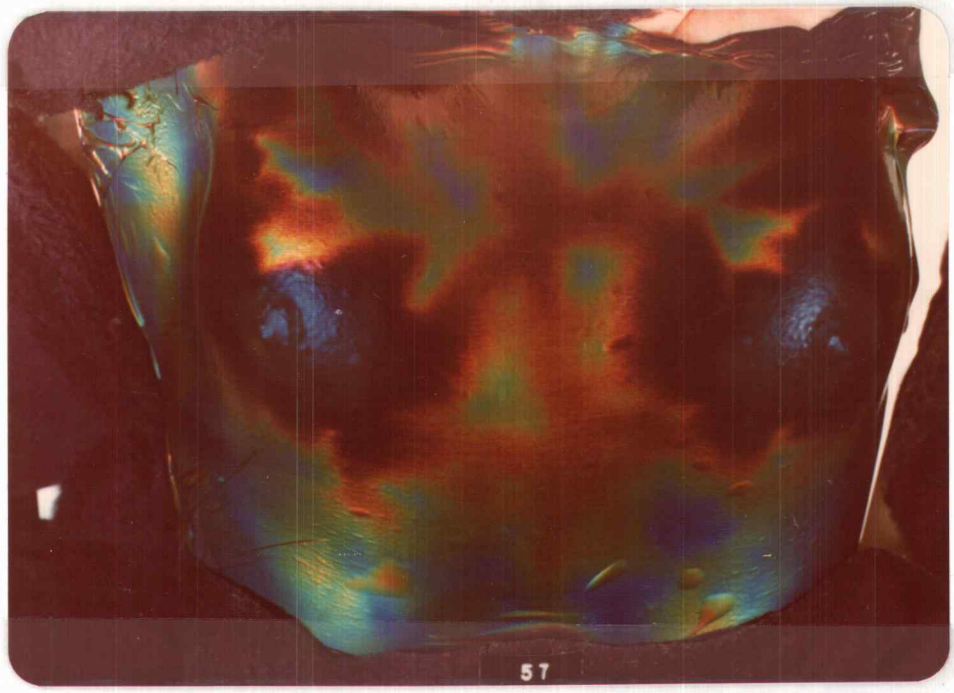

B

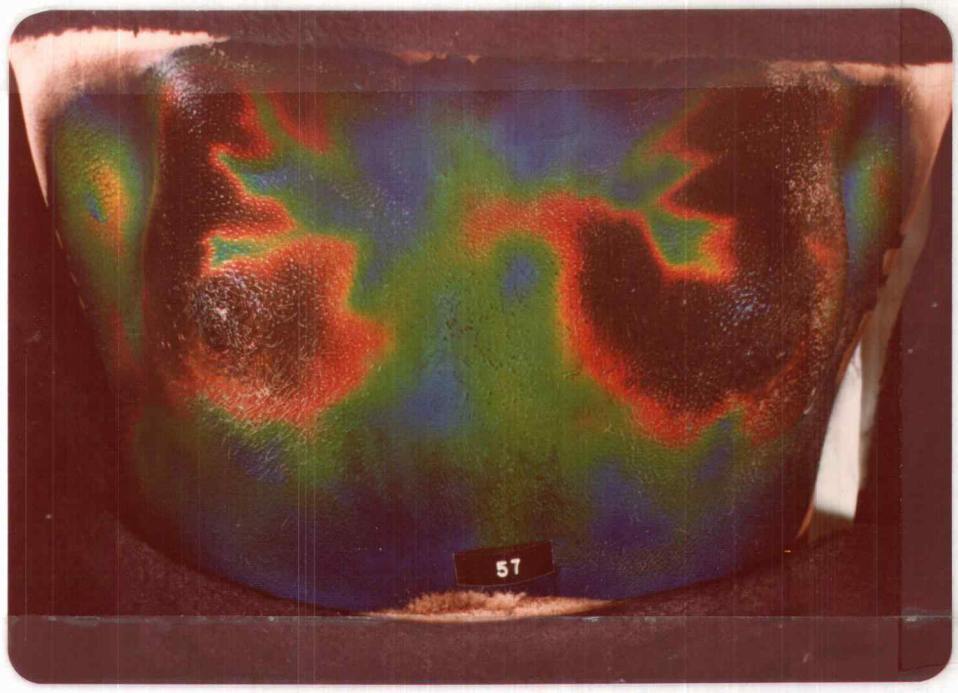

C

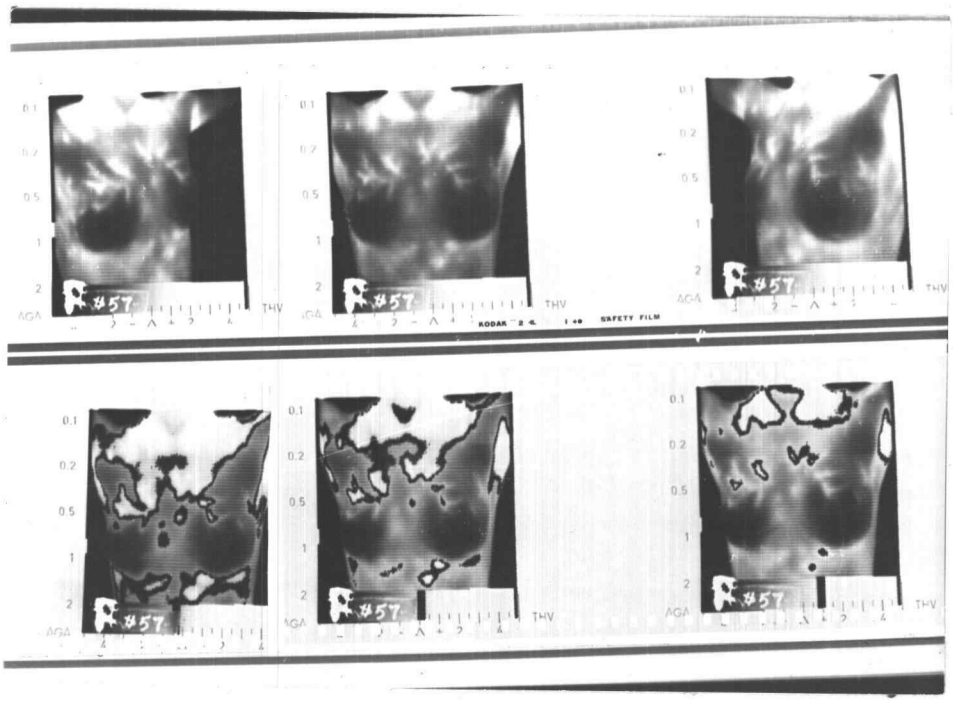

V. RESULTS AND DISCUSSION: PART II

INTERPRETATION SCHEME

The abnormal thermogram

In general the abnormal thermogram is recognized by the quantitative differences in temperatures (L.C.) or heat emission (IR) from symmetrical locations of the two breasts. The exact threshold of abnormality has not yet been established. In the presence of an inflammation of the breast, it is established that additional heat is caused.

Biologic behavior may be influenced by the histologic characteristics of a lesion, and vascularity may be altered by the metabolic activity at a cellular level (Isard,1974). It is clear that the temperature gradient between a particular tumor and the overlying skin will be influenced by the depth of the lesion and the conductivity of the subcutaneous and cutaneous lesions as Stoll (1971) and Isard (1974) have indicated.

The high resolution, temperature sensitivity and ease of interpretation of the liquid crystal thermographic method developed in this study made it possible to define all the positive thermographic signs. Some signs were considered of primary importance and others were considered of secondary importance.

Therefore, an interpretation scheme was developed based on a trinary point system which penalizes each sign by 0, 1 or 2 points depending on its abnormal significance in relation to cancer of the breast.

In this method the primary signs are penalized by 2 points, and the secondary signs are penalized by 1 point and any other signs present in the thermogram would be assigned 0 points. The primary signs are:

(1) Unilateral periareolar heat emission

(2) Unilateral inferior vascular pattern

(3) Any combination of the following unilateral vascular conditions:

A. Medial

B. Superior

C. Lateral

(4) Unilateral vascularity radiating from a point other than areola.

The secondary signs are:

(1) Unilateral focal heat emission (hot spot)

(2) Unilateral vascular condition (medial, superior or lateral)

(3) Edge sign

(4) Unilateral excess heat other than previously described.

Figure 29 shows a diagram of the different regions of the breast section.

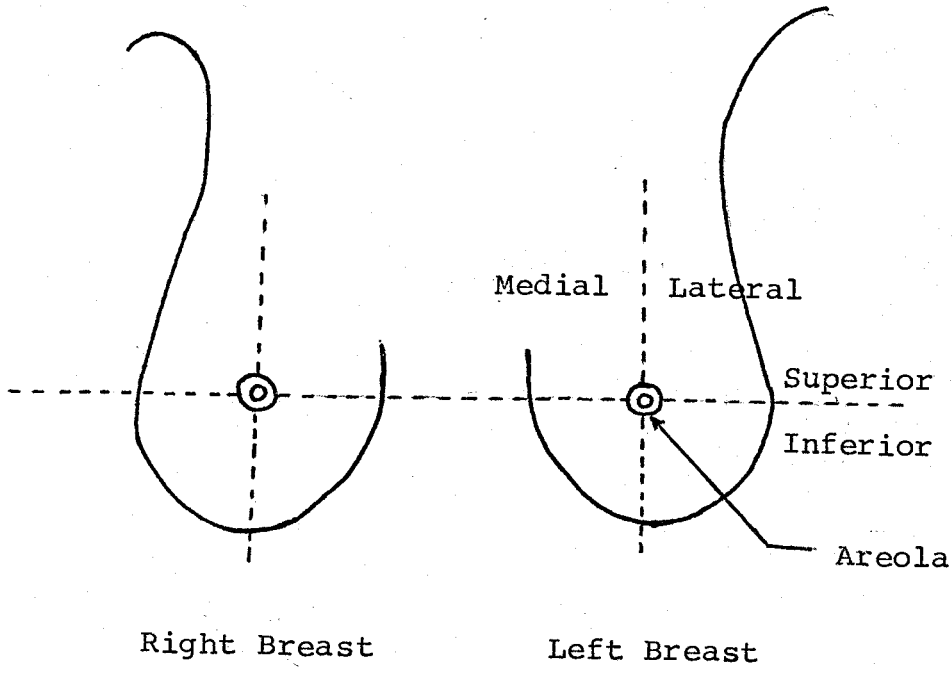

Figure 29. Diagram of the breast section

The total number of points assigned to a given thermogram are added. If the total number of points is greater than 2 points, the thermogram is considered abnormal; otherwise, it is considered normal.

In using this method, the significance level for temperature differences is $\Delta T \geq 1^{\circ}C$.

Focal heat can be a very misleading factor in the thermographic interpretation especially when associated with an avascular pattern. Then the spot will catch the attention as it stands out as an isolated phenomenon about 2-4 mm in diameter with no connection with a vessel as illustrated in Figure 30. In association with a vascular pattern, there may be a confluence of warmer vessels in a local area or an increase in heat which may be confined to a single vein. Figure 31 illustrates this case associated with a fibrocystic disease in the left breast.

It is believed that this sign accounts for a large percentage of the false positive rate encountered in IR thermography. Isard (1974) showed that this is often a characteristic of benign lesions and cysts, particularly those with pericystic inflammation and fibroadenomata.

Diffuse heat is another thermographic characteristic that deserves special attention, as it can often be confused with other vascular signs. Diffuse heat is recognized by a rather extensive zone of increased temperature

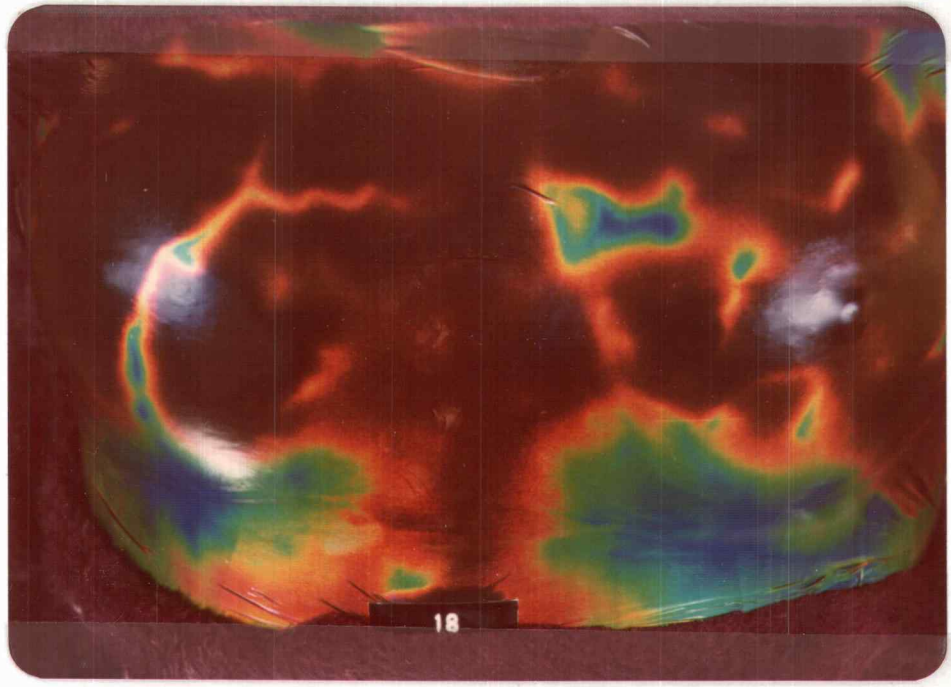

Figure 30. Liquid crystal thermogram of a case with focal heat in the left breast associated with an avascular pattern.

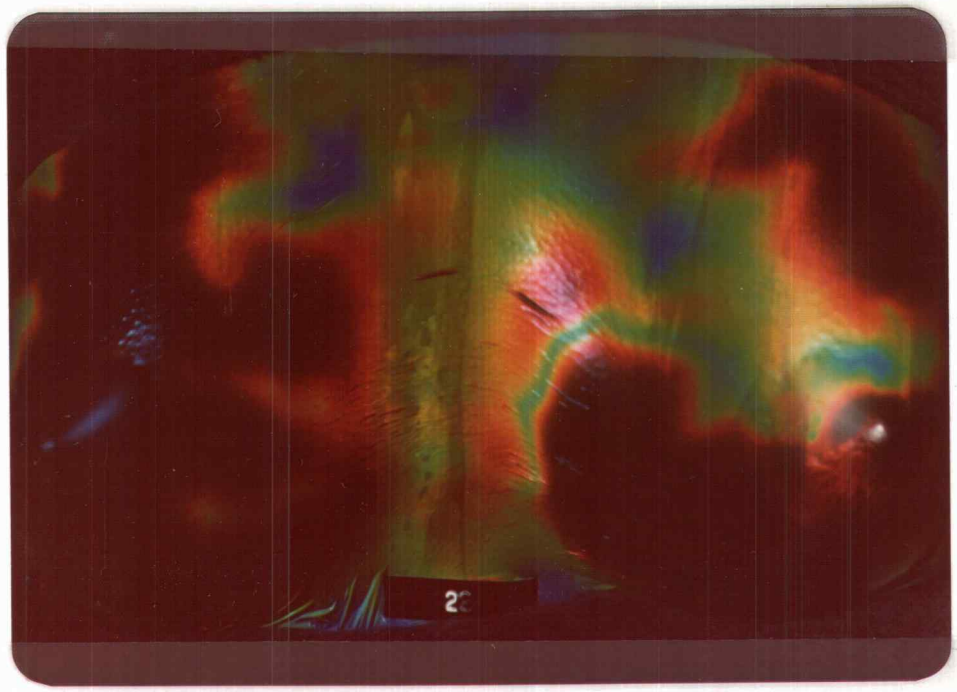

Figure 31. Liquid crystal thermogram of a case with fibrocystic disease of the left breast represented by an increase in heat confined to a single vein.

which tends to obliterate the linear vascular marks. Isard (1974) reported that it is usually quite obvious and readily discernible and that it is commonly found in the presence of acute mastitis or breast abscess with marked heat in the perialeolar area. The more severe forms of fibrocystic disease will frequently be associated with diffuse heat usually in the upper outer quadrants of the breasts (Isard, 1974). Figure 32 shows a case of diffuse heat in this study.

An additional parameter in thermographic analysis that was introduced by Isard (1972) is the "edge sign." It is the thermographic representation of skin retraction and can be recognized by the loss of the smooth symmetrical contour of the normal breast. The combination of the edge sign and any other unilateral vascular condition accentuates the suspicion of malignancy.

Figure 33 illustrates a case with a unilateral vascularity of the left breast radiating from the areola. Figures A, B are the liquid crystal thermograms using the thin film and the direct spraying respectively. The L.C. color-temperature range used in the film is 0.3°C higher than the range of L.C. material used in Figure B. Despite the slight change in ranges, it is noticed that the thermal pattern resulting from the isothermal contours in each case would be similar.

Figure 34 illustrates the comparative findings using the three modalities of a case with unilateral medial vascularity of the left breast.

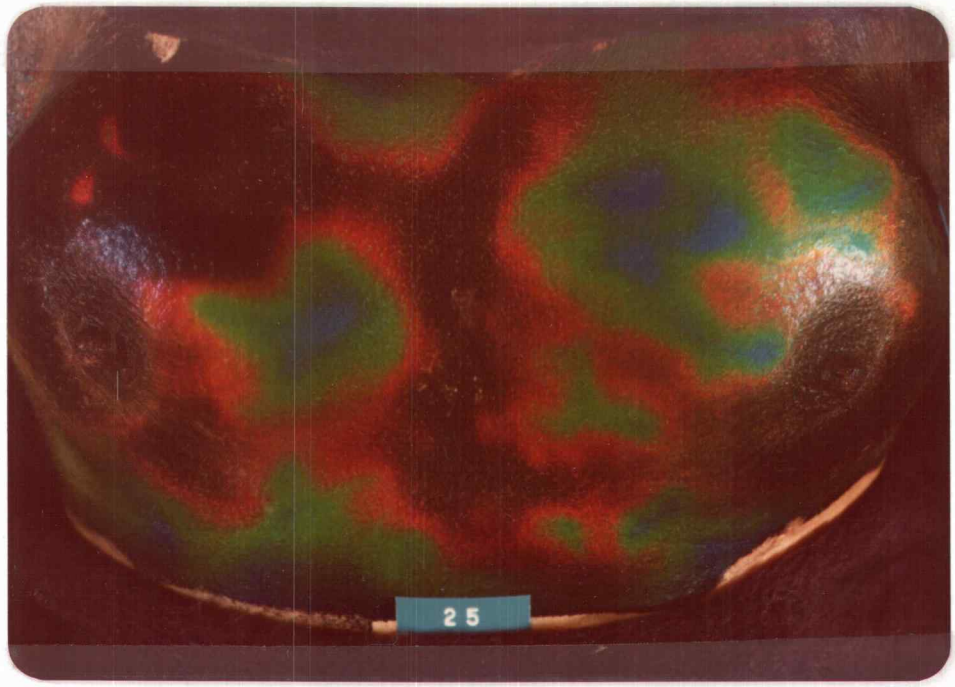

Figure 32. Liquid crystal thermogram of a case with unilateral diffuse heat in the left breast.

Figure 33 shows the comparative thermograms of a case with a unilateral vascularity of the left breast radiating from the areola. (A) shows the L.C. film thermogram showing T_1(red) = 28.3°C, T_4(green) = 29.3°C, T_5(blue) = 30.3°C; (B) shows thermogram with direct application of the liquid crystal showing T_1(red) = 28°C, T_4(green) = 29°C, T_5(blue) = 30°C; (C) shows the corresponding IR thermograms and the isotherms taken at MTL, at Δ = -1°C, at Δ = + 1°C.

A

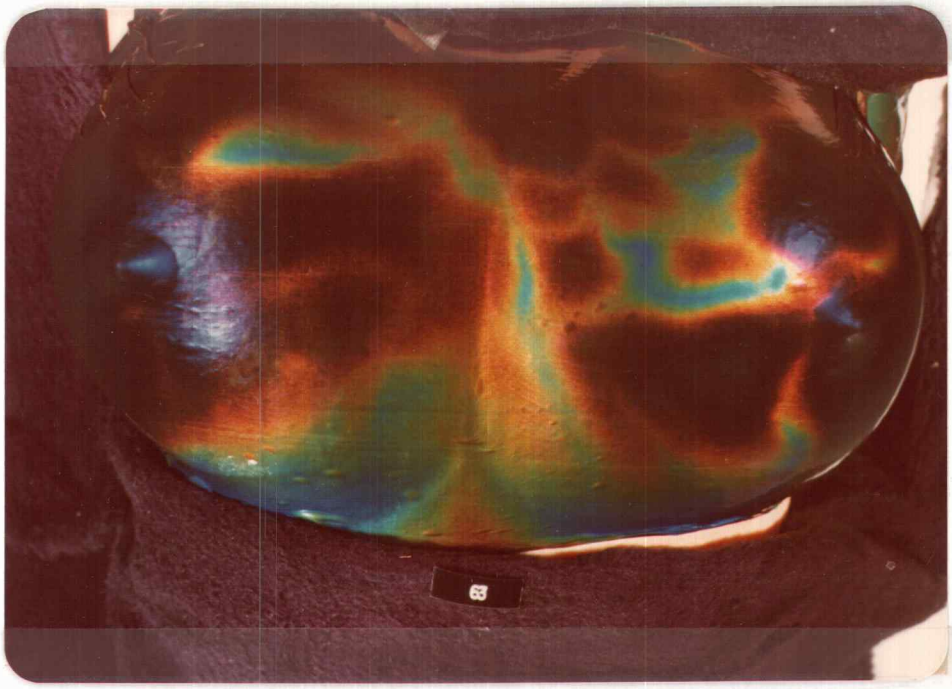

B

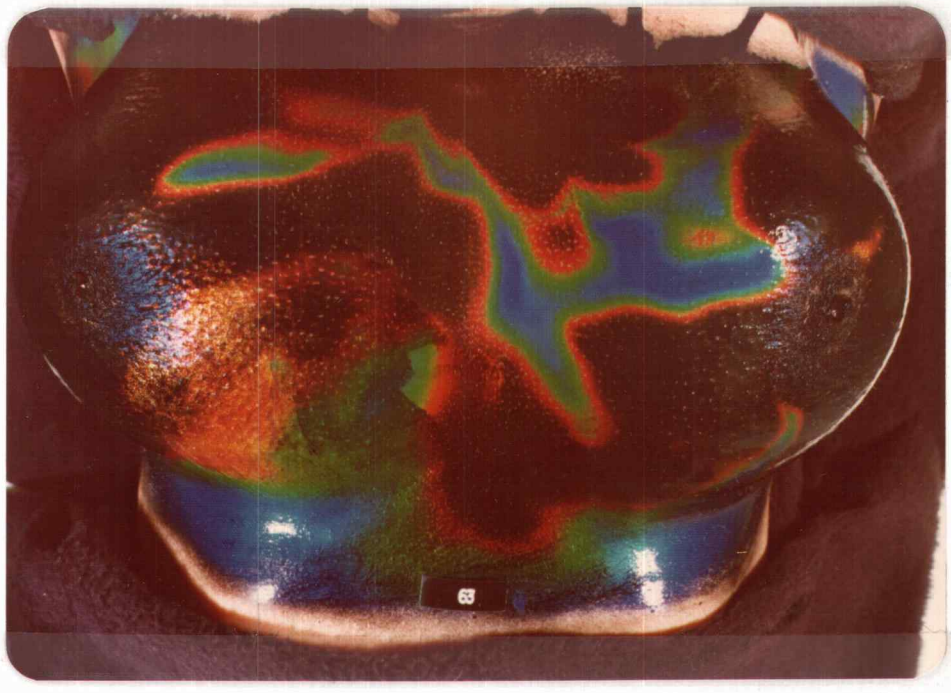

C

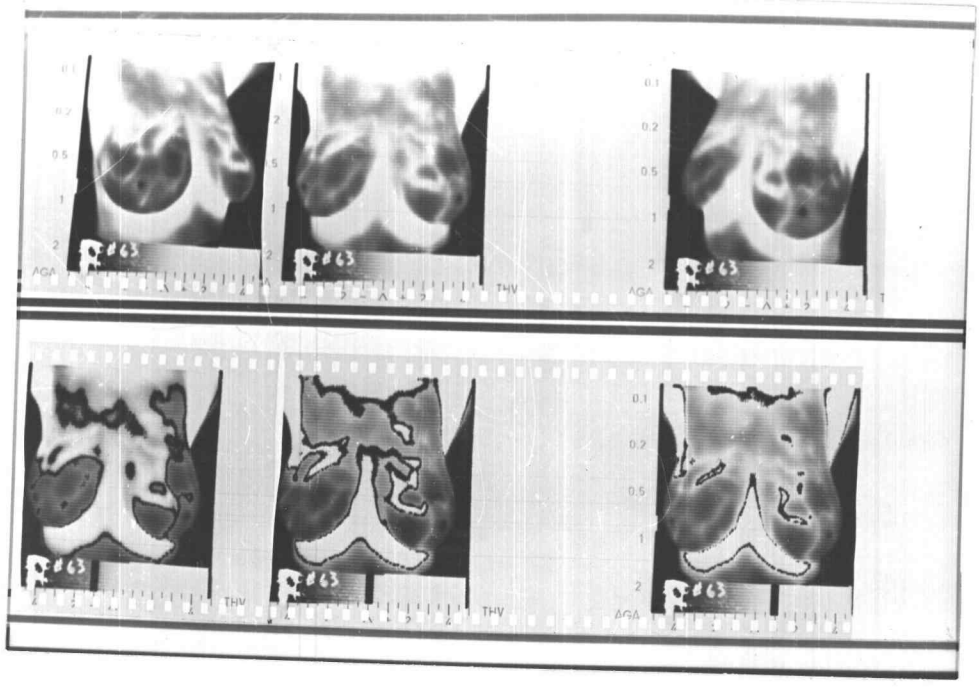

Figure 34. Comparative thermographic findings of a case showing unilateral vascular medial left breast

A. Liquid crystal elastic film

B. Liquid crystal direct spraying

C. Infrared thermogram

A

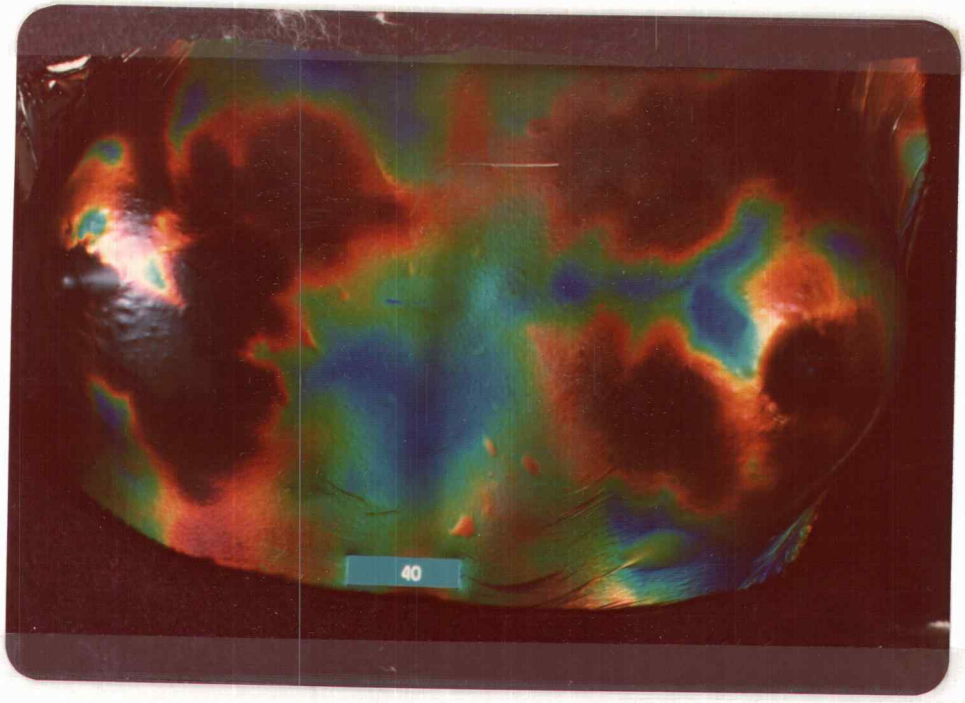

B

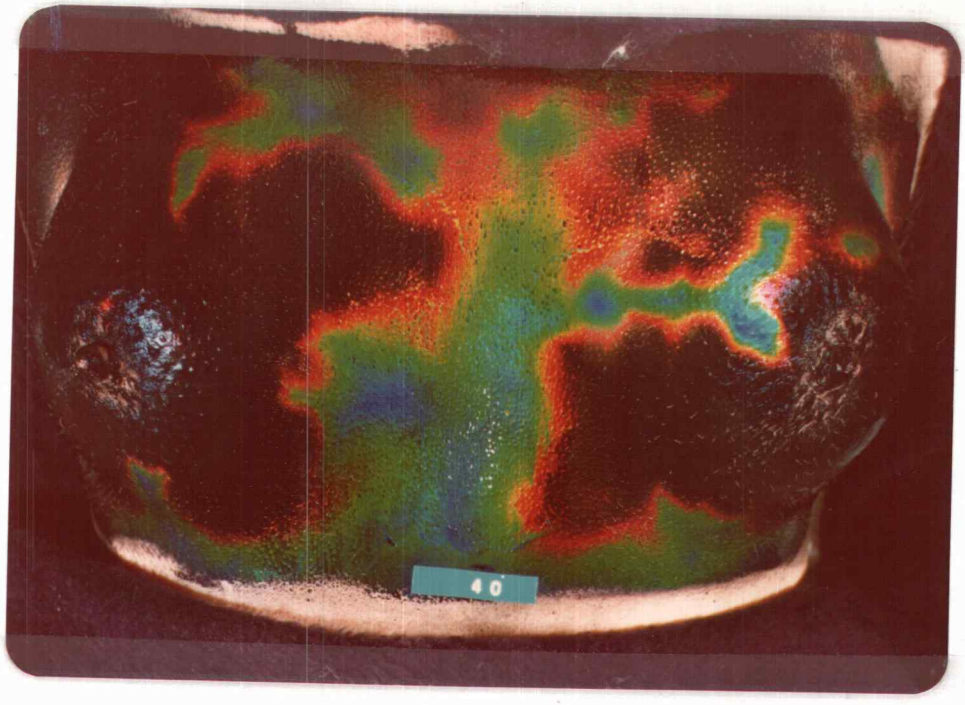

C

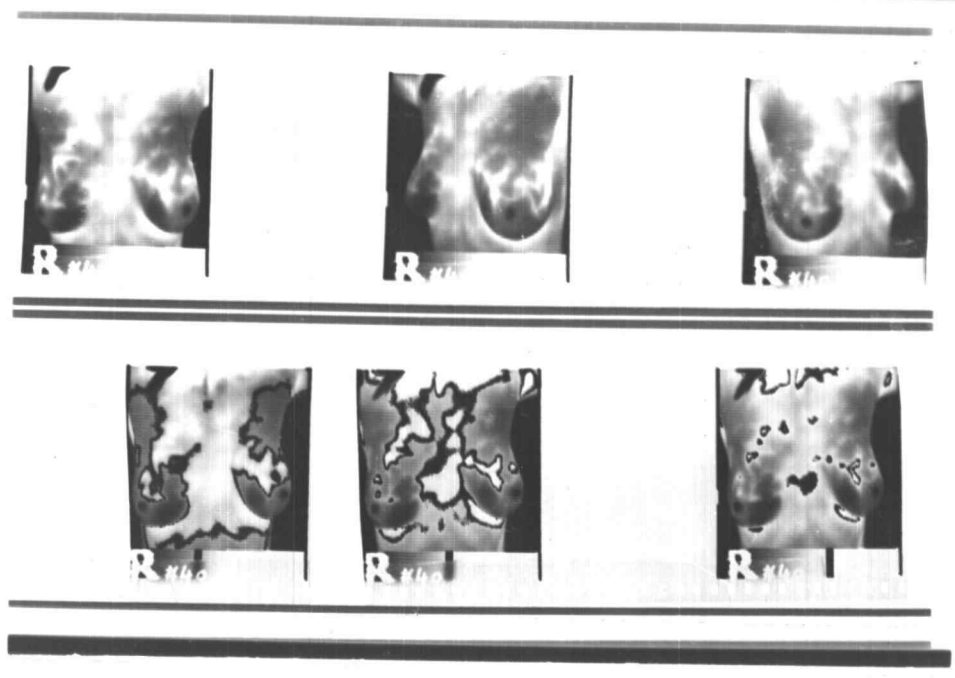

VI. RESULTS AND DISCUSSION: PART III
THE CLINICAL EVALUATION OF THE INTERPRETATION SCHEME

In this study a random sample was selected of one thousand (1000) cases of women who reported to Akron City Hospital for examination of the breast in 1974 and 1975. The age distribution of this sample is shown in Figure 35. Eight hundred twenty-four cases (82.4%) were symptomatic consisting of women who had clinically suspicious signs or who had previous history of cancer, 176 (17.6%) cases were asymptomatic.

All 1000 women had infrared thermographic examination. The thermograms were interpreted using the conventional interpretation method. There were 416 (41.6%) positive cases and 584 (58.4%) negative cases. Five hundred eighty-nine cases were examined by xeroradiography, 362 of those cases (61.46%)were cases whose thermographic findings were positive. The remaining 227 cases had a negative thermogram. The results of the xerographic examination showed 119 (20.2%) positive cases and 470 (79.8%) negative cases. One hundred one of the positive xerograms were cases that had a positive thermogram.

The 1000 IR thermograms were interpreted using the new interpretation scheme, which assigns each sign 0, 1 or

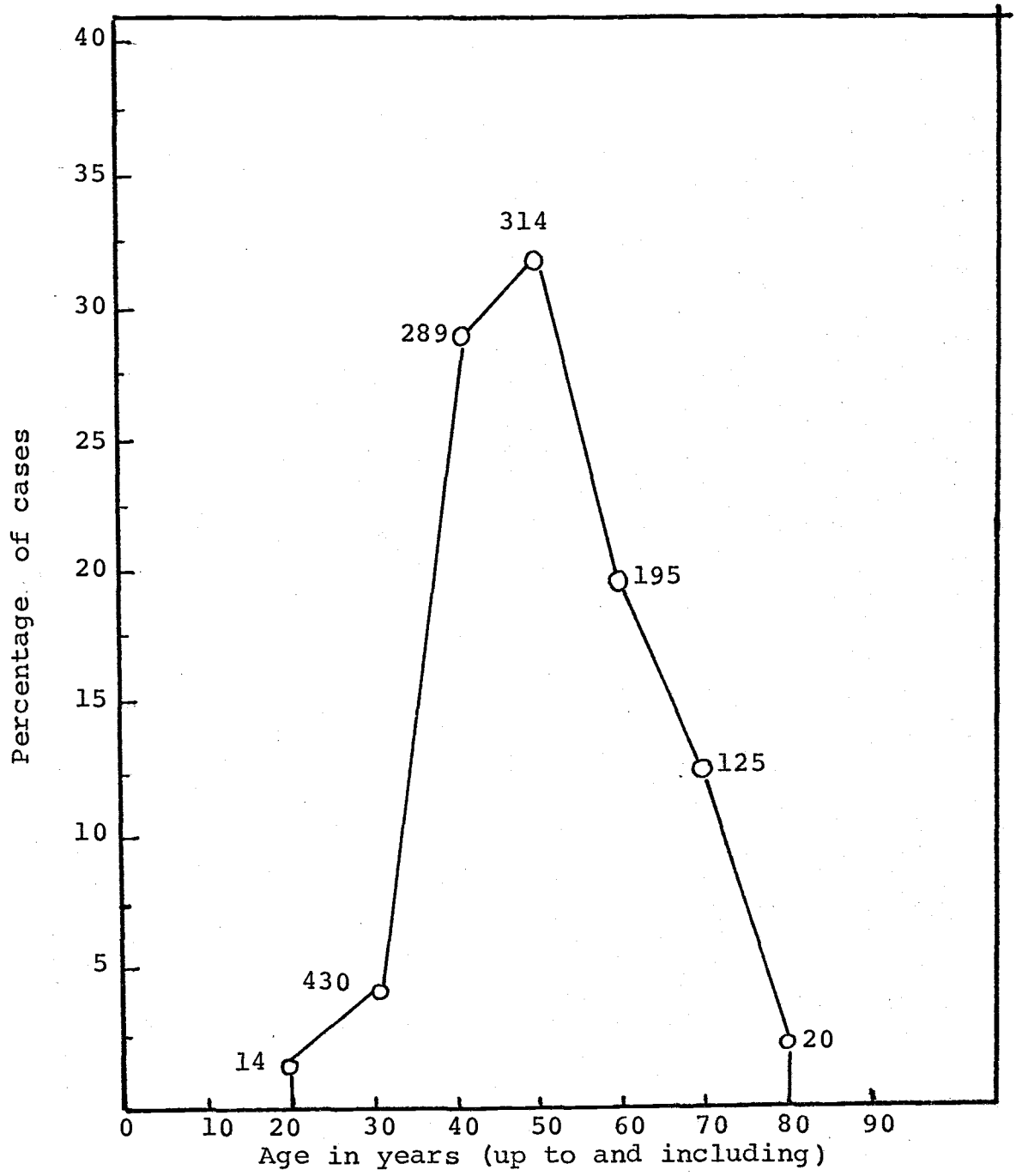

Figure 35. Age distribution of 1000 cases

2 points if the thermographic sign is nonsignificant, secondary positive or primary positive respectively, following the significance code described previously. The results showed 162 (16.2%) positive cases, 838 (83.8%) negative cases.

Seventy-one cases had histologically confirmed tissue specimens. Those represent cases that had IR thermographic, xeroradiographic and biopsy examinations. Therefore, quantitative conclusions could be drawn.

Table 3 shows the results using each modality and in the case of the thermographic results, it shows them when interpreted by conventional method and using the point system introduced in this study.

TABLE 3.--Thermographic results of 1000 patients using conventional and point system interpretation and xeroradiographic results of 589 patients

	Thermogram with Conventional Interpretation	Xerogram	Thermogram with Trinary point System
Positive	416(41.6%)	119(20.2%)	162(16.2%)
Negative	584(58.4%)	470(79.8%)	838(83.8%)
Total	1,000	589	1,000

The 71 cases that had thermographic, xerographic and biopsy studies were analyzed in detail since only through histologically confirmed tissue specimens can one

make a definite judgment of a case as being true positive, true negative, false positive involving fibrocystic disease or other benign disease of the breast or false positive involving no abnormality, or false negative.

Of the 71 cases biopsied, 17 cases (23.94%) showed evidence of malignancy (carcinoma of the breast). Fifty-four cases (76.06%) had negative biopsy reports. Of the 54 negative cases, 26 cases had a negative thermographic report and 28 cases had positive thermographic report. Of special interest it was found that out of the 28 cases that had positive thermographic findings and nonmalignant tissue specimens 17 cases (60.7%) were associated with different kinds of fibrocystic disease and represented cases with benign lesions.

The thermographic and xeroradiographic results of those 71 patients were analyzed and the findings were correlated with the biopsy reports using each of the conventional and point interpretation system independently for the thermographic evaluation. The IR conventional results showed 14 cases (82.35%) true positive, 31 cases (57.4%) false positive, 23 cases (42.6%) were true negative and 3 cases (17.65%) were false negative. The IR point interpretation system results showed 15 cases (88.23%) were true positive, 11 cases (20.37%) were false positive, 43 cases (79.6%) were true negative and 2 cases (11.77%) were false

negative. The xeroradiographic results showed 16 cases (94.12%) were true positive, 18 cases (33.33%) were false positive, 36 cases (66.67%) were true negative and 1 case (5.88%) was false negative. Table 3 shows those results grouped.

Discussion and sample cases

The results shown in Table 4 indicate the effectiveness of the point system in thermographic interpretation. As a result of the point system, the true positive rate was increased by 7.14% and most importantly the false positive was decreased by 64.5%. This also resulted in an increase in the true negative rate by 86.8% and a decrease in the false negative rate of 33.18%.

TABLE 4.--Thermographic, xeroradiographic and biopsy comparative diagnosis of 71 histologically confirmed tissue specimens

	Thermography	Xerography	Biopsy	Thermography with Point System
Positive	45(63.4%)	34(47.8%)	17(23.9%)	26(36.6%)
Negative	26(36.6%)	37(52.2%)	54(76.1%)	45(63.4%)
True Positive	14(82.4%)	16(94.1%)	17(100%)	15(88.2%)
False Positive	31(57.4%	18(33.3%)		11(20.4%)
True Negative	23(42.6%)	36(66.7%)	54(100%)	43(79.6%)
False Negative	3(17.6%)	1(5.9%)		2(11.8%)
Total	71	71	71	71

The most important change was in the false positive rate as it consisted the major drawback in the use of infrared thermography. Naturally, as a result of the large decrease in the false positive rate using the point system, the other reliability statistics have improved accordingly. It is also important to note that of the 11 cases reported as false positive using the point system, 9 cases (81.8%) were associated with fibrocystic disease.

The value of xeroradiography in the localization of malignant tumors should not be ignored. This sutdy has shown that the use of thermography with the new interpretation scheme in conjunction with xeroradiography in a mass-screening situation would result in highly reliable diagnostic findings.

Figure 36 shows the thermographic and xeroradiographic findings of a case involving a large carcinoma in the subareolar region of the left breast. The thermogram illustrates a case involving the edge sign in the left breast in addition to unilateral vascular and periareolar heat emission of the left breast. The localization of the cancerous lesion is shown in the xerogram, an important factor in the surgical procedure.

Figure 37 shows another case of carcinoma of the left breast. In this case the thermographic signs are very distinct as unilateral vascular involving the lateral

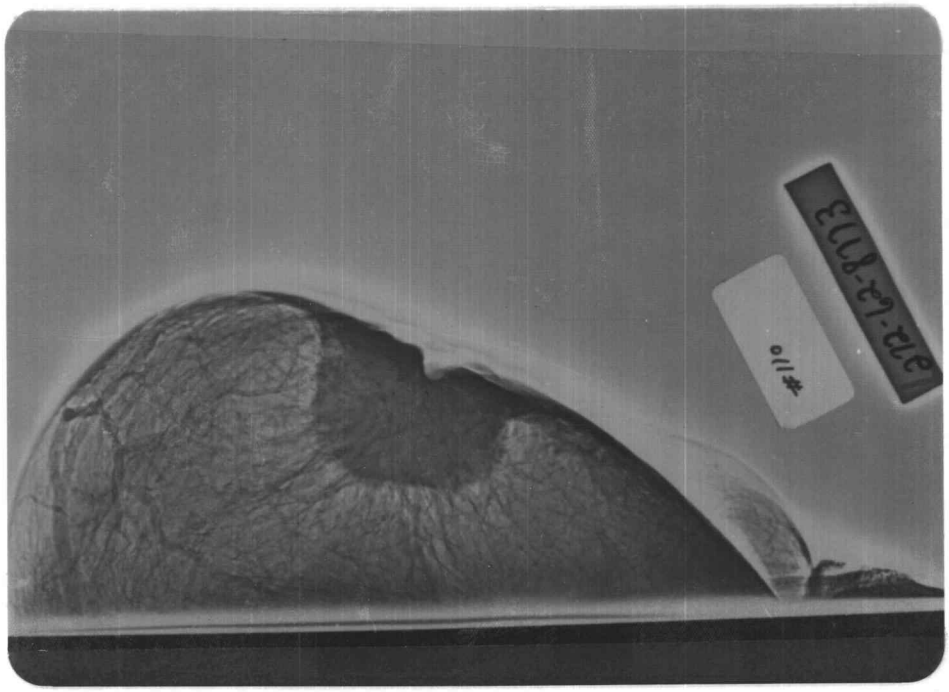

Figure 36. Xerogram of a case with large carcinoma in the subareolar region of the left breast.

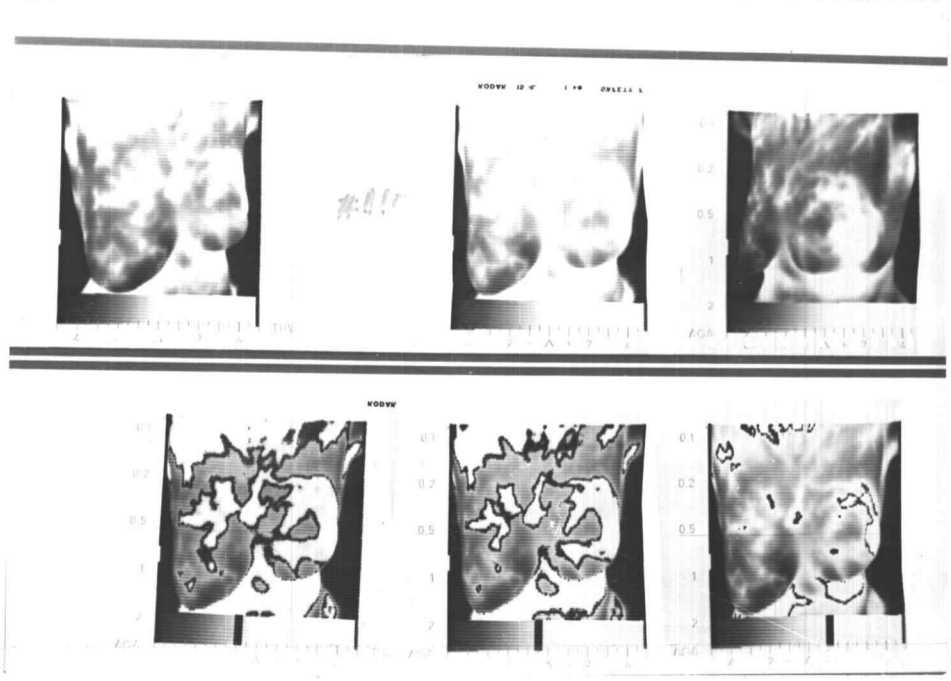

Corresponding thermogram with edge sign, unilateral vascular and periareolar heat emission in the left breast.

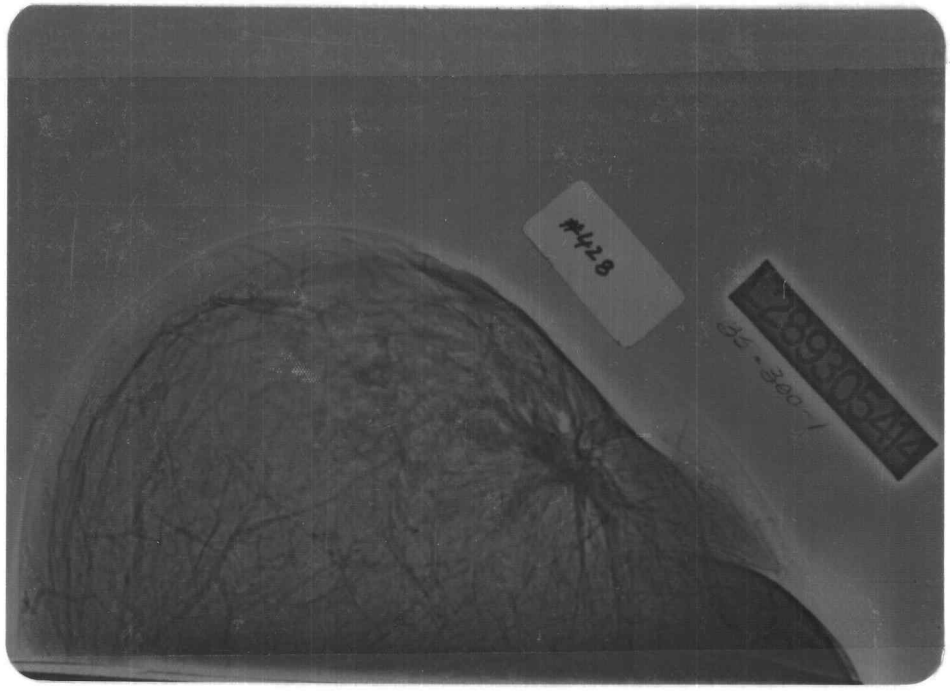

Figure 37. Xerogram of a case with carcinoma within the upper and lateral quadrant of the left breast appearing as less than one millimiter calcification.

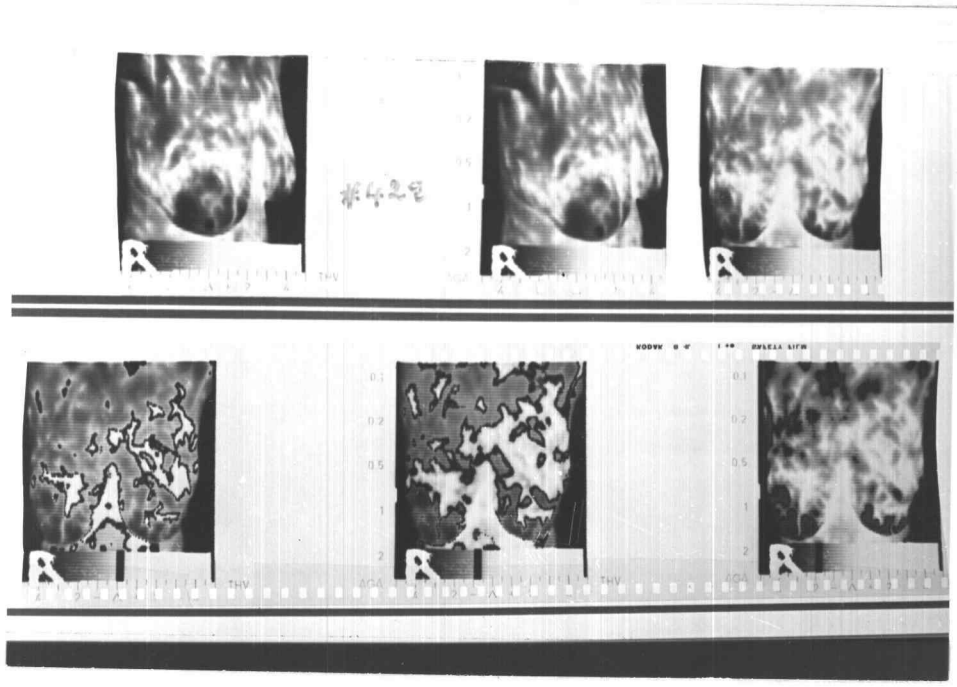

Corresponding thermogram; a very clear evidence of abnormality involving the upper and lateral quandrant of the left breast.

quadrant of the left breast. The xerogram findings were positive, but, as shown in the figure, the abnormality is not as obvious in the xerogram as in the thermogram.

Figure 38 shows a case of carcinoma of the left breast above and just lateral to the subareolar area. The thermographic signs in this case are univascular medial and lateral and inferior and periareolar heat emission in the left breast. The mass lesion is well defined in the xerogram as shown by the darker approximately 6 mm diameter region.

Figure 39 is an illustration of a case of carcinoma of the right breast. The thermogram shows an intense unilateral inferior vascular and periareolar heat emission of the right breast. The corresponding xerogram shows an area of soft tissue mass density with irregular margins and containing a number of microcalcifications in the lateral quadrant of the right breast at the level of the nipple.

Table 5 shows the diagnosis of different thermographic findings presented in this study using the trinary point system and the corresponding positive signs in each case.

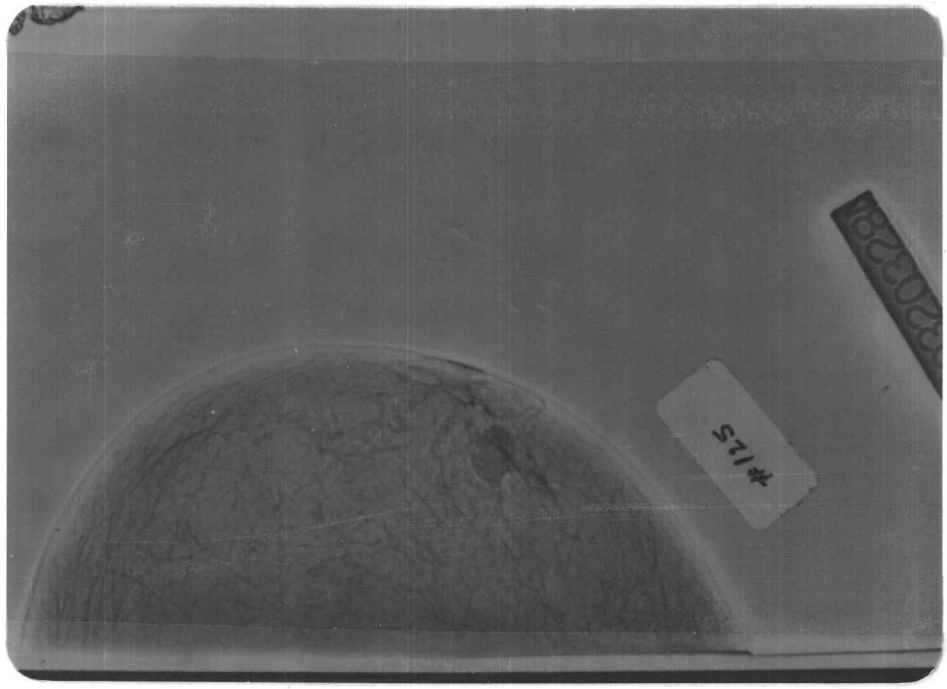

Figure 38. Xerogram of a case of carcinoma of the left breast above and just lateral to the subareolar area.

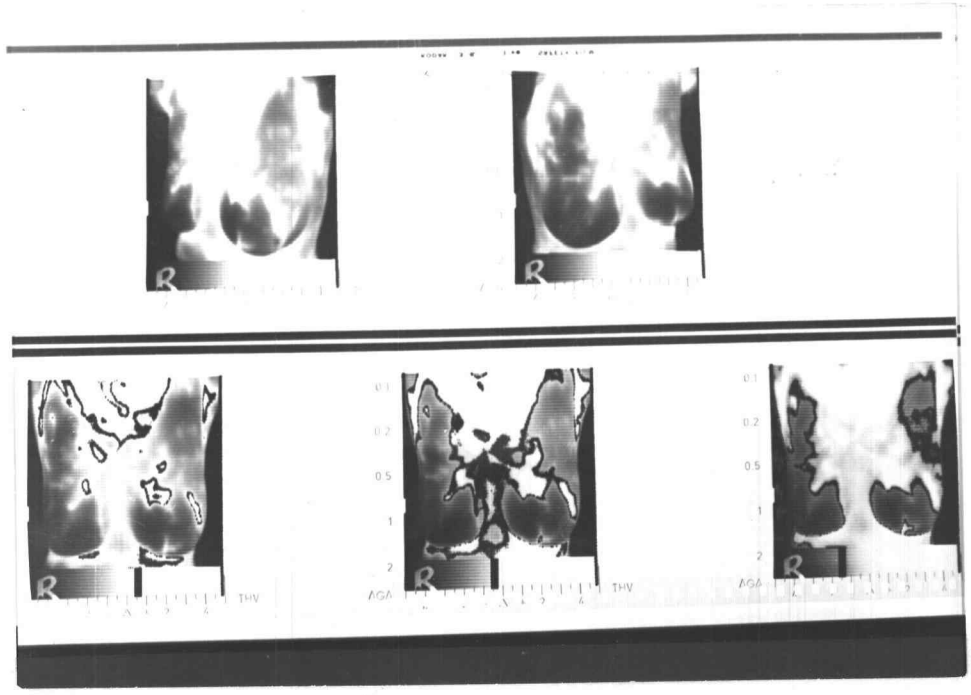

Corresponding abnormal thermogram showing intense unilateral vascular and inferior heat emission of the left breast.

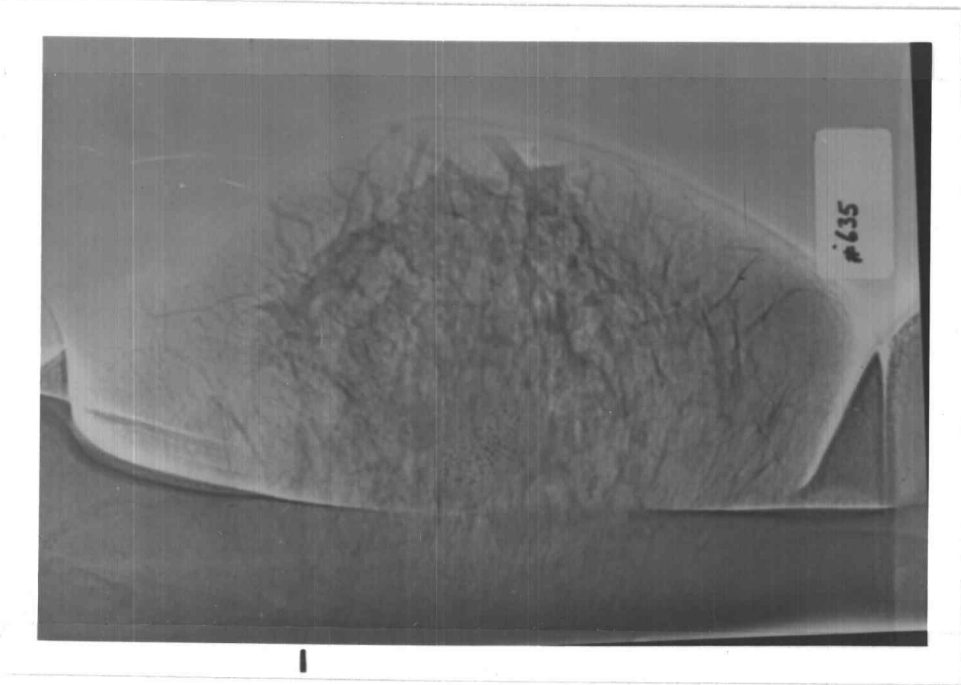

Figure 39. Xerogram of case of carcinoma of the right breast shown as multitudes of micro-calcifications in the lateral quadrant at the level of the nipple.

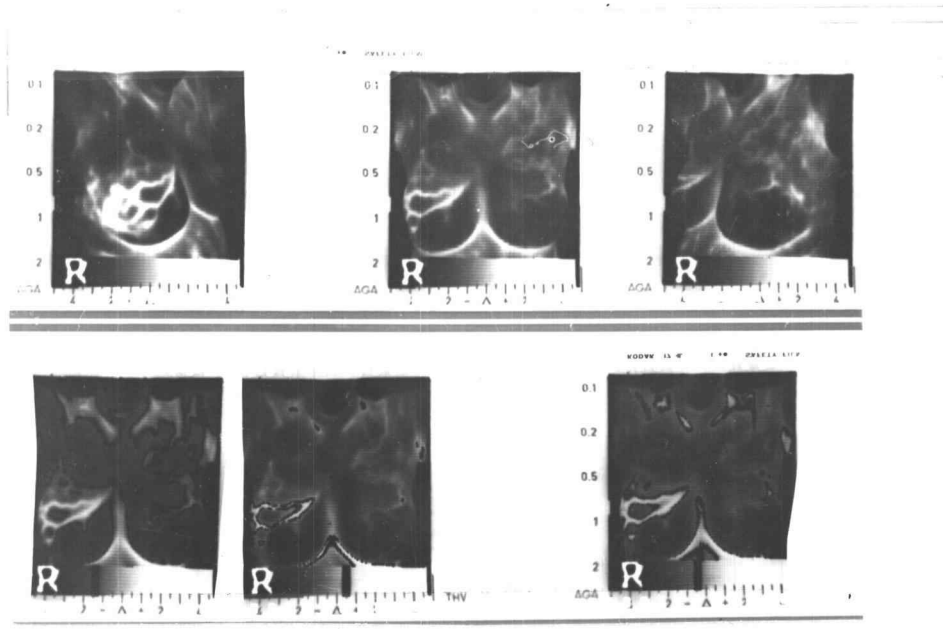

Corresponding thermogram with abnormal signs showing an intense unilateral inferior vascular and periareolar heat emission of the right breast.

TABLE 5.--Illustration of thermographic evaluation using trinary point system

Figure Number	Total No. of Points	Positive Thermographic Signs	Diagnosis
26	0	None	Negative
28	0	None	Negative
30	1	Hot spot (left breast)	Negative
32	1	Diffuse heat (left breast)	Negative
31	2	Unilateral medial + hot spot (left breast)	Negative
33	2	Unilateral periareolar heat emission (left breast)	Negative
37	3	Periareolar + unilateral superior heat emission (left breast)	Positive carcinoma of the left breast
39	3	Periareolar + unilateral medial heat emission (right breast)	Positive carcinoma of the right breast
36	4	Unilateral inferior + lateral heat emission + edge sign (left breast)	Positive carcinoma of the left breast
38	5	Periareolar + unilateral inferior + lateral heat emission (left breast)	Positive carcinoma of the left breast

As can be seen from those cases, the use of the new interpretation scheme makes the thermographic evaluation a systematic procedure that can be applied easily and in doing so, transforms it from an art that is totally dependent on the experience of the reader to a science that yields consistent results regardless of the experience of the reader.

VII. CONCLUSIONS AND SUGGESTIONS

This study has demonstrated that the elastic thin film liquid crystal thermography system developed through the course of this work is a reliable inexpensive tool that can be used in hospitals and clinics. The comparative study using three thermographic modalities is the first of its nature and has proven that liquid crystal thermography offers all the thermographic features of infrared thermography, and in addition, offers other desirable characteristics in terms of spatial resolution, ease of interpretation and cost.

The point system for thermographic interpretation developed in this study proved to be effective and consistent in the 1000 case study and resulted in a 64.5% decrease in the false positive rate obtained otherwise. The adoption of this scheme in thermographic evaluation is expected to change the scope and reliability of both infrared and liquid crystal thermography.

Breast cancer is the major malignant lesion and the leading cause of death from cancer in women in the United States. The necessity of a method to screen women in order to detect early breast cancer is obvious. A survey of the existing methods for breast cancer detection reveals that the high initial cost of infrared thermography and

xeroradiography and the time and efforts required by technicians and radiologists in xeroradiography result in long waiting periods until tumors are palpable. Carcinomas then are found large and spread. Also, the use of X-ray radiation in xeroradiography suggests its use as a follow up method in cases with positive thermograms rather than as a screening tool since periodical check up may result in excessive radiation which in itself could induce cancer.

The initial cost for a liquid crystal thermography set up is estimated to be less than 1,000 U.S. dollars, and the thermographic examination is estimated to cost approximately $5.00 per patient in a mass-screening situation. This should be compared to a current charge of $20.00-$30.00 for infrared thermography per patient and $35.00-$50.00 for xeroradiography examination per patient depending on the place of the examination.

While thermography does not localize cancer and in some cases does not differentiate malignant from benign cases, it can serve as a thermal signal of abnormality. Furthermore, its total safety, lack of irradiation and minimal expense make it a very attractive modality. Its use as a primary screening tool in conjunction with xeroradiography as a follow up on positive thermograms as was done in this study is recommended as it yields optimum results.

The total potential of the elastic thin film liquid crystal thermography technique is yet to be realized. This work has been just a starting point of an entirely new branch of liquid crystal thermography. Researchers have started using the technology developed in this study to explore its full potential in clinical diagnosis. It is suggested to evaluate the new technique developed in this study in the potential diagnosis of pulmonary and occlusive vascular disease, peripheral vascular disease, placental location and other related studies that have been done previously using infrared thermography because the liquid crystal thin film technique offers a less expensive, easier and equally reliable tool.

It is suggested for future comparative thermographic study that every case with positive thermographic findings be followed up by a xeroradiographic examination and a tissue specimen study regardless of the xeroradiographic diagnosis. A study of this nature would answer some of the questions concerning the false positive occurrence in thermography and its relation to early detection of breast cancer. A follow up examination of all the false positive cases after a period of six months from the original examination is also suggested.

It is clear that none of the existing diagnostic tools for breast cancer including thermography is able to detect every malignant lesion. A question that deserves

further investigation is whether the lack of confirmation is related to the size, location, or biologic behavior of the tumor or to the nature of the underlying breast matrix, and whether some subtle thermal changes defy recognition.

BIBLIOGRAPHY

Aartz, N. J. 1967. Some experience with thermography. Journal de Radiologie d'Electrologie et de Medecine Nucleaire. Paris, 48:76-79.

Aartz, N. J. 1969. The use of thermography in the detection of breast cancer. Bibliotheca Radiologica. 5:40-52.

Adams, J. et al. 1969. Light-scattering properties of cholesteric liquid crystals films. Molecular crystals and liquid crystals. 8:9-18.

Bothmann, G., F. Kubli. 1974. Vortrag auf dem I Europe Thermographiekongreb, Amsterdam.

Brasfield, R. D., J. S. Laughlin, and R. S. Sherman. 1964. Thermography in the management of cancer: A preliminary report. Annals New York Academy of Sciences. 121-135.

Brebner, D. M. et al. 1974. An introduction to xeroradiography. South Africa Medical Journal. 43(55):2289-2291.

Carroll, P. 1973. Cholesteric liquid crystals: Their technology and applications. London, Ovum Ltd. 280 pp.

Crissey, J. T., E. Gordy, J. L. Fergason, and R. B. Lyman. 1964. A new technique for the demonstration of skin temperature patterns. Journal of Investigative Dermatology. 43:89-92.

Crissey, J. T., J. L. Fergason, and J. M. Bettenhausen. 1965. Cutaneous thermography with liquid crystals. Journal of Investigative Dermatology. 45(5):329-333.

Davey, J. B., W. P. Greening, J. A. McKinna. 1970. Is screening for cancer worthwhile? Results from Well Woman Clinic for Cancer Detection. British Medical Journal. 3:696-699.

Davison, T. W. 1971. Liquid crystal thermographic patterns of normal and abnormal human breast. Master's thesis. Kent, Kent State University. 80 numb. leaves.

Davison, T. W., K. L. Ewing, J. L. Fergason, M. Chapman, A. Can, and C. C. Vorrhis. 1972. Detection of breast cancer by liquid crystal thermography: A preliminary report. Cancer. 29(5):1123-1132.

Delarue, N. C. 1969. The challenge of breast cancer. Time for reappraisal of management. Applied Therapeutics. 11:381-386.

De Vries, Hl. 1951. Rotary power and other optical properties of certain liquid crystals. Acta Crystal Lographica. 4:219-226.

Dodd, G. D., J. D. Wallace, I. M. Freundlich, L. Marsh, and A. Zermino. 1969a. Thermography and cancer of the breast. Cancer. 23:797-802.

Dodd, G. D., A. Zermino, L. Marsh, D. Boyd, and J. D. Wallace. 1969b. New developments in breast thermography: High spatial resolution. Cancer. 25:468-477.

Draper, J. W., and C. H. Jones. 1969. Thermal patterns of the female breast. The British Journal of Radiology. 42:401-410.

Evers, R. et al. 1973. Principles and techniques of xeroradiography. Roentgenbaetter. 26:544-553.

Farrell, C., J. D. Wallace, and C. M. Mansfield. 1971. The use of thermography in detection of metastatic breast cancer.

Farrow, J. H. 1969. The James Ewing Lecture, current concepts in the detection and treatment of the earliest of breast cancers. Cancer. 25:468-477.

Fergason, J. L. 1964. Liquid crystals. Scientific American. 211:75-85.

Fergason, J. L. 1965a. Cholesteric structure--Part I optical properties. Proceedings of the International Conference on Liquid Crystals held at Kent State University, August, 1965.

Fergason, J. L. 1965b. Cholesteric structure--Part II Chemical significance. Proceedings of the International Conference on Liquid Crystals held at Kent State University, August, 1965.

Fergason, J. L. 1966. Cholesteric structure--Part III Thermal mapping. New York Academy of Sciences. 29:26-34.

Fergason, J. L. 1968. Liquid crystals in non-destructive testing. Applied optics. 7(9):1729-1739.

Fochem, K. et al. 1974. Plate thermography: A new method of mammary examination. A preliminary report. Wiener Klinische Wochenschrift. 86(21):664-666.

Forrest, A. P., and I. H. Gravelle. 1969. Diagnosis of cancer of the breasts with special reference to mammography and thermography. Practicioner. 203: 137-145.

Freurdlich, I. M., J. D. Wallace, and G. D. Dodd. 1968. Thermography and the venous diameter ration in the detection of non-palpable breast carcinoma. American Journal of Roentgenology, Radium Therapy and Nuclear Medicine. 102(4):927-932.

Gautherie, M., Y. Queneville, and C. Gros. 1974. Thermographie Cholesterique, Feuilles de cristaux liquides. Applications cliniques, pharmacologiques et physiologiques et confrontation avec la thermographi-infrarouge. Pathologie et Biologie (Paris). 22(7): 553-566.

Gershon-Cohen, J. 1964. A short history of medical thermometry. Annals New York Academy of Sciences. 121:4-11.

Gershon-Cohen, J., J. D. Haberman-Brueschke, and E. E. Brueschke. 1965. Medical thermography: A summary of current status. The radiologic Clinics of North America. 3:403-431.

Gershon-Cohen, J., M. B. Hermel, M. G. Murdock. 1970. Priorities in breast cancer detection. New England Journal of Medicine. 283(2):82-85.

Gershon-Cohen, J. 1971. Imperative changes in detection methods for breast cancer. Southern Medical Journal. 64:387-391.

Hardy, J. D., H. Hammel, and D. Murgatroyd. 1956. Spectral transmittance and reflectance of excised human skin. Journal of applied physiology. 40:257-264.

Harris, D. L., W. P. Greening, and P. M. Aichnoth. 1966. Infrared in the diagnosis of a lump in the breast. British Journal of Cancer. 20:701-721.

Hensel, H. 1952. Physiologie der Thermoreception. Ergebnisse der Physiologie. 47:166-368.

Hitchcock, C. R., D. F. Hitchcock, J. Sancheray, T. Moulton, and R. Baker. 1968. Thermography in breast cancer screening. Journal of the American Medical Association. 204:419-422.

Hoffman, R. L. 1967. Thermography in the detection of breast malignancy. American Journal of Obstetrics and Gynecology. 98(5):681-685.

Isard, H. J., and R. Shilo. 1968. Breast thermography. American Journal of Roentgenology. 103(4)921-925.

Isard, H. J., B. J. Ostrum, and R. Shilo. 1969. Thermography and breast carcinoma. Surgery, Gynecology, and Obstetrics. 128:1289-1293.

Isard, H. J. 1972. Thermographic "edge sign" in breast carcinoma. Cancer. 30:957-963.

Isard, H. J., and B. J. Ostrum. 1974. Breast Thermography--The Mammatherm. Radiologic Clinics of North America. XII(1):167-188.

Jones, C. H. 1969. Interpretation of problems in thermography of the female breast. Bibliotheca Radiologica. 5:96-108.

Lapayowker, M. S., H. L. Kundel, and M. Ziskin. 1971. Thermographic patterns of the female breast the their relationship to carcinoma. Cancer. 27:819-822.

Lawson, R. 1956. Implications of surface temperatures in the diagnosis of breast cancer. Canadian Medical Association Journal. 75:309-310.

Lawson, R. 1957. Thermography--A new tool in the investigation of breast lesions. Canadian Service Medical Journal. 13:517.

Lilienfield, A. M., J. M. Barnes, R. B. Barnes, R. Brasfield, J. F. Cannel, E. Diamond, J. Gershon-Cohen, J. Haberman, H. J. Isard, N. Z. Lane, R. Lottis, J. Miller, W. Seaman, and R. Sherman. 1969. An evaluation of thermography in the detection of breast cancer. Cancer. 24:1206-1271.

Lloyd-Williams, K., F. L. Lloyd-Williams, R. S. Handley. 1960. Infrared radiation thermometry in clinical practice. The Lancet. 2:1378-1381.

Lloyd-Williams, K., F. Lloyd-Williams, and R. S. Handley. 1961. Infrared thermometry in diagnosis of breast disease. The Lancet. 2:1378-1381.

Lloyd-Williams, K. 1964. Temperature measurement in breast disease. Annals New York Academy of Sciences. 121: 272-281.

Malone, L. J., G. Frankl, R. Dorazio, and J. Winkley. 1975. Occult breast carcinomas detected by xeroradiography: Clinical considerations. Annals of Surgery. 181(2): 133-136.

Massapust, L. C., and W. D. Gardner. 1953. The infrared phlebogram in the diagnosis of breast complaints. Surgical Gynecology and Obstetrics. 97:612-626.

McMahon, H. O. 1950. Thermoradiation from partially transparent reflecting bodies. Optical Society of America. 40:257-264.

Selawry, O. S., H. S. Selawry, and J. F. Holland. 1966. The use of liquid cholesteric crystals for thermographic measurement of skin temperature in man. Proceedings of the International Conference on Liquid Crystals held at Kent State University, August 16-20, 1965.

Shaw, G. D. 1969. Experience with thermography in mass-screening of breast tumors. Bibliotheca Radiologica. 5:109-119.

Steketee, J. 1973. The effect of transmission on temperature measurements of human skin. Physics in Medicine and Biology. 18(5):726-729.

Stoll, B. A. 1971. The thermoprofile as an early indicator of breast cancer response to hormonal therapy. Cancer. 27:1379-1382.

Swearingen, A. G. 1965. Thermography: Report of the radiographic and thermographic examination of 100 patients. Radiology. 84:818-824.

Wallace, J. D., H. Goldman, G. Dodd, G. Staugger, and U. Taylor, Jr. 1965. Rapid scanning thermography in suspect evaluation. Radiology. 84:132.

Watmough, D. J., and R. Oliver. 1969. Wavelength dependence of skin emissivity. Physics in Medicine and Biology. 14(2):201-204.